Project no.: AST5 – CT-2006 - 030800

COSEE

Cooling Of Seat Electronic boxes and cabin Equipment

Thematic Priority: Specific Targeted Research Projects (STP)

FINAL PUBLISHABLE REPORT

Period covered: June 2006 to February 2009

Date of preparation: March 28th, 2009

Start date of project: June 14th, 2006

Duration: 33 months

Project coordinator name : **THALES AVIONICS**

Project coordinator organisation name : **THALES AVIONICS**

Revision 00

Project co-funded by the European Commission within the Sixth Framework Programme (2002-2006)		
Dissemination Level		
PU	Public	X
OO	Restricted to other programme participants (including the Commission Services)	
RE	Restricted to a group specified by the consortium (including the Commission Services)	
CO	Confidential, only for members of the consortium (including the Commission Services)	

TABLE OF CONTENT

1 PUBLISHABLE FINAL ACTIVITY REPORT

1.1 WP 1000

New generations of (IFE) In-flight Entertainment Systems are required to provide more and more services (Audio, video, Internet, flight services, multimedia, games, shopping, phone, etc…) at an affordable cost.

But unlike other avionics systems installed in temperature controlled bays most of the IFE equipment and boxes are installed inside the cabin, they may be buried in small enclosed zones and they are not connected to the aircraft cooling system ECS.

This situation creates thermal management problems that affect the reliability, the safety and the cost of the equipment.

The most critical equipment is the SEB (Seat Electronic Box) installed under each passenger seat.

To face the increasing power dissipation, fans are used with the following drawbacks: extra cost, energy consumption when multiplied by the seat number, reliability and maintenance concern (filters, failures, …), risk of blocking by passengers belongings, and noise coupled with unpleasant smells creating disturbance in the overall cabin area.

The objectives of the project are therefore to develop and evaluate an alternate advanced cooling technique to the fans based on loop heat pipes phase change passive systems, adequately integrated inside the seat structure and taking benefit of the seat frame as a heat sink or of the aircraft structure when installed in the ceiling.

The architecture and installation of a typical Thales IFE system is illustrated below.

System features and functions are tailored per class.

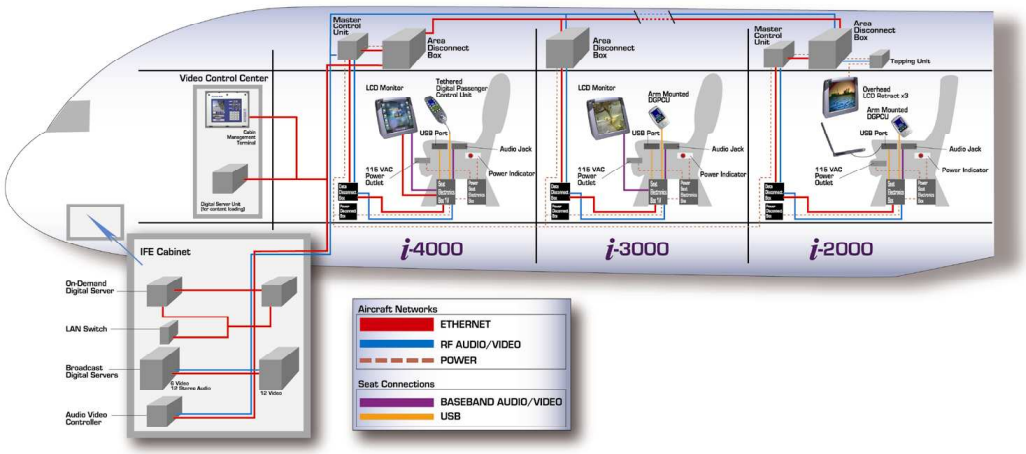

For the installed equipment in the cabin like the SEBs, ADB, MCU and TU and having no access to the ECS

(Environment Cooling System) forced convection, the thermal management is therefore critical.

- SEB (Seat Electronic Box) = 35 W to 75 W (one per seat)
- ADB (Area Distribution Box) = 25 W to 45 W (2 to 8 per aircraft)
- PMCU (Power Master Control Unit) = 25 W to 45 W (2 to 5 per aircraft)
- Tapping Unit (Overhead video display) = 20 W (6 to 14 per aircraft)

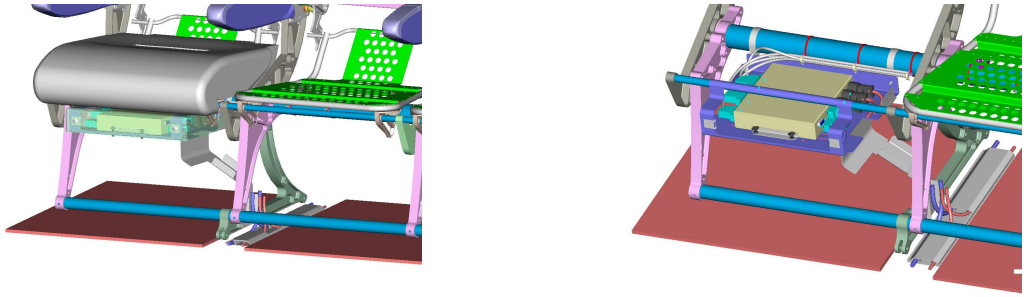

Figure 1: Examples of installation under seat

The cooling alternatives are:

Free convection whenever possible with very limited power dissipation capabilities and possible obstruction drawbacks

When the power increases, forced stand alone convection using fans is necessary with reliability cost, consumption and blocking risks concerns

- Most of the seat structures are based on large aluminum frames offering excellent heat spreaders.

The problem to be solved is then to channel the heat from the dissipative box sources to these frames with a minimum thermal resistance and weight.
A direct connection through an additional plate to the frame would generate an unacceptable weight that has been removed with great difficulties from the seat main structure.
A new technique has emerged in the PC world that was first developed for space application: Heat pipes and Loop Heat pipes
The challenge to use this innovative technique in the aeronautic world is the capability to design new loops Heat Pipe adapted to the specificities of the aerospace use (vibration, acceleration, variable orientation, temperature, …) and within the boundaries of several very specific and demanding constraints, such as reliability, weight, power consumption, volume, standardization, scalability, maintainability, cost of implementation, implementation planning, cost of ownership, upgradeability, possibility of retrofit, etc..

The project quantified objectives are therefore to develop a new cooling enhanced thermal link dedicated to the cabin IFE (In Flight Entertainment) equipment based on heat pipe technique and having the following characteristics:

- Transfer capacity up to 100 W
- Thermal conductivity equivalent or greater than 800 W/m/°K (twice that of copper)
- Heat transportation distance 500 mm (max)
- Resistance to aircraft cabin environment (vibrations, acceleration, shocks, airbus specifications)
- Minimum volume and weight
- Ease Maintainability
- Affordability: cost target ≤ cost of a fan system

1.1.1 WE 1100 : Sytem specifications

The aim of this Work Package is the establishment of common specification for the different cabin

equipment in term of environment conditions, power dissipations, heat densities, installation configurations, size, and expected cost.

Meeting with the end-user club to collect additional constraints coming from the airlines and Airbus has been held in Hamburg during the Aircraft Interior Expo once a year.

The objectives of this Work element are to define the requirements of the cooling system to be developed at the equipment level, at the seat level, and in term of thermal performances.

New generations of (IFE) In-flight Entertainment Systems are required to provide more and more services (Audio, video, Internet, flight services, multimedia, games, shopping, phone, etc…) at an affordable cost.

But unlike other avionics systems installed in temperature controlled bays most of the IFE equipment and boxes are installed inside the cabin, they may be buried in small enclosed zones and they are not connected to the aircraft cooling system ECS.

This situation creates thermal management problems that affect the reliability, the safety and the cost of the equipment.

The most critical equipment is the SEB (Seat Electronic Box) installed under each passenger seat. The Seat Electronic Box shall supply the passenger seats in the Cabin and beds/seats in the Rooms with audio, video, games, telephone, etc…by peripherals as PCUs and SDUs.

The mechanical interfaces at seat level and at SEB level have been defined.
The thermal performances with the functional specifications have been established.

Performance	Requirement for COSEE LHP
Evapo max operating thermal interface T°	85℃
Heat sink operating T°range (Tseat)	20℃ to 55℃
Non operating T°range (T0)	-55℃ to 85℃
Maximal heat load (Qmax)	50 W
Minimal start-up heat load (Qmin)	20W
Evaporator thermal interface dimensions	40mmx40mm
Flux density at evaporator	< 4 W/cm²
Adverse tilt of evaporator	The static head between reservoir and evaporator shall be sufficient to respect all 1G testability orientations of evaporator.
Proof pressure	1.5 x MNOP with Psat (T= 85℃)
Burst pressure	3 x MNOP with Psat (T= 85℃)
Life time	25 years
Mass	Shall be minimized
Vertical distance between evaporator and condenser	300 mm
Cost	≤ Cost of a fan system(*)

Table 1: Specifications summary for COSEE LHP

(*) 2 "Aeronautic Standard" fans in parallel assessed at 600Euros.

1.1.2 WE 1200 : Comparison of existing cooling

Challenge of electronic thermal management

In the field of the electronic industry, the component development is conducted by the performance and the miniaturization of electronic systems, resulting in an increase of the heat dissipation. As conduction or air convection cooling systems are no more efficient to transfer such high heat rates, alternative cooling techniques have to be used. Among the available techniques, two-phase capillary thermal control devices are specially promising. They are self-circulating devices where heat is removed and released by phase change (i.e. at a constant temperature) and working fluid is circulated by thermodynamic forces. This basic idea is available in many devices as Heat Pipe (HP), micro Heat Pipe, Heat Spreader, Capillary Pumped Loop (CPL), and Loop Heat Pipe (LHP). The two-phase capillary pumped loops, as CPL or LHP, alternatively offer many advantages over heat pipes in terms of operability against gravity, the maximum heat transport capability, smooth-walled flexible transport lines, and fast diode action (Bugby, 2006).

Phase change technologies: Two-phase capillary pumped loop CPL and LHP

A two-phase capillary loop consists of an evaporator, a condenser, a compensation chamber (also called reservoir), and vapour and liquid transport lines. Like a conventional heat pipe, a two phase capillary loop utilizes capillary action to circulate the working fluid in a closed loop and, in the process, to transfer waste heat from one location (heat source) to another (heat sink). But unlike heat pipes, the two-phase loop wick structure is confined only to the capillary pump (i.e. evaporator section) affording the wick to have ultra fine pores (without inducing an excessive pressure drop to the loop). Note that the maximum capillary pumping head generated by the wick is inversely proportional to its pore size. Therefore, the available pumping pressure of the two-phase capillary loop is at least one-order-of-magnitude higher than those of heat pipes (Hoang and Ku, Ipack2003). Moreover, a two-phase capillary loop allows vapour and liquid to flow in separate smooth-wall conduits, greatly reducing viscous flow losses in the transport lines. As a consequence, CPL or LHP can transport a large amount of waste heat over a long distance for rejection. Consequently, the original conception of the two-phase capillary loop allows a wide variety of different designs, as the flexibility in evaporator/condenser locations, which essentially extends the sphere of functional possibilities and practical application of these devices (Maydanik, 2004).

The major difference between LHP and CPL is the position of the compensation chamber. In a LHP, the compensation chamber is directly attached to the evaporator while in a CPL the compensation chamber is connected to the evaporator through a piping system. This distinction has a large impact on the design and operation of the capillary loop (Maidanik and Fershtater, 1997, Nikitkin and Cullimore, 1998, Baumann and Rawal, 2001). The physical proximity of the reservoir to the evaporator, connected by the use of a secondary wick, simplifies the LHP start-up and makes the LHP operation vapour-tolerant. Both contribute to the robustness of the LHP operation under various conditions. However, it is also a disadvantage of the LHP, since it adds some integration and packaging difficulties near the evaporator. The preconditions required for a CPL is a major disadvantage that makes the LHP a good replacing and competing technology.

Despite the design simplicity and theoretical operational robustness, the LHP is a complex system where thermal and hydrodynamic physical mechanisms between the various LHP components are strongly coupled. As an example, temperature and pressure dynamic instabilities, such as under- and overshoot, have been experimentally observed, suited to transient changes, such as start-up or variations in power load and sink temperature. Moreover, under certain conditions, the LHP can never really reach a true steady-state, but instead displays an oscillating behavior (Ku, 2003, Ku and Rodriguez, 2003, Chen and al., 2006). Such dynamic behaviours can induce possible types of failure, like eventual evaporator dry-out, degradation of characteristics, temperature oscillations, which ones

are not suitable for the thermal control of electronics.

Loop heat pipe architectures

Maydanik (1999, 2005) has presented an overview of various examples of the LHP designs. The development of LHPs was a response to the specific demand of aerospace technology, which requires high operational reliability and robustness (Orlov et al. 1997, Baker et al. 1998, Cheung et al. 1998, Douglas et al. 1999, Amidieu et al. 2000, Mena et al. 2000, Baumann and Rawal 2001, Hoang and Ku 2002, Grob et al. 2003). LHP are currently baselined as integral thermal control components of several spacecraft, including Granat in 1989, Obzor in 1994, Mars 96 in 1996, LHPFX aboard STS-87 in 1997, and ALPHA aboard STS-83 and STS-94 in 1997. Also mentioned are NASA's GLAS, CNES's STENTOR, ESA's COM2PLEX, and high power communication satellites.

Currently, miniaturization of LHPs is at the forefront of an extensive research and development to provide cooling solution for advanced electronic packaging. In spite of excellent results for LHP with ammonia as working fluid, water is probably the only available fluid that satisfies requirements for these applications regarding flammability/toxicity limits and environmental friendliness. The constrained space requires configuring specific mini-LHPs (Hoang and Ku, Ipack2003) (figure 1). Flexibility of the small transport line helps them to be routed around tight spaces. The main difficulty arising as the LHP is miniaturized (Maydanik, 2004) is connected with the decrease of the evaporator diameter, which causes a corresponding decrease in the thickness of the wick. As a result, the parasitic heat flows from the evaporation zone to the compensation chamber increases, increasing the LHP operating temperature. The use of wicks made of less heat-conducting materials does not solve the problem of parasitic flows on the whole as flows over the evaporator body may increase.

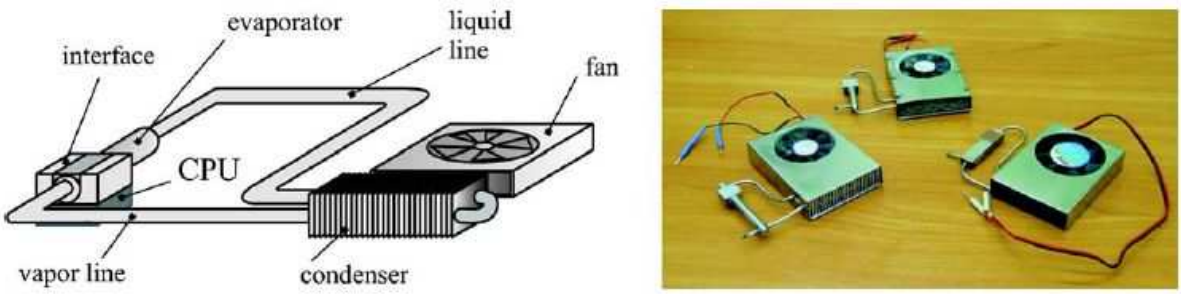

Fig. 1: Scheme and general view of CPU coolers with an LHP (Maydanik, 2005)

Review of LHP experimental studies

Numerous LHP papers have been published since the mid-1990's. Numerous experimental and numerical studies have been conducted in order to improve the LHP operation understanding. In this section, experimental results obtained for miniature LHP are presented. Some further information can be found in Launay et al. (2007). Typical experimental results for some miniature LHP studied in the literature are given in the table of appendix 1.

Numerous experimental studies have been conducted since a few years (Delil et al. 2002, Delil et al. 2003, Hoang and Ku, Ipack2003, Kaya and Ku 2003, Pastukov et al. 2003, Maydanik 2004, etc). The experimental studies pay particularly attention to the evaporator design, porous characteristics and the working fluid. Miniature LHPs with cylindrical and flat evaporators have been created. They are capable of transferring heat flows up to 200 W for a distance up to 1 m at operating temperatures from 10 °C to 100 °C and have a thermal resistance of 0.1-0.3 K/W. It has been shown that the use of new-used materials for miniature LHPs, such as aluminium and copper, makes it possible to increase

considerably the heat transfer characteristics of these devices.

The heat load, which ensures a LHP stable operation, ranges between a minimum value Q_{min} and a maximum value Q_{max}. It should be mentioned that for miniature LHPs, Q_{max} does not correspond to the capillary limit in most cases, but it corresponds to the heat load to which the system limit temperature is achieved. Boiling or wick partial dry-out may occur as the heat flux increases as the LHP evaporator is miniaturized. At the difference of heat pipes, heat spreaders, or CPL, LHP may still operate for wick partial dry-out conditions, but such phenomena will tend to increase the evaporator thermal resistance, and consequently, the heat source temperature. The value of Q_{min} is defined as the power load at which the LHP can start. Q_{min} is largely dependant of the LHP initial position previous to start-up.

Flat evaporator design

Experimental results on a miniature LHP with a flat evaporator was presented by Delil et al. (2002). The study consisted of testing various types of capillary structures in order to define the heat transfer coefficient at the vaporization interface and to study its effect on the LHP performances. Ethanol was used as working fluid. The best LHP thermal resistance is of around 0.7 K/W for a thermal load of 100 W at horizontal position. A strong influence of the anti-gravity height *H* on the thermal resistance of LHP having capillary structures with large pores has been observed.

A small-scale loop heat pipe with polypropylene wick was fabricated and tested for its thermal performances (Boo and Chung, 2004. The container and tubing of the system were made of stainless steel and several working fluids including methanol, ethanol, acetone, R134a, and water were used to study their effect on the LHP performance. A minimum thermal load of 10 W (0.8 W/cm²) and a maximum thermal load of 80 W (6.5 W/cm²) were achieved using methanol as working fluid with a condenser temperature of 20 °C for the horizontal position (the compensation chamber above the evaporator). The maximal thermal load was characterized by the maximum heater surface temperature of 90 °C, value beyond which the PP wick may be permanently deformed. For the top heating mode position (the evaporator is above the condenser), the time to reach the steady-state was more than 4 times longer than that for horizontal position and the maximum thermal load was 38 % less than that for horizontal position.

Experimental results for a miniature LHP with a flat evaporator design have been presented by Lee et al. (2004). Two different sintered metal wicks were tested: a sintered brass and a stainless steel powders with pore diameters of 9.6 μm and 19.1 μm, and porosities of 40 % and 53 %, respectively. Distilled water was used as the working fluid and the fill charging ratio was changed, ranging from 40 % to 60 % of the total LHP volume. The best performances were obtained for the LHP with a fill charge of 51 %, although the LHP start-up was easier for the lowest fill charge. For heat flux ranging from 1.48 W/cm² to 5.91 W/cm², the thermal resistance decreases from 45 K/W to 14 K/W. By comparing results measured for the two types of sintered metal wick, the LHP show almost similar performances.

Delil et al. (2003) have experimentally tested two miniature LHPs with different evaporator designs, using ammonia as the working fluid. The LHP1 evaporator has a cylindrical shape (40 mm long; diameter 8 mm) and a titanium porous wick. The LHP2 evaporator has a flat shape of diameter 28 mm, a nickel-titanium layered wick and a bi-porous thermal contact wall layer. Results indicate that the cylindrical LHP cannot be operated at powers higher than 20 W because of the inherent thin wick thickness dictated by the packaging dimensions. The flat evaporator LHP showed good performances up to 110 W. The effect of the heat sink temperature on the LHP operating temperature becomes significant for power load higher than 10 W. The LHP vapour temperature is generally roughly 5 °C lower in the horizontal orientation than in the vertical one, at powers above 10 W. At a heat sink temperature of 20 °C and for a heat load equal to 70 W, the thermal resistances in the horizontal and vertical orientations are equal to 0.14 K/W and 0.21 K/W, respectively.

Cylindrical evaporator design

A miniature LHP was tested for horizontal and four vertical orientations under various sink temperatures (Figure 2; Chen et al., 2006). The LHP has a cylindrical evaporator of 5 mm outer diameter and 29 mm length. A grooved titanium porous wick with a pore radius of 17.2 μm and a

porosity of 0.78 has been used and ammonia is used as the working fluid. The subcooled liquid comes directly into the porous wick and there is no secondary wick between the evaporator and the compensation chamber. The steady-state operating characteristics are similar for various orientations except for the orientation where the evaporator is above the compensation chamber (2). Particularly, for a sink temperature of 25 °C and the maximum allowed evaporator temperature of 75 °C, a heat load of 70 W can be dissipated. The resulting thermal resistance is 0.7 K/W.

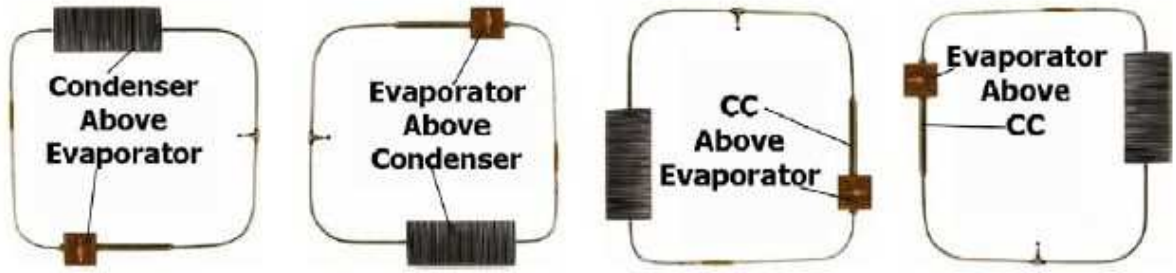

Fig. 2: Four vertical orientations (Chen et al., 2006)

Two different configurations of the compensation chamber were experimentally investigated by Riehl and Siqueira (2004, 2005). Acetone has been chosen as the working fluid to operate between -60 and 80 °C. One of the LHP has the compensation chamber detached from the capillary evaporator (LHP1) while the other one is in integral part (LHP2). A polyethylene wick (pore diameter of 12 µm, porosity of 50 %) was used. At steady-state, the LHP configuration 1 presented lower operating temperature. Several factors, as liquid charge distribution into the evaporator core, heat transfer between the compensation chamber and the ambient, or axial conductive heat leak may induce such results. The thermal resistance of the LHP1 and 2 is around 0.9 K/W when the LHP operates at 80 W (2.3 W/cm²). By varying the LHP elevation between ± 110 mm, the LHP thermal resistances are around 1 K/W and 0.7 K/W for the adverse (evaporator above condenser) and the positive elevations (evaporator below condenser), respectively (Riehl, 2004).

Review of LHP parametric studies

A parameter study on the LHP operation is difficult as strongly coupled physical mechanisms are involved in LHPs. Each parameter effect has been deduced from theoretical analysis, experimental observations or numerical studies. We should keep in mind that in most of the studies, ammonia is the working fluid. The use of fluids of lower pressure may amplify the sensitivity of the LHP operation to some parameters.

Effect of fluid charge

Contrarily to the LHP steady-state operation, the LHP start-up is strongly influenced by the fluid charge, and particularly by the fluid distribution in the LHP before starting. Even with the same boundary conditions imposed on a same LHP, drastic random discrepancies of the wall superheat prior to the LHP start-up were experimentally observed (Cheung et al. 1998). The presence of vapour bubbles/slugs in the evaporator grooves and/or in the evaporator core may modify the heat flux ratio going to the compensation chamber, which affects the temperature evolution in the evaporator section (Cheung et al. 1998, Maydanik and Fershtater 1997, Ku et al. 2001, Ku 1999). The way a LHP starts can have residual effects in its subsequent operation, as a temperature hysteresis (Ku 1999).

Effect of the porous wick characteristics and of the groove design

The porous wick characteristics, such as the effective thermal conductivity, the pore diameter, the porosity and the permeability, may have a significant effect on the LHP performance. Numerous 2D - 3D numerical studies of heat and mass transfer in a capillary structure of a LHP have been conducted (Cao and Faghri 1994, Figus et al. 1999, Zhao and Liao 2000, Yao et al. 2004) in order to determine the heat transfer coefficient in the evaporation zone. The heat transfer coefficient is strongly correlated to the vapour front position in the porous structure. From the numerical results, it seems interesting to use a relatively high permeable wick in order to make the vapour flow easier.

Platel et al. (1996) experimentally observed an increase of the heat transfer coefficient in the evaporation area up to a factor 2.5 when transversal micro grooves machined in the evaporator wall were added to the longitudinal grooves. A parametric analysis has been provided by Yao et al. (2004) in order to study the effect of the vapour groove design on the capillary and boiling limits for a LHP. Calculation results are presented for a sintered nickel porous wick with ammonia as the working fluid. Yao et al. noted that: 1/ the boiling limit increases with the number of grooves; 2/ the boiling limit is maximum for a fin/groove width ratio of 0.5; 3/ the capillary limit increases with the fin width; 4/ both the boiling and capillary limits increase as the porous wick thickness decreases. The boiling phenomena first appears in the porous wick located close to the heated fin, where the liquid is at its most superheated state as compared to the liquid distributed in the other part of the porous wick. It could be noted that the boiling limit (around 3 W/cm²) appears at a heat flux one order of magnitude lower than that of the capillary limit (around 60 W/cm²). According to Figus et al. (1999), the wick thermal conductivity does not modify significantly the vapour front position in the porous wick, but significantly affects the wall temperature and consequently, the axial heat leak.

Delil et al. (2002) have tested various types of capillary structure in order to define the heat transfer efficiency at the vaporization interface and to study its effect on the LHP performance. The heat transfer coefficient for a flat interface between the heating surface and the porous structure has been studied for heat fluxes up to 30 W/cm². The experimental results for one tested LHP are presented in figure 3. At a horizontal position, a maximum heat transfer coefficient of 52000 $W.m^{-2}.K^{-1}$ has been measured. Several observations are made: 1/ The heat transfer coefficient for vapour grooves machined in the wall of the evaporator body is higher than for vapour grooves machined in the porous wick; 2/ A decrease in the maximum pore diameter of the wick considerably increases the potential to operate against a gravitational head; 3/ A decrease in the maximum pore diameter in the evaporator shifts the maximum heat transfer coefficient to larger thermal loads. Values of around 80000 $W.m^{-2}.K^{-1}$ are quite feasible for ammonia LHPs with cylindrical evaporators (Maydanik, 2004).

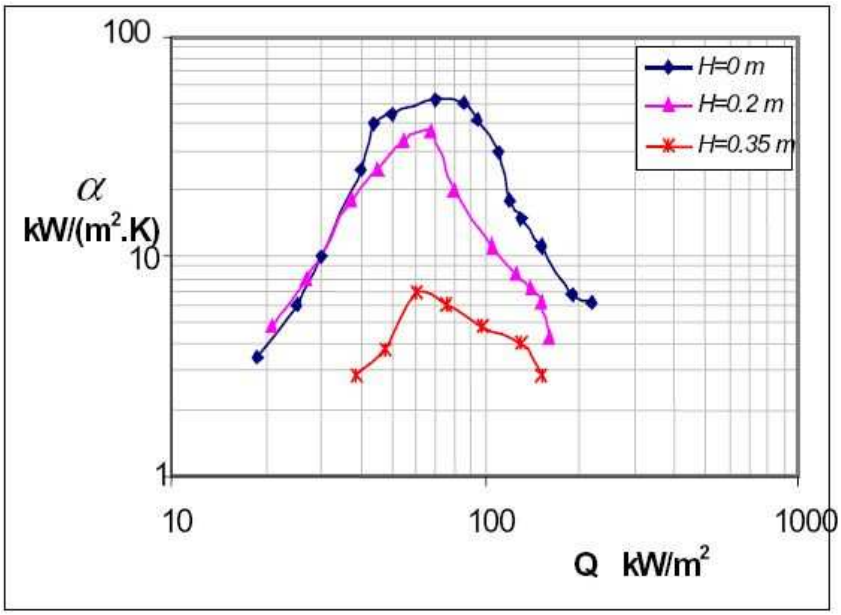

Fig. 3: Heat transfer coefficient vs. heat flux under a variable height (Delil et al. 2002).

Lee et al. (2004) have compared the thermal resistances of two different metal wick LHPs. The stainless steel powder wick has a porosity of 0.4 with a 9.6 µm effective pore diameter, whereas the sintered brass one has a porosity of 0.53 with a 19.1 µm effective pore diameter. The experimental results indicate similar performance, with a small advantage to the stainless steel powder at low heat flux.

Boo and Chung (2004) have tested several polypropylene wicks. As the pore size was reduced from 25 µm to 0.5 µm, the maximum thermal load was increased by 45 %. At the same time, the thermal resistance of the system was decreased by 33 %. A small pore size is recommended when the LHP operates close to the capillary limit. Otherwise, there exists an optimum pore size for which the wick permeability does not damage the evaporator heat transfer coefficient. Similar trends were observed by Liao and Zhao (1999).

The effect of the wick characteristics on the LHP operating limits has been presented by Hamdan et al. (2002, 2003). Calculation results have been obtained for a coherent porous silicon wick. Reducing the pore size increases the capillary pressure but at the same time it increases the pressure losses due to friction. So, there exists an optimum value of the pressure build-up across the wick, which depends on the heat flux. The nucleate boiling limit is correlated to the liquid superheat. A high superheat is desired since it will delay the bubble formation and hence any interface oscillation. As the superheat needed for nucleation is inversely proportional to the pore radius, a decrease in the pore radius will increase the boiling limit.

Effect of the working fluid

Although LHPs were first developed and tested with water or acetone as working fluids for power electronic cooling, most of the detailed results on LHP performance were presented when ammonia was used as the working fluid for the spacecraft thermal control. With the new interest of using LHPs for computer cooling, fluids like water, acetone, methanol or ethanol have been used. The first experimental results showed a significant effect of the working fluid on the LHP performance.
While ammonia exhibits many desirable heat transfer characteristics, its freezing point is too high to prevent freezing in the condenser line during a safe mode on a satellite platform. According to Rodriguez and Pauken (2000), propylene is a good fluid since it has a lower freezing point and relatively good heat transfer properties. A prototype LHP has been tested with both ammonia and propylene as working fluids. At low sink temperature, the LHP performance was similar for heat loads lower than 100 W. For higher heat loads, the thermal conductance of the ammonia LHP was approximately four times greater than that of the propylene LHP one.

Working fluids including methanol, ethanol, acetone, R134a and water were used by Boo and Chung (2004) to compare their performance in a small-scale loop heat pipe containing a polypropylene wick. Methanol, acetone, and ethanol are suitable working fluids for PP-wicks if the temperature remains moderate (< 90 °C), while R134a and water are incompatible or inappropriate with PP-wicks. At horizontal position, the minimum heat load required for the LHP operation was equal to 10 W for methanol and acetone, and higher than 10 W for ethanol. For a heat load lower than 60 W, the best performance is obtained for acetone. Methanol was considered as the best working fluid for heat loads higher than 60 W, with a maximum heat load equal to 80 W for heat sink temperatures varying from 10 to 30 °C.

According to Baumann and Rawal (2001), the liquid thermal conductivity has two significant effects on the LHP performance. Firstly, a low liquid conductivity reduces the heat transfer coefficient in the evaporator, thus limiting the heat transport capability. Secondly, a low liquid thermal conductivity reduces the LHP operating temperature by reducing the wick effective conductivity.

Effect of the gravity (elevation and tilt)

Varying the LHP elevation and tilt are two different ways to study the effect of gravity on the LHP performance. The LHP elevation corresponds to the position of the evaporator with respect to the condenser, while the LHP tilt corresponds to the position of the evaporator with respect to the compensation chamber. An adverse elevation means that the evaporator is above the condenser and an adverse tilt means that the evaporator is above the compensation chamber.
In a gravity environment, a tilt modification will change the fluid distribution, especially between the compensation chamber and the evaporator core. At adverse tilt, the evaporator core may be filled with vapour and consequently, this may increase the LHP operating temperature. Kaya and Ku (1999) studied experimentally the performance of a LHP for positive and adverse tilts. The LHP operating temperatures at adverse tilts were much higher than those at positive tilts for low heat loads. At positive tilts, where the evaporator core is completely flooded with liquid, the low steady-state temperatures for low heat loads can therefore be attributed to a substantial reduction of the heat leak and to a more efficient cooling of the compensation chamber, caused by an increase in the mass flow rate. Indeed, at the evaporator outlet, liquid may be pushed by vapour bubbles (Chuang, 2003). The experimental results presented by Chen et al. (2006) show that their miniature ammonia LHP can work under all test conditions except for adverse tilts. The fact that there is no secondary wick to pump the fluid from the compensation chamber to the primary wick may explain this result.

The effect of the relative elevation of the evaporator against the condenser on the LHP performance has been presented by numerous experimental works (Chen et al. 2006, Chuang 2003, Boo and Chung 2004, Kaya and Ku 1999, Rodriguez and Pauken 2000, Dickey and Paterson 1994, Wolf and Bienert 1994, Riehl 2004). All experiments agree well. At low heat loads, adverse elevations tend to increase the LHP operating temperature, compared to the horizontal position, whereas positive elevations tend to decrease it (figure 4).

The difference in operating temperatures decreases with an increase of the heat load and eventually disappears at large heat loads. Then, for large heat loads, the elevation has usually no effect on the LHP performance.

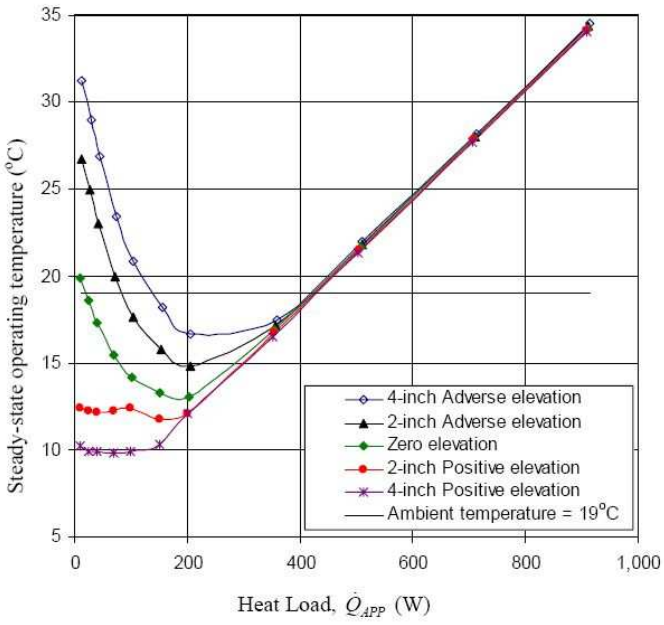

Fig. 4: Effect of the elevation on the steady-state operating temperature

(T_{sink} = 5 °C, T_{amb} = 19 °C) (Chuang 2003)

The operating temperature increase with the elevation has been explained by Ku (1999). As the pressure difference across the wick increases due to gravitational head, the difference in saturation

temperatures also increases, which induces an increased heat leak. Since the liquid enthalpy entering to the compensation chamber does not change, the compensation chamber temperature increases in order to provide enough subcooling to compensate for the increased heat leak. At high heat loads, as the gravitational head becomes negligible compared to the frictional pressure drop, the difference in saturation temperatures across the wick is not dependent on the elevation anymore.

Using ammonia (Chuang 2003, Wolf and Bienert 1994) or propylene (Rodriguez and Pauken 2000) as working fluids, with an adverse elevation ranging from 0.05 to 2.7 m, experimental measurements showed an increase of about 50 % in the LHP thermal resistance at 20 W. Using acetone as the working fluid (Rhiel, 2004) and with an adverse elevation of 0.11 m, the thermal resistance was increased by 100 % for the same heat load. The experimental results presented by Boo and Chung (2004) with a methanol LHP have shown a great effect of the gravity on the operating temperature, which vary from 50 °C at the 5 cm-positive elevation to 72 °C at the 10 cm-adverse elevation. It is then clear that the effect of the elevation on the LHP performance is strongly correlated to the working fluid.

The effect of gravity on the evaporation heat transfer in the porous wick has been experimentally observed by Delil et al. (2002) (figure 3). It is observed that the adverse elevation *H* has a negative effect on the evaporation heat transfer, which induces a decrease of the LHP performance. Moreover, the effect of *H* increases with the pore diameter.

Effect of the evaporator/reservoir design on the heat leak

The amount of heat leak is composed of two parts: the axial heat leak and the radial heat leak. The axial heat leak refers to the heat conducted from the evaporator metal mass to the compensation chamber through the connection in between. Then, the axial heat leak may depend on the configuration of the compensation chamber, which is connected to the evaporator. The radial heat leak depends on the combination between the thermal and hydrodynamic effects in the porous medium. Detailed calculations of the radial heat leak for cylindrical or flat evaporator can be found in references (Hoang and Ku 2003, Chuang 2003, Hamdan 2003).

An experimental investigation of two identical LHPs with different compensation chamber designs was presented by Riehl (2004) and by Riehl and Siquiera (2006). The chamber design affects the axial heat leak and the heat transfer between the compensation chamber and the ambient, which is in relation to its external surface area. According to Van Oost et al. (2002), the evaporator/compensation chamber design plays a fundamental role on the LHP performance. The compensation chamber and the evaporator have to be thermally disconnected and their hydraulic coupling could be ensured via a secondary wick or a bayonet. The purpose of the bayonet is to vent or directly condense the vapour inside the evaporator core. Advantages and disadvantages of designs with or without bayonet are discussed for LHPs at steady-state and transient operations.

Conclusion

The LHP performance is characterized by their thermal resistance and maximum heat transport capability. Providing a parametric analysis is not easy, because the LHP governing parameters are strongly coupled. The fill charge ratio has a significant effect if the void fraction in the evaporator core varies, leading to a radial heat leak variation. The radial heat leak, as well as the ratio of radial to axial heat leak, is affected by the wick characteristics, and the evaporator and compensation chamber designs. The pore size is an important parameter, which should be as low as possible to increase the capillary and boiling limits. The fluid selection mainly depends on its saturation pressure, which should be sufficiently high at the considered operating temperature. Thus, ammonia and propylene are used for low temperature applications; water, alcohols, acetone and R134a may be used for higher temperature applications. In addition, the compatibility of the fluid with the loop materials should be carefully considered. The gravity effect is important for terrestrial applications: an

adverse elevation or tilt decreases the LHP performance, especially at low heat loads. Likewise, a fluid pressure drop increase tends to decrease the performance. The temperature difference between the ambient and the heat sink affects the transition heat load between variable and fixed conductance modes of the LHP operation.

In terms of dissemination of scientific knowledge, a paper has been published in the International Journal of Thermal Sciences (Launay et al., 2007).

1.1.3 WE 1300 : System mock up definition

The objectives of Work Element 1300 are to design and develop the module demonstrator in accordance with:
Test configuration selected
Number of seat box necessary for the demonstration
Number and type of seat selected
Experimental measurement method
Demonstration preparation: interface with ECAB project
Visualisation of the results

SEB has been described with its components. Different configurations of SEB mounting have been evoked with the seat adaptation needed.

To check the performance of the LHP and the fulfilment of the environment specifications a LHP mock-up will be developed.

This mock-up will be representative of the final system but easier to handle then a seat structure.

A dissipative device with monitor able power will replace the SEB and a temperature will replace the seat controlled plate with a liquid circulation.

Such a mock up will permit to check the thermal performance the influence of tilt angle and the most of the environment testing.

These test with a SEB and real seat mounting are important to integrate the real value of thermal resistances and also to evaluate the integration problems with the tubing distribution and installation constraints.

These tests were planned on three type of seat :

- PAIG : Business double
- RECARO : Carbon fiber type
- AVIO : Economy class type
-

PAIG being enable to send its seat it has been partially replaced by a Recaro seat.

The complete LHP will be mounted on each seat and will be checked at ambient temperature with increasing levels of temperature in the SEB.

Thales will provide the different SEB mock-up. These SEB mock-ups will have a system to generate the power on the equipment and to measure the temperature on specific component and on the pcb.

Thales has to find a system to bring all the hot points in only one where the evaporator of the LHP will be fixed.

1.1.4 WE 1400 : Test File Definition

The objective of task **1400** is to define the test conditions for the evaluation of the cooling system performance.

Test condition shall include increased power dissipation, different external boundary condition (increased temperature) and also evaluation of system performance under accelerations and vibrations.

Preliminary test under increasing power has been realised in WP 5000 in Thales facilities.

The following thermal test configuration can be applied.

- A precise definition of the power configuration will be given, according to the different possible thermal schemes offered by the demonstrators.
- The boundary conditions are clearly explained in the following diagram.

POWER CONFIGURATIONS

INCREASING POWER FROM 10W to 100W in the SEB

⇒

BOUNDARY CONDITIONS :

- Ambient temperatures
- Orientation effects

The purpose of this general test is to determine the maximum heat dissipation of the SEB and the temperature gradients in accordance with the specified temperature maxima for a given configuration and environment.

The maximum temperature for the component junction of hot spots is T=125°C.

For each measurement, specific conditions must be defined and the following procedure applied.

The criterion for stabilization is a temperature oscillation between ±2°C/minute around the average value.

Dynamic test includes vibrations and acceleration these test will complement the test performed on the LHP mock up and will concern only the test that have a meaning at this level.

The three seats will be tested in VZLU premises and will be submitted to the following test sequence:

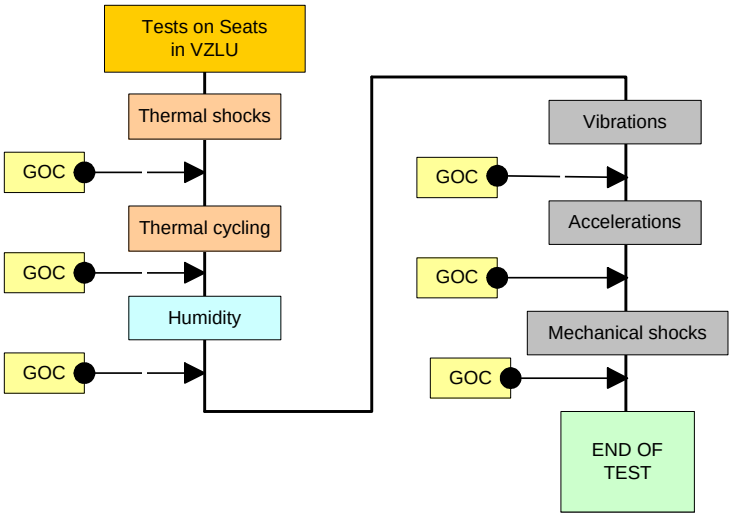

GOC : Good Operational Checkout

The schedule of the different tests and theirs specificities have been re-evaluated after the first serie of test on LHP, the following table shows the matrix of the tests that have been realised in Thales and VZLU between december and end of february:

		Order of Tests	MOCK-UP			Analogy	Equipment Status	Location of the test	SEATS	
			LHP Mock-up	Seat + SEB Mock up	Full System				AVIO	RECARO
Temperature variations ambient to +55°C 25°- 35°- 45°- 55°C	Increasing Power	1			X		ON	VZLU	X	X
Storage temperature	High temperature	2			X		ON	VZLU	X	NO
	Low temperature	Test not realised				X	Test not realised			
Linear Acceleration	Mid power	3			X		ON	VZLU	X	X
	Maximum power	4			X		ON	VZLU	X	X
Atmospheric pressure	Decompression	5			X		ON	VZLU	X	X
	Overpressure	Test not realised				No risk	Test not realised			
Random Vibrations		6			X		ON	VZLU	X	X
Thermal shocks		7			X		ON	VZLU	NO	X
Humidity	All these tests will be not realised they will be validated by analogy					X				
Mechanical shocks						X				
Sand and dust						X				
Fungus						X				
Fluids contamination						X				
Toxicity Inflammability						X				

The power must be increased step by step for a given temperature until the maximum power with the differents powers indicated in the following table:

	Steps of power applied					
Ambient Temperature	RECARO SEAT			AVIO SEAT		
25°C	25 W	50 W	60 W	25 W	50 W	100 W
35°C	25 W	50 W		25 W	50 W	
45°C	25 W			25 W	50 W	
55°C	10 W			25 W	50 W	

All the tests have been realised on the two types of seats Recaro and Avio.

1.2 WP 2000 : LOOP HEAT PIPES STUDIES

1.2.1 WP 2100 : THEORETICAL APPROACH

The scope of WE2000 is to design a LHP adapted to the specifications defined in WP1000. LHPs are superior to conventional heat pipes in terms of capillary pumping head, operational robustness, etc… However, as two-phase heat transfer devices, LHPs are delicate in the sense that their performance greatly depends on the structure of loop components in connection with various operating conditions. For a given LHP, since all loop components are thermally and hydro-dynamically interrelated, the operating characteristics can also be strongly influenced by the pre-start-up conditions and the operating history.

The structure of LHPs can be various in terms of size, geometric shape, number of components, relative position of the loop components, material, working fluid, fill charge, etc… This great flexibility of a LHP structure allows an optimum design for a specific application. Therefore, for the proposed application a new LHP configuration has to be designed, based on extensive technology mock-up experimentation results and parametric simulation studies. A simulation approach is required to

handle the large number of possible design variations. The simulation model must allow predicting the steady-state performance of LHP under given boundary conditions. The LHP studies will result in an optimum LHP design with the appropriate material and working fluid.

The objective of this study is to develop a simulation tool in order to determine the maximum heat transfer capability and the thermal resistance of the loop heat pipe.

For the simulation of LHP behavior, the model should include following parameters:

- capillary structure parameter (porosity, permeability, …)
- fluid type and characteristics,
- thermal operating conditions (heat flux level, cooling fluid temperature, elevation),

The theoretical results will be compared to the experimental values, given by the WE2200, for one LHP geometry.

DEVELOPMENT OF A GENERAL LHP THERMO-HYDRAULIC MODEL AND SIMULATIONS

Figure 1 presents the functional schematic of the modeled LHP, which consists of a capillary pump, a reservoir (also called compensation chamber), a condenser and vapour and liquid transport lines. Although cylindrical shape capillary pumps hold higher working fluid pressure, a flat evaporator is usually more convenient for electronic cooling as it fits better the component shape. In addition, the prototype produced by ITP and to be tested at IKE was chosen to be of flat type. However, a cylindrical evaporator model was also developed for purposes of model validation with experimental data from the open literature.

The ***steady-state model*** (appendix 2) developed in this study is based on momentum and energy conservation equations and thermodynamic relationships. The following assumptions are adopted:

1/ the fluid in the reservoir is isothermal;

2/ The energy balance at the evaporator expresses that a part of the heat input Q_i is transferred to the reservoir by conduction through the evaporator wall (axial heat leak), and another part to the liquid-vapour interface:

$$Q_i = \frac{T_E - T_R}{R_{wall}} + \frac{T_E - T_v}{R_E}$$

where R_E is the thermal resistance between the heat source to the vaporization interface at the porous wick surface, R_{wall} the conductive thermal resistance between the heat source and the reservoir, T_E the evaporator wall temperature, T_R the reservoir temperature and T_v the vapour temperature. The heat transferred to the liquid-vapour interface includes latent and sensible heat, plus heat transfer by conduction/convection to the evaporator core through the wick (radial heat leak);

3/ incompressible laminar or turbulent fluid flows are considered;

4/ the vapour temperature variations in the grooves and in the vapour line are neglected;

5/ the desuperheating length in the condenser is neglected;

6/ the phase change process in the condenser is isobaric.

7/ the fluid thermophysical properties vary with the temperature;

8/ LHP heat exchange with ambient is considered.

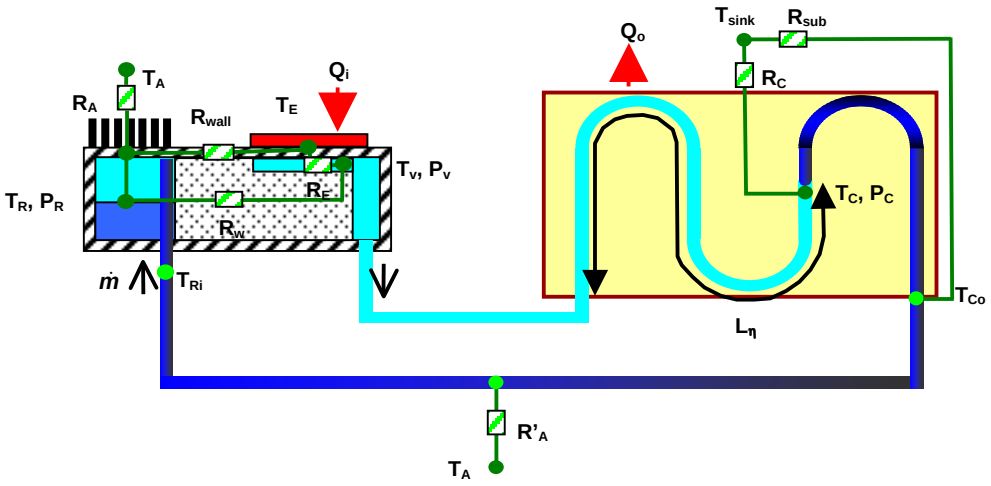

Figure 1: LHP schematic and thermal resistance network

A ***preliminary validation*** (appendix 3) of the model was performed from experimental or numerical results available in the open literature. Detailed experimental results are presented by Boo and Chung (2004), using methanol, ethanol and acetone as working fluids. The LHP is made of stainless steel and a polypropylene porous wick is used as the capillary structure. It was shown that the temperature difference between the evaporator and the vapour is strongly linked to the thermal resistance of the evaporator R_E. R_E is difficult to estimate as it depends on the mechanical contact between the container and the wick, and also on the wettability of the liquid with the porous wick. The simulation results were also compared to Chuang's results (Chuang, 2003), who studied a cylindrical evaporator LHP filled with ammonia of which condenser elevation above the evaporator is varied. A good accordance was obtained between our model results and Chuang's results.

A ***parameter sensitivity analysis*** was performed, including the effect of the fluid properties and fluid type (figure 2), of the evaporator thermal resistance (figure 3), of the mesh properties (figure 4 and 5) and mesh geometry (figures 6 to 8), and of the LHP elevation (figure 4 to 8).

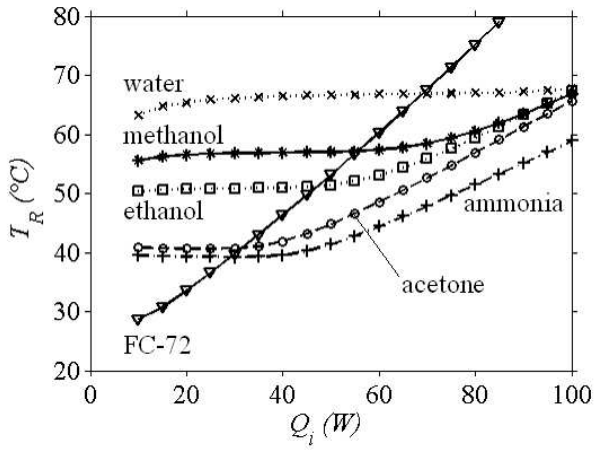

Figure 2: Effect of fluids on the LHP operating temperature

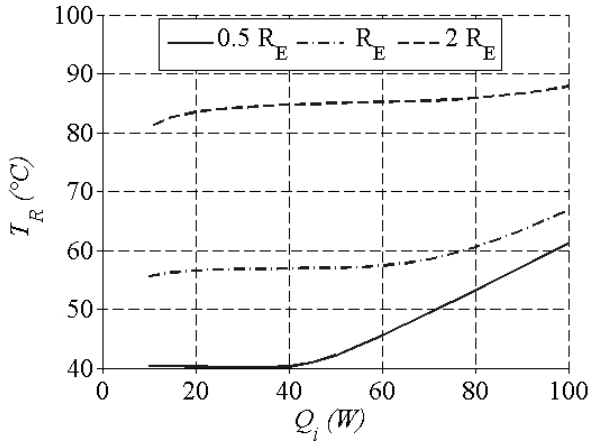

Figure 3: Evaporation resistance effect on the LHP operating temperature

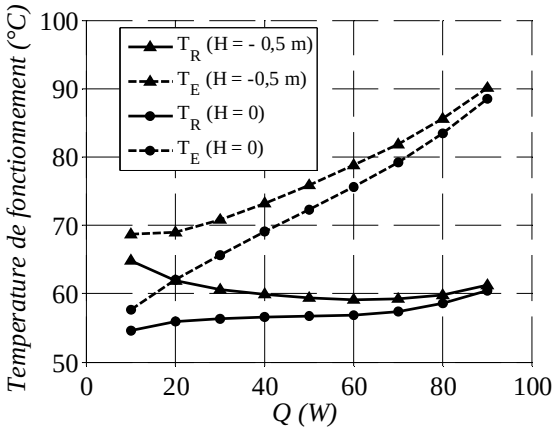

Figure 4: Condenser elevation effect on the LHP temperatures; polypropylene mesh (k_w= 0.20 $Wm^{-1}K^{-1}$, k_{eff}= 0.19 $Wm^{-1}K^{-1}$)

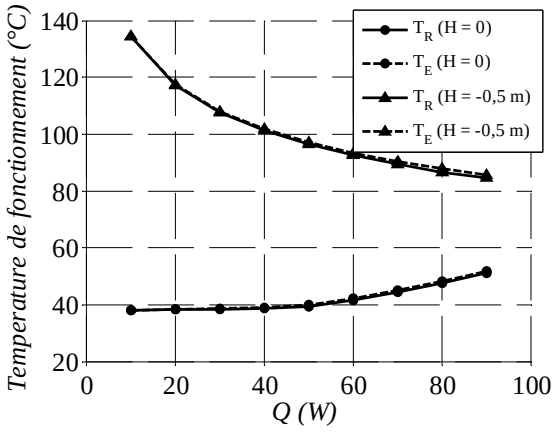

Figure 5: Condenser elevation effect on the LHP temperatures; nickel mesh (k_w= 90 $Wm^{-1}K^{-1}$; k_{eff}= 50 $Wm^{-1}K^{-1}$)

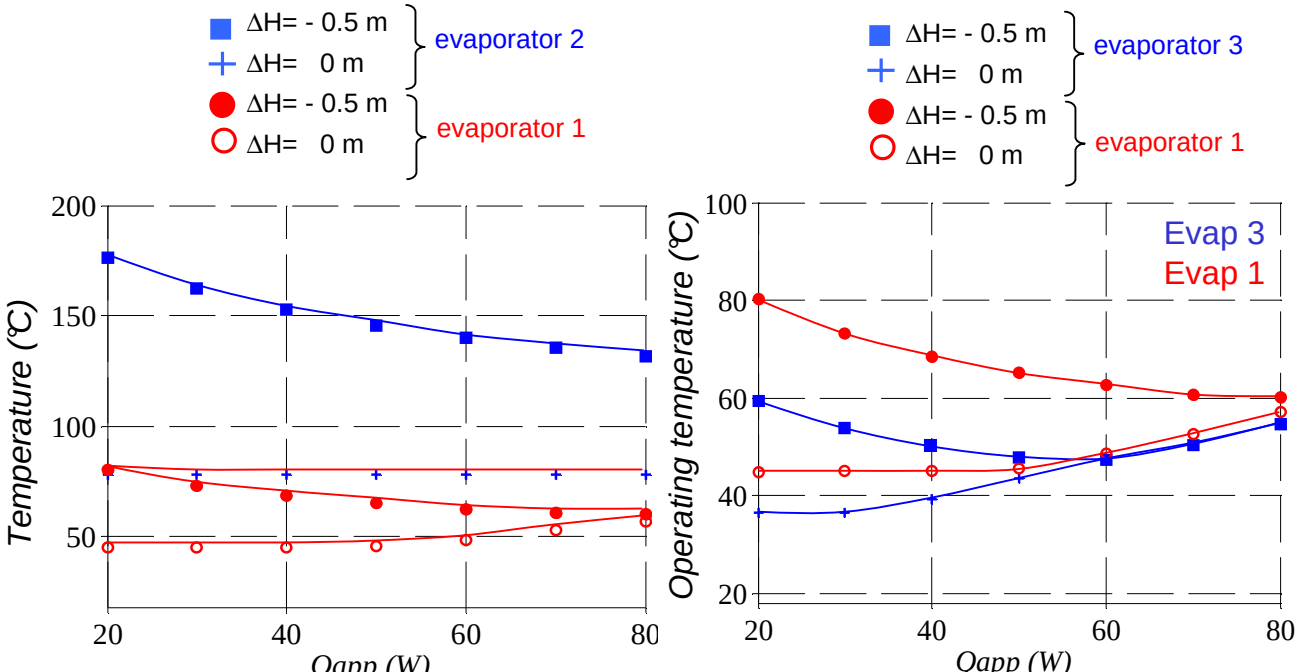

Figure 6: Comparison of the performance of LHP (1) and (2) at horizontal and vertical positions

Figure 7: Comparison of the performance of LHP (2) and (3) at horizontal and vertical positions

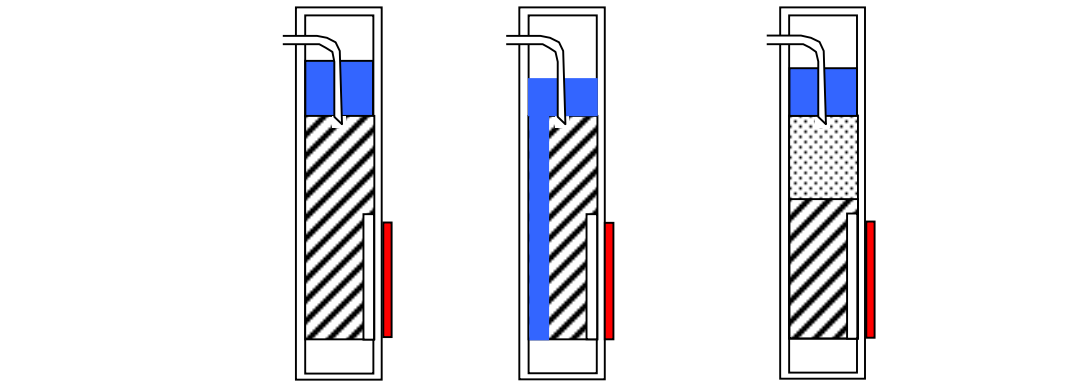

(1) (2)

(3)

Figure 8: Studied mesh configurations

(1) basic geometry: copper mesh (k_{eff} = 40 $Wm^{-1}K^{-1}$, thickness 6 mm)

(2) thinner mesh: copper mesh (k_{eff} = 40 $Wm^{-1}K^{-1}$, thickness 5 mm)

(3) composite mesh: copper mesh (k_{eff} = 40 $Wm^{-1}K^{-1}$, thickness 6 mm) + low thermal conductivity mesh (k_{eff} = 5 $Wm^{-1}K^{-1}$, thickness 6 mm)

The ***main conclusions*** arising from this study are:

- when using a low conductivity capillary structure, the LHP performance is sensible to the latent heat of vaporization, the liquid specific heat and the evaporator thermal resistance R_E (which includes container/wick mechanical contact and fluid/wick wettability), particularly when the LHP operates at variable conductance mode,

- when operating at fixed conductance mode, the LHP performance mainly depends on the heat transfer resistance between the working fluid and the heat sink,

- the LHP is more sensitive to elevation or acceleration forces when using a high conductivity capillary structure rather than a plastic mesh.

- a composite wick enables to decrease the operating temperature at low heat inputs and reduces the sensitivity of the LHP performance to the elevation.

VALIDATION OF THE MODEL WITH THE IKE EXPERIMENTAL RESULTS

A new LHP model was developed, to account for the specificities of the LHP fabricated by ITP and of the experimental test bench of IKE (appendix 4). As the convective and radiative heat exchanges of a LHP with its environment have a predominant influence on its thermal behaviour, as compared to the heat exchanges within the system, it was decided to limit the heat exchanges with the surrounding and to cool the condenser by means of forced water circulation.

The numerical results of the LHP model were compared to the experimental measurements performed by IKE, for an ambient temperature and a cooling fluid temperature fixed either to 20 °C

or to 55 °C, a heat input at the evaporator ranging from 20 to 100 W and four LHP orientations: horizontal, vertical, with a tilt angle of 30° and 60°. The validation is based on the comparison between two leading temperature values, viz. the evaporator wall temperature T_E and the vapour temperature T_v. Two parameters, R_E and R_{wall}, were adjusted to minimize the difference between experimental and theoretical evaporator temperatures T_E. It was shown that the model correctly predicts the evolution of the LHP temperatures with the heat input, the tilt angle and the heat sink temperature (figures 9 to 16)

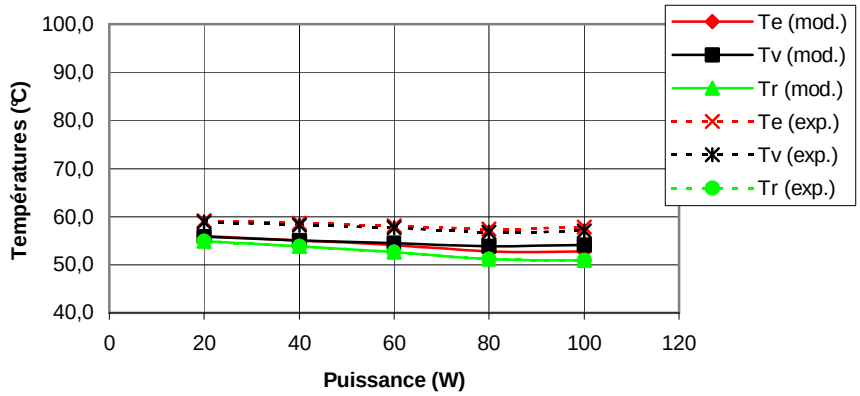

Figure 9: Comparison of experimental and predicted temperatures (T_e, T_v, T_r) – Horizontal position, T_{sink} = 20 °C

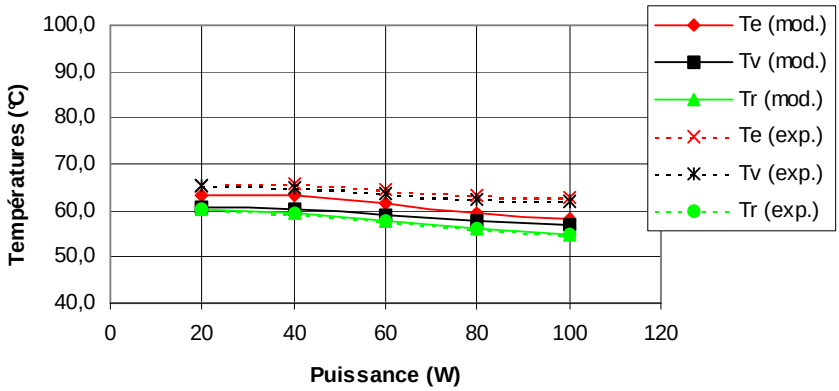

Figure 10: Comparison of experimental and predicted temperatures (T_e, T_v, T_r) – Tilt angle of 30°, T_{sink} = 20 °C

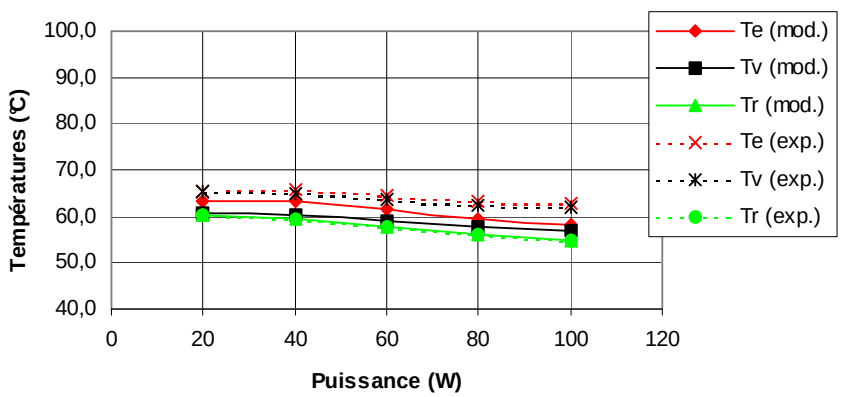

Figure 11: Comparison of experimental and predicted temperatures (T_e, T_v, T_r) – Tilt angle of 60°, T_{sink} = 20 °C

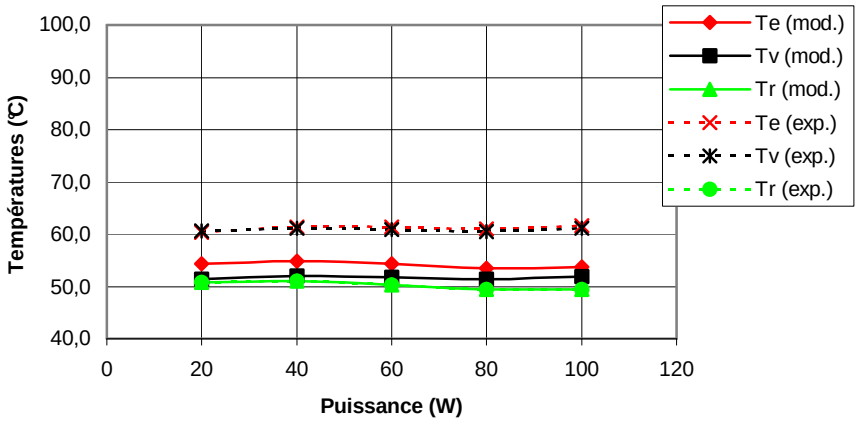

Figure 12: Comparison of experimental and predicted temperatures (T_e, T_v, T_r) – Tilt angle of 90°, T_{sink} = 20 °C

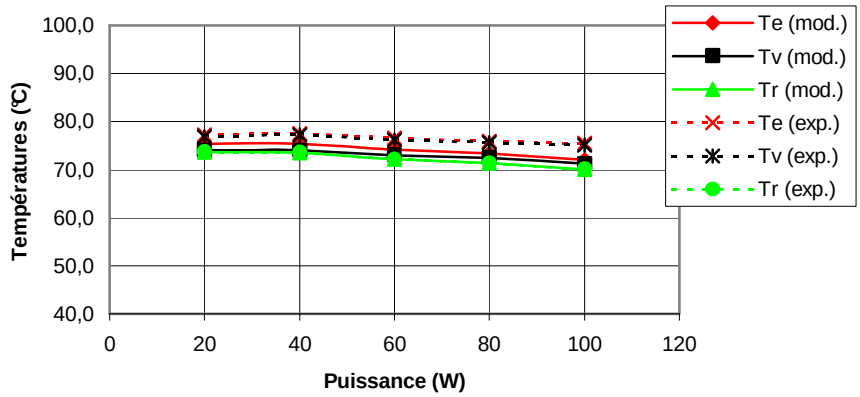

Figure 13: Comparison of experimental and predicted temperatures (T_e, T_v, T_r) – Horizontal position, T_{sink} = 55 °C

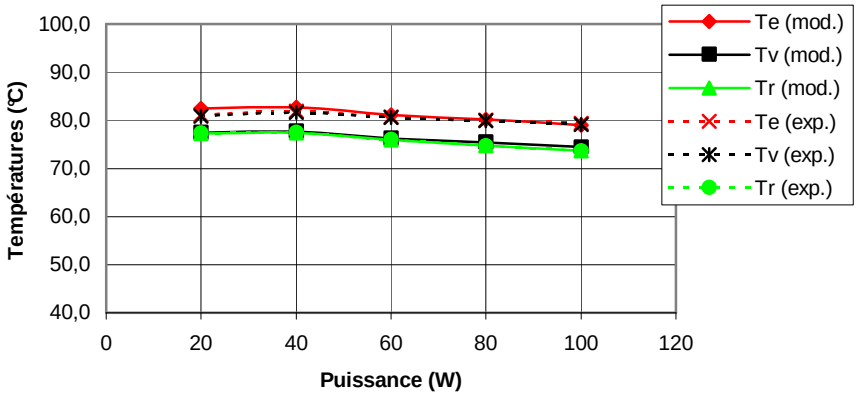

Figure 14: Comparison of experimental and predicted temperatures (T_e, T_v, T_r) – Tilt angle of 30°, T_{sink} = 55 °C

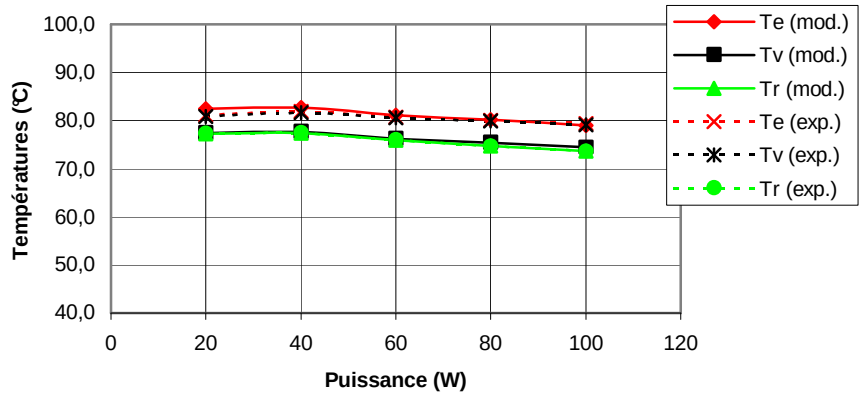

Figure 15: Comparison of experimental and predicted temperatures (T_e, T_v, T_r) – Tilt angle of 60°, T_{sink} = 55 °C

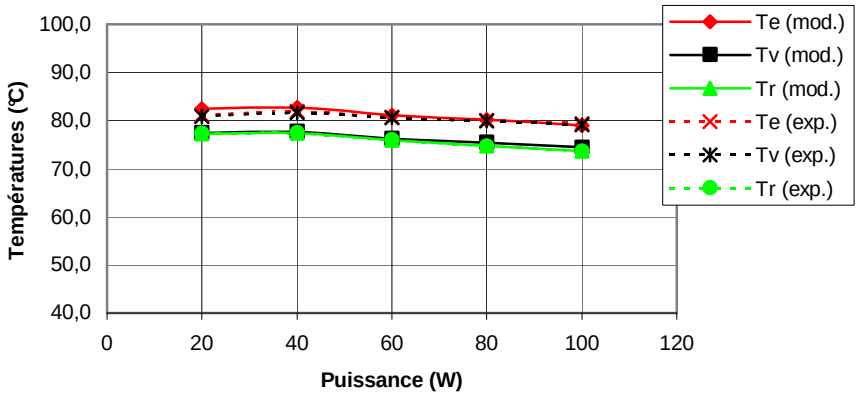

Figure 16: Comparison of experimental and predicted temperatures (T_e, T_v, T_r) – Tilt angle of 90°, T_{sink} = 55 °C

The values obtained for R_E during the ***identification stage*** (appendix 5) were depicted as a function of the heat load, the LHP tilt angle and the heat sink temperature (figure 17). Whatever the tilt angle and the heat sink temperature, R_E decreases with the heat load. The shape of these curves is similar to the typical curves R_E *(Q)* described by Chuang in its PhD thesis (2003).

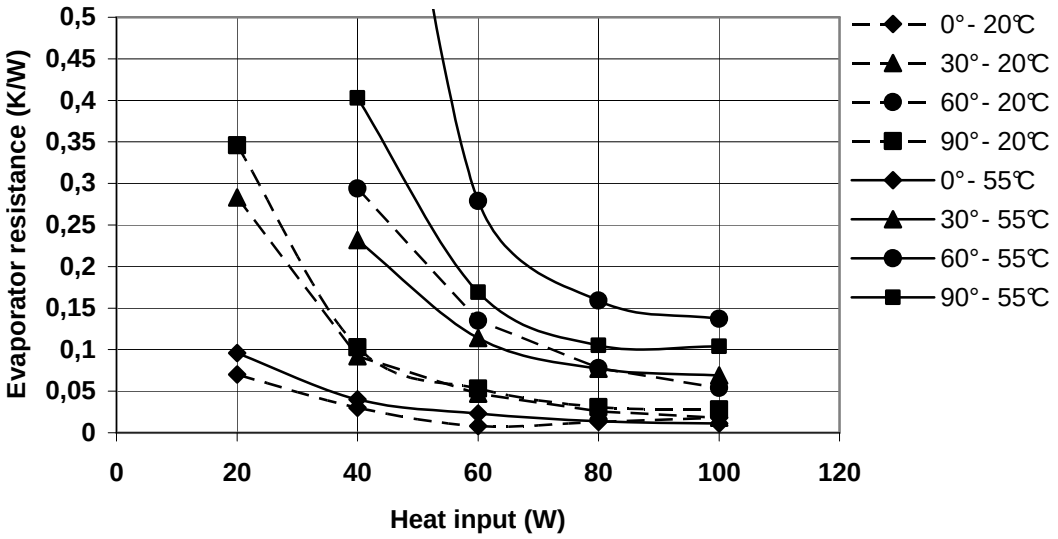

Figure 17: Evolution of the evaporator thermal resistance as a function of the heat load, the tilt angle and the heat sink temperature

COMPARISON OF THE PERFORMANCE OF THE LHP DESIGNED BY EHP AND BY ITP

A flat disk-shaped Loop Heat Pipe was designed by EHP. The LHP evaporator/reservoir, made of titanium, has a diameter of 40 mm and a thickness of 4.8 mm. The characteristics of the titanium capillary structure were found in the open literature (Maydanik, 2005). The liquid and vapour lines, 2.5 mm ID, are bended to provide a 300 mm elevation between the evaporator and the condenser. The working fluid is ultra-pure water. The model of the EHP geometry was developed, using the geometrical data of the appendix 3. In order to compare the performance of both LHP designs, the same operating conditions have to be considered. As no experimental data are available at the present time for the EHP Loop Heat Pipe, the values are R_E can not be identified and were estimated on the basis of simplifying assumptions.

An example of the simulation results is shown in figure 18. In this figure, the copper LHP fabricated by ITP is called "LHP1" and the titanium LHP fabricated by EHP, "LHP2". The model predicts higher temperatures for the titanium LHP than for the copper LHP, at the evaporator wall, in the reservoir, in the vapour. The increased reservoir temperature in the titanium LHP is due to weak heat exchange between the reservoir and the ambient, linked to the small heat transfer surface area of the reservoir. Thus, the parasitic heat flux is not dissipated to the environment but in the fluid that fills the reservoir. The radiator pressed onto the reservoir of the copper LHP is very efficient to decreases the LHP operating temperature, although the parasitic heat flux is greater.

A simulation performed with identical values of R_E for both LHP showed that the results are strongly dependant on the evaporator thermal resistance (figure 19). This time, the temperatures are higher for the copper LHP. Therefore, to perform a reliable comparison between the LHP, this parameter has to be accurately identified from experiments with the EHP Loop Heat Pipe.

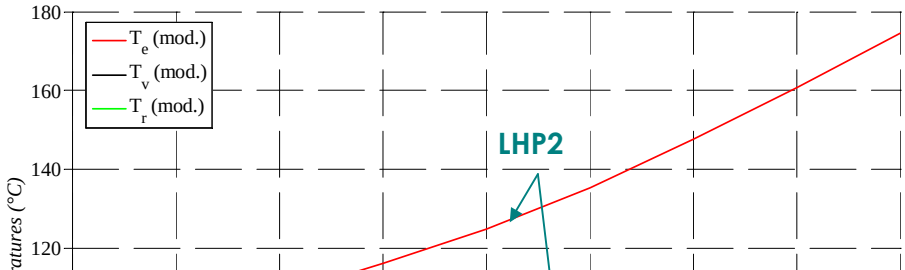

Figure 18: Comparison of T_e, T_v and T_r for the LHP designed by EHP and by ITP

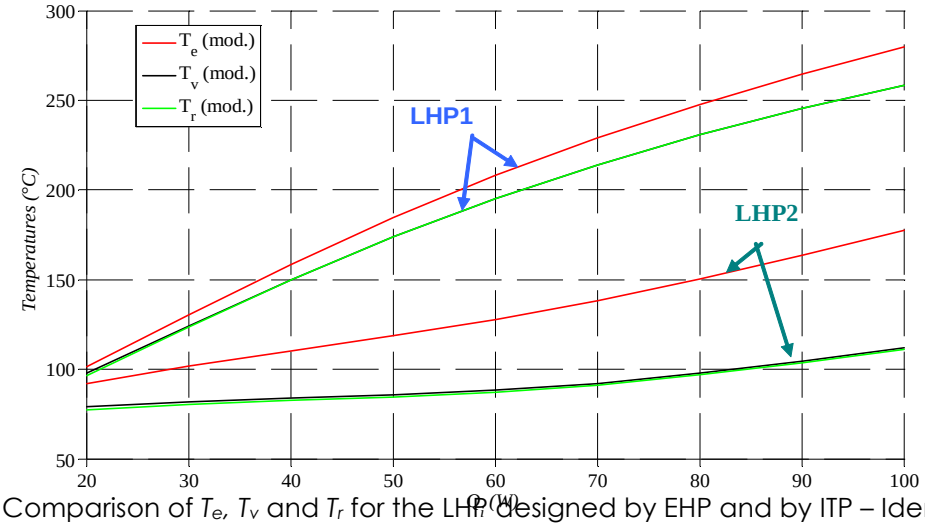

Figure 19: Comparison of T_e, T_v and T_r for the LHP designed by EHP and by ITP – Identical R_E values

PARAMETER SENSITIVITY ANALYSIS

A parameter sensitivity analysis has been performed with the LHP geometry designed by ITP. As in some actual seat configurations, the heat sink might be located further away from the LHP than initially considered, the effect of the liquid line length has been studied (figure 20). When the liquid line length is increased by 50 %, the liquid pressure drops increases, inducing an increase of the LHP operating temperature. In terms of T_E, this increase is not very sensitive to the heat flux and is about 6 K.

The selection of the working fluid will play a major role for this type of application. Water is certainly a good candidate, but suffers from the risk of freezing. FC72 performance as LHP working fluid is usually considered as limited. Lastly, R-245fa is a recently-developed fluid which is more and more used in electronics cooling applications. However, it presents some limitations, particularly at high pressure. These three working fluids were investigated and compared, for both horizontal orientation (figure 21) and vertical adverse orientation (figure

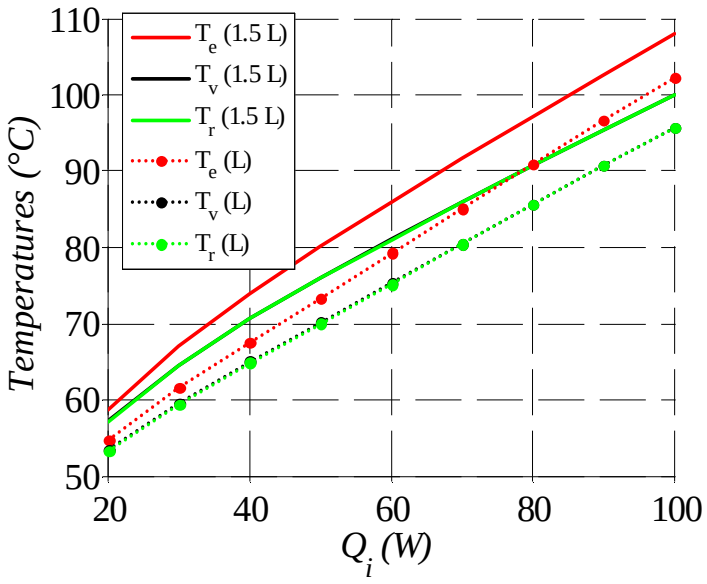

Figure 20: Effect of the liquid line length (T_e, T_v, T_r) – Horizontal position

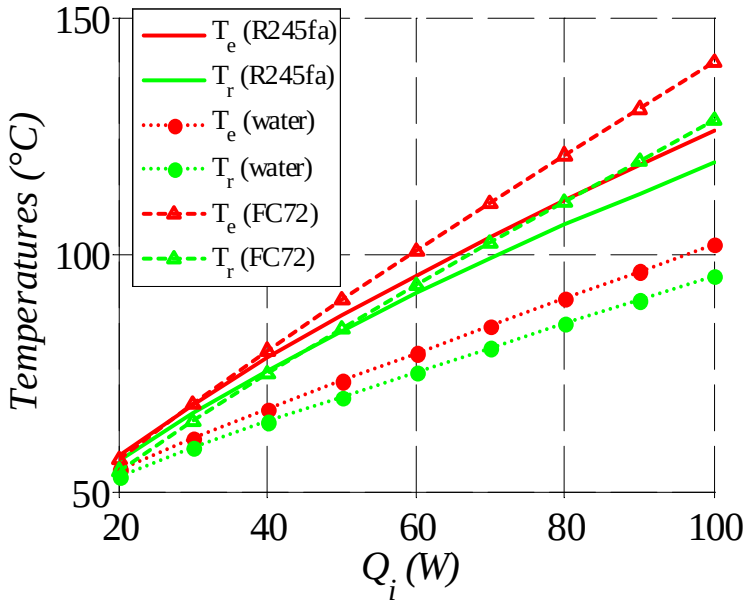

Figure 21: Effect of the liquid line length (T_e, T_r) – Horizontal position

22). At horizontal position, the best performance is achieved with water. The highest operating temperature is reached with FC-72 as the working fluid. Moreover, with FC-72, the LHP capillary limit is reached at a heat transfer rate of 90 W. For a vertical orientation, and for low heat inputs, the LHP operating temperature is lower with R-245fa than with water. However, with R-245fa, the capillary limit is reached for very small heat inputs (about 20 W). This low value is due to its very low surface tension with respect to water.

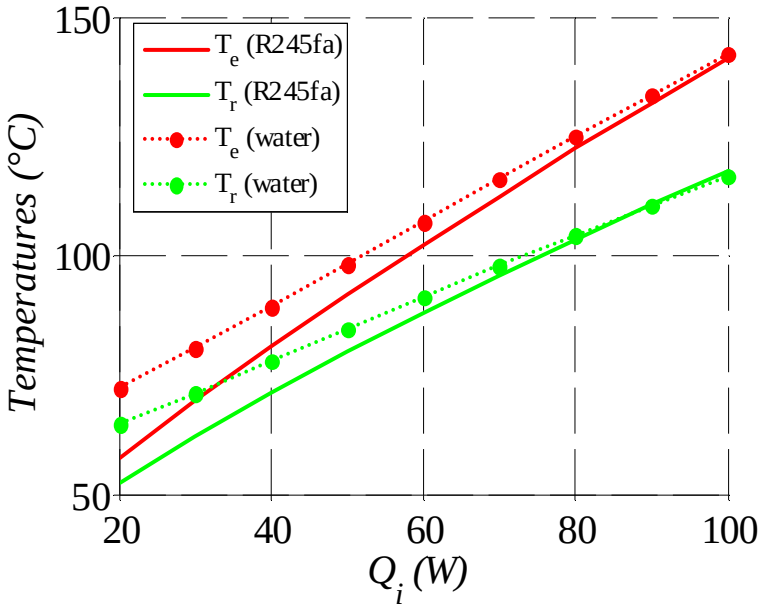

Figure 22: Effect of the liquid line length (T_e, T_r) – Vertical adverse position

DEVELOPMENT OF A SIMPLE TOOL FOR THE LHP DESIGN

The numerical model involved in the design of LHP has a certain degree of complexity. We have therefore developed a simplified analytical model that allows plotting the LHP operating curve reasonably accurately with respect to the whole model from a very basic mathematical formulation. This methodology and the result were published in the Journal of Thermophysics and Heat Transfer (Launay et al., 2008). This new approach of the LHP modeling presents many advantages. It facilitates the identification of the physical mechanisms which influence the variation of LHP operating temperature. Moreover, the simplified analytical expressions are able to highlight those parameters, which have a significant influence on the LHP performance. This, it is believed will assist researchers and thermal engineers when performing the system analysis during the design phase.

CONCLUSIONS

A LHP steady-state model has been developed to investigate the system thermal behaviour when subjected to various operating conditions, and to highlight the effect of some geometrical and thermophysical parameters on its performance. The model is of nodal type and consists of a set of equations taking into account the conservation of mass and energy. A preliminary validation has been done with experimental and numerical results from the open literature (Chuang, 2003, Boo and Chung, 2004). From the first simulations, carried out with a geometry found in the literature (Boo and Chung, 2004), the following conclusions can be drawn:

- when using a low conductivity capillary structure, the LHP performance is sensible to the latent heat of vaporization, the liquid specific heat and the evaporator thermal resistance R_E (which includes container/wick mechanical contact and fluid/wick wettability), particularly when the LHP operates at variable conductance mode,
- when operating at fixed conductance mode, the LHP performance mainly depend on the heat transfer resistance between the working fluid and the heat sink,
- the LHP is more sensitive to elevation or acceleration forces when using a high conductivity

capillary structure rather than a plastic mesh.

Thanks to this model, some enhanced wick designs have been suggested (thinner mesh, composite wick). The composite wick could decrease the operating temperature at low heat flux and reduce the sensitivity of the LHP to orientation.

The experimental data provided by IKE allow the identification of the evaporator wall – vapour thermal resistance R_E and of the evaporator wall thermal resistance, corresponding to the longitudinal heat leak, for various operating conditions. The R_E values and their evolution as a function of the heat load are in good agreement with the literature results. Using the identified parameters, the maximum difference between the experimental and predicted temperatures is of 10 K.

The simulations performed with the geometry of the LHP manufactured and delivered by ITP to IKE lead to the following conclusions:

- the increase of the liquid line length results in an increase of the LHP operating temperature. This increase is about 6K when the liquid line length is increased by 50%.
- FC-72 or R-245fa are probably not good candidates as working fluids (as compared to water), in that sense that they lead to a low or very low capillary limit (about 90 W and 20 W, respectively) with respect to the specifications, especially under vertical orientation or when subjected to acceleration forces.

A model was developed to simulate the loop heat pipe designed and manufactured by EHP. Simulations were performed to compare the performance of the ITP and EHP loop heat pipes. The ITP performance seems to be better due to the enhanced heat exchange from the reservoir to the ambient. However, this result has to be confirmed after identification of the thermal resistances R_E and R_{wall} of the EHP loop heat pipe, using experimental data.

Besides, a simple analytical tool for the LHP design was developed and presented: it will constitute a help for the future for engineers aiming at designing LHPs, as its formulation is relatively simple.

To conclude, it should be recalled that diffusion of knowledge by means of publications in scientific journals or conferences is one of the core missions of academic laboratories like CETHIL. Therefore, two journal papers (Launay et al., 2007a, Launay et al., 2008) and two conference communications (Launay et al., 2007b, 2007c) were published from the knowledge developed by this WP.

1.2.2 WP 2200 : TECHNOLOGICAL MOCK UP EXPERIMENTATION

The objective is to investigate the steady-state and transient performance of a LHP with respect to the system specifications. The experimental investigations will provide:

- data to verify the estimated thermal performance and operating margins of selected phase change configurations,
- data to improve the computational models.

A test set-up and procedure will be devised for the investigations. The set-up will allow:

- testing of articles representing the modeled configurations,
- recording of thermal performance of test articles, i.e. heat transport capability, temperature distribution, thermal resistance.

TEST RIG

a) b)

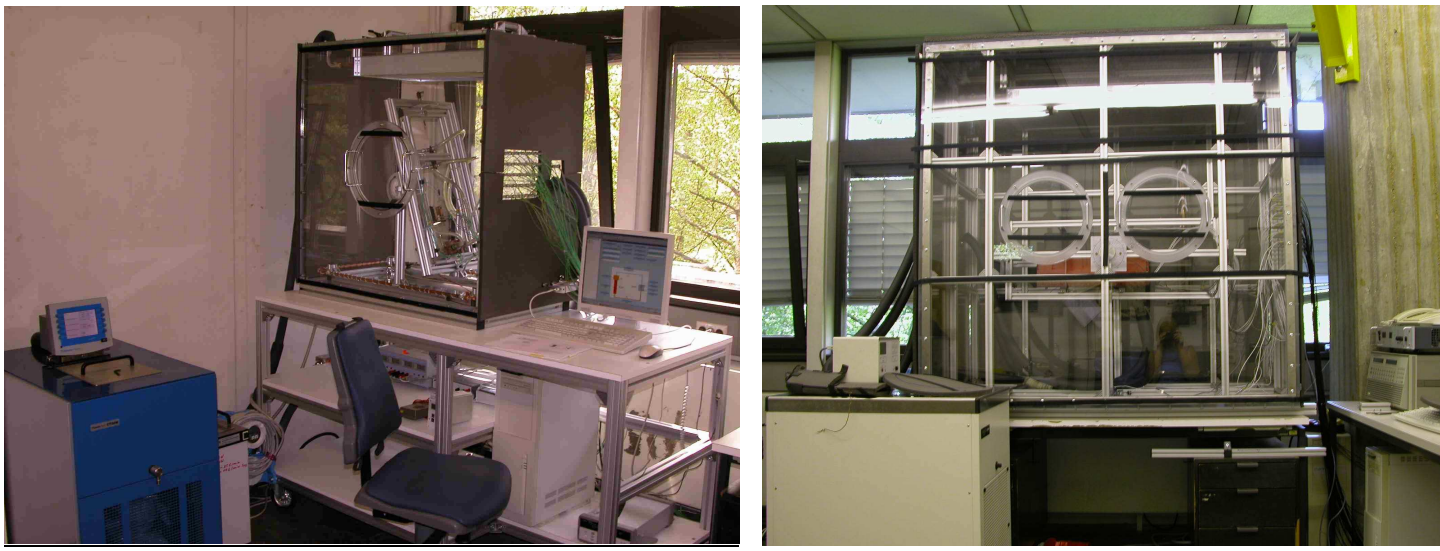

Figure 2: a) First test rig, b) Second test rig

The first test rig was build regarding the maximum given dimensions of the LHP. Experimental results of the first LHP required a second LHP with a larger heat sink than that of the first one. This second LHP did not fit into the first test rig. Therefore a second test rig was necessary. Both test rigs provide almost the same features.

The LHP is fixed on a movable construction that can be set to different angles in two orientations. Therefore it is possible to simulate all orientations which can occur during the use of LHP application.

The heat source is a copper block attached to the evaporator, employed with two heater cartridges. The condenser of both LHPs can either be cooled by forced liquid cooling or by free or forced convection. Temperatures are measured at different positions of the LHP using thermocouples at the first and using RTD (typ Pt100) at the second LHP. The number of temperature sensors is related to the size of the LHP.

The whole construction is embedded into a box made of PMMA (first test rig: 1000 mm x 1000 mm x 600 mm, second test rig:1500 mm x 1500 mm x 800 mm), where different ambient conditions can be

set. The box is isolated with a high efficient isolation material to avoid heat transfer between the box and the ambient as much as possible. Flanges are employed at the front side and one at the top of the box, so that the experimental parameters inside the box can be set easily to the requested experimental conditions.

Several feed-throughs are employed to connect the lines for the measurement sensors, heating and cooling devices.

The condenser section of the LHP can be cooled by free or forced convection. Another possibility is using coolant liquid circulating from a cryostat to the condenser. Measuring the cooling water inlet temperature $T_{CW,in}$ and outlet temperature $T_{CW,out}$ and the volume flow V of the cooling liquid and assuming an adiabatic heat transfer at the condenser facilitates the calculation of the amount of heat leaving the heat pipe at the condenser. Here the density and specific heat capacity are functions of the temperature of the cooling liquid flowing through the flow meter.

Most of the experimental work with LHP's are done under adiabatic conditions which is not the real case in general. Therefore the LHP's behaviour is also tested under different ambient conditions simulating the real conditions around the LHP in the cabin of an aircraft. The whole box can be heated up and cooled down.

MEASUREMENT SET UP

At the left side there is the box with the heat exchanger, the LHP, the copper block with the cartridge heaters (simulating the heat source), the condenser (simulating the heat sink) and the temperature sensors.

The blue lines illustrate the flow of coolant. The red lines represent the data flow from the temperature sensors. The green lines represent data flow in voltage or current form.

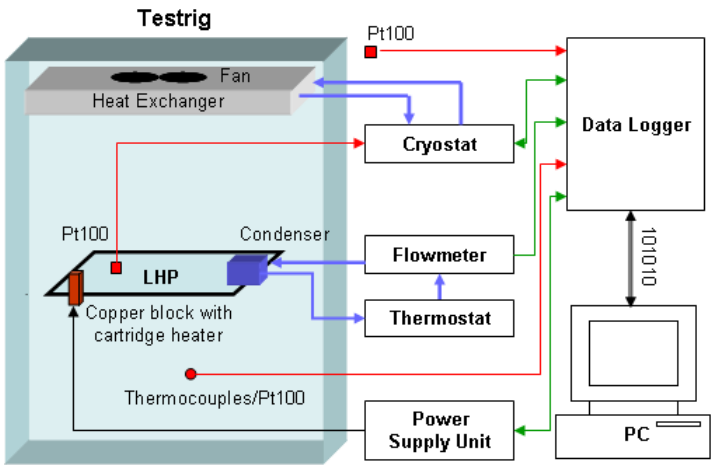

Figure 3: Overview of measurement setup

All the measurements, outputs and inputs are programmed under HP VEE which is an object oriented programming language that allows to create programs by connecting icons. The result in HP VEE resembles a data flow diagram.

PARAMETER VARIATION

The following table gives an overview which parameters have been varied and in which range.

Parameter	Variation / explanation
Type of cooling	Natural air convection: · an aluminium radiator is screwed to the aluminium plate · thermal conduction is enhanced by a copper paste between plate and radiator · no insulation along the loop heat pipe · air cooling (no significant air flow) Forced liquid cooling: · A condenser is attached to the condenser section with water as coolant · Insulation along the loop heat pipe except at compensation chamber heat sink
Coolant temperature	$T_{Coolant}$ = {20;55}°C
Box ambient temperature	$T_{Box,amb}$ = {20;55}°C
Orientation	Orientation in y-z direction γ · evaporator above condenser : positive angles · evaporator below condenser : negative angles · γ= {-90;-60;-30;0;+30;+60;+90}° Orientation in x-z direction δ · vapour line above liquid line: positive angle · vapour line under liquid line: negative angle · δ = {-90;-60;-30;0;+30;+60;+90}°
Power input	Electrical power input P_{el} P_{el} = {0;20;40;60;80;100}W

Table 2: Parameter variation

In order to clarify the orientation of the LHP the following figure is presented.

a) Front view / angle γ

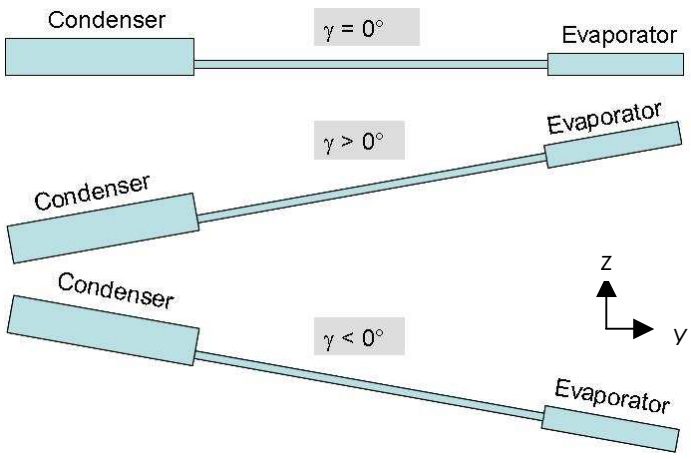

b) View from right side / angle δ

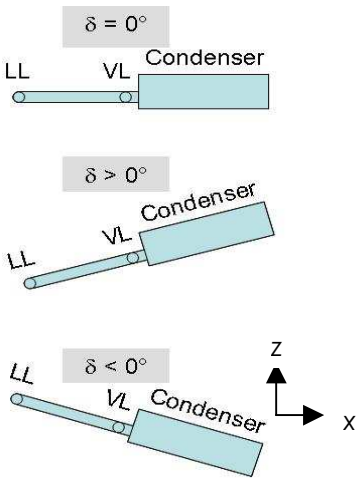

Figure 4: Orientation of LHP

POSITION OF TEMPERATURE SENSORS

Figure 10 shows the positions of the temperature sensors at the first LHP.

On the first LHP measurements have been realised with natural convection air cooling and with forced liquid cooling as the vapour and liquid lines have been wrapped by insulation material. The temperature sensors at position VL_5, HS_Fin_1 and HS_Fin_2 are not installed in the forced convection case. But there are two additional temperature sensors measuring the coolant temperature at the condenser section (CW_in, CW_out).Tests with different angles and with different power have been realised.

a) natural convection, air cooling

b) forced convection, liquid cooling, insulation

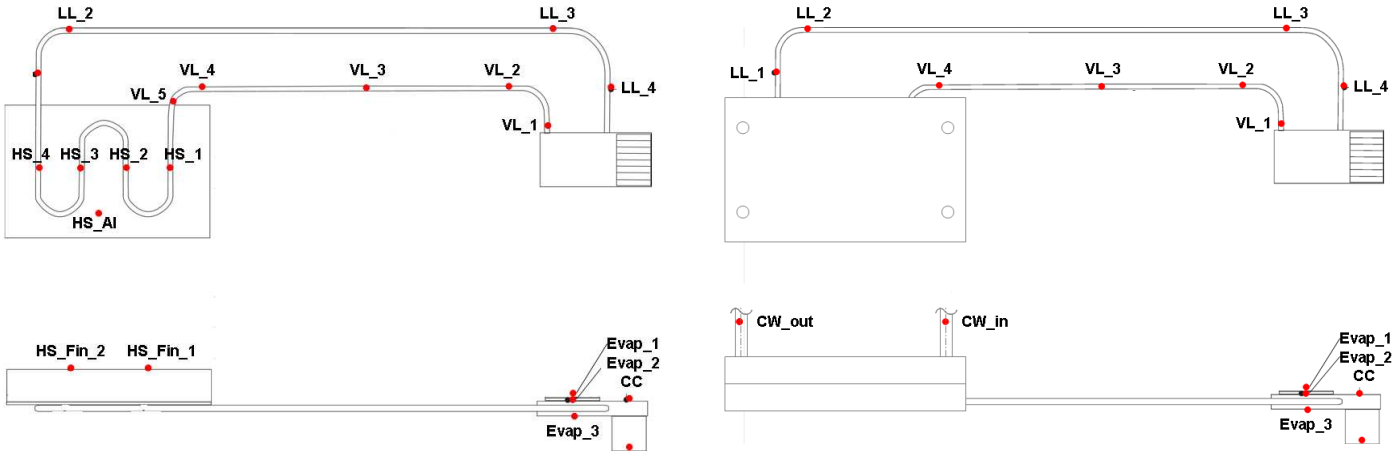

Figure 5: Positions of temperature sensors at the first LHP

On the second LHP only measurements with forced liquid cooling have been realized. The condenser attached to the condenser section of the second LHP is not shown in figure 11. There are two additional temperature sensors measuring the coolant temperature. The vapour as well as the liquid lines have been wrapped by insulation material. Also tests with different angles and with different power inputs have been realized.

Figure 11 shows the positions of the temperature sensors at the second LHP.

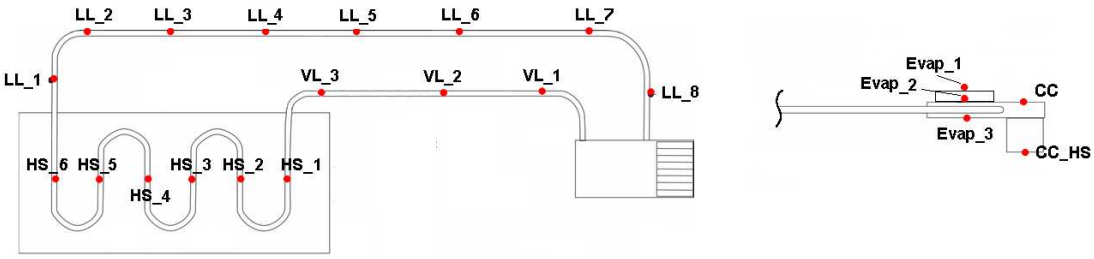

Figure 6: Positions of temperature sensors at the second LHP

RESULTS OF THE FIRST LHP

a) natural convection, air cooling

b) forced convection, liquid cooling, insulation

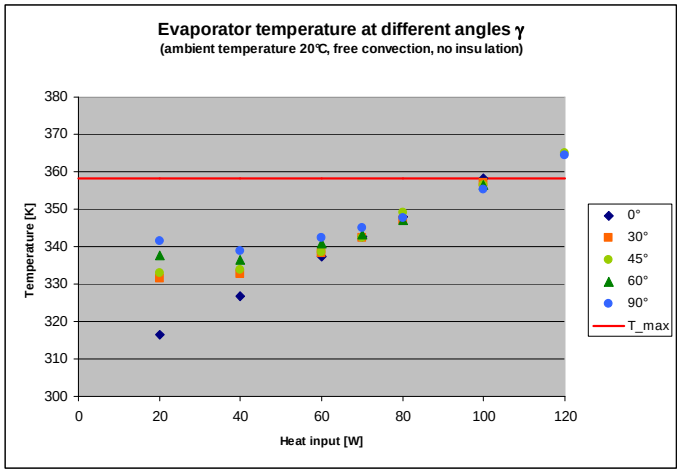

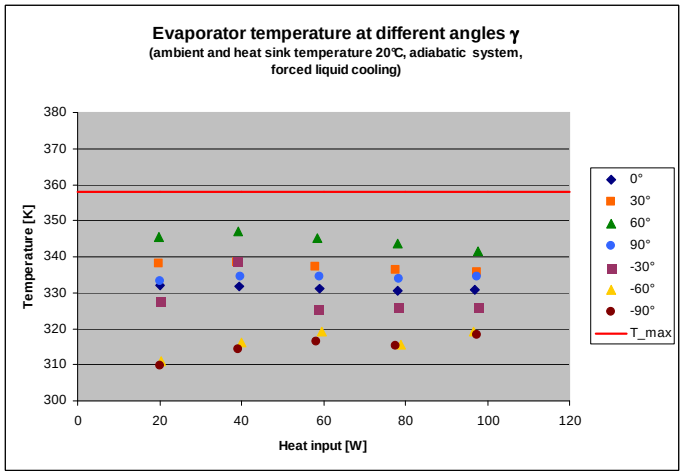

Figure 7: Evaporator temperatures at different angles γ for an ambient and heat sink temperature of 20 °C

As claimed in the requirements the LHP maximum evaporator temperature is 85 °C (358.15 K). For an ambient and heat sink temperature of 20 °C all measurements showed good results. The evaporator temperature at natural convection and an angle of 90 ° exceeds the maximum evaporator temperature but only at a heat input of 120 W which is out of the specified maximum heat input that is 100 W.

Furthermore, it can be seen on the left figure that a higher evaporator temperature for bigger angles results from the higher pressure loss in the liquid line as the position of the condenser is lower than that of the evaporator.

Similar observations can be made for forced convection liquid cooling. Here the evaporator temperatures for positive angles are higher than that for negative angles.

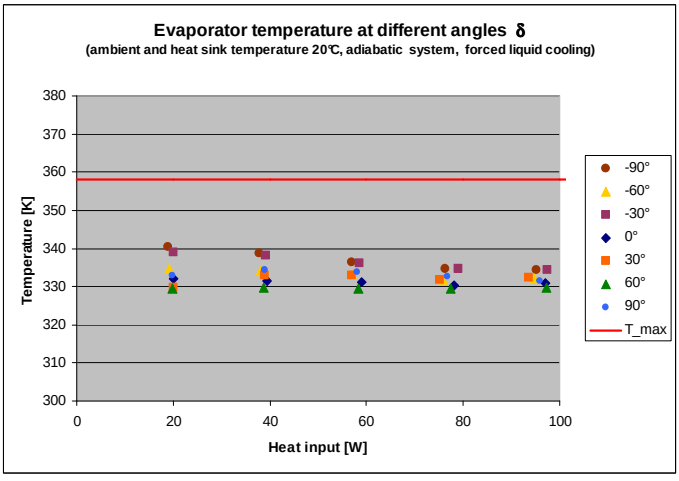

Figure 8: Evaporator temperatures at different angles δ for an ambient and heat sink temperature of 20 °C

The variation of the angle δ has almost no influence on the evaporator temperature. The highest temperature difference is about 10 K at low heat inputs.

a) natural convection, air cooling

b) forced convection, liquid cooling, insulation

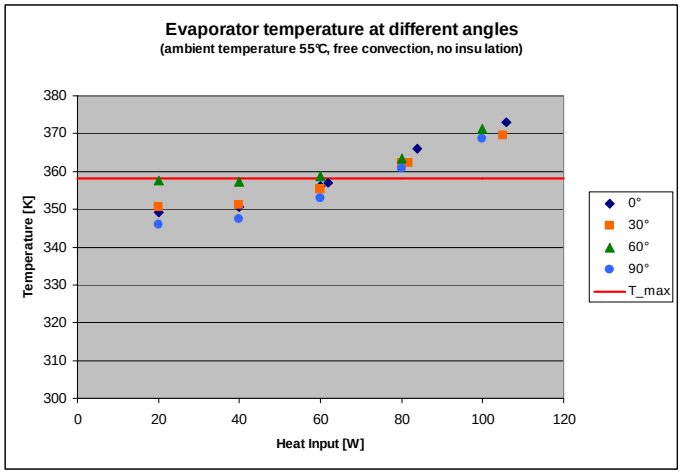

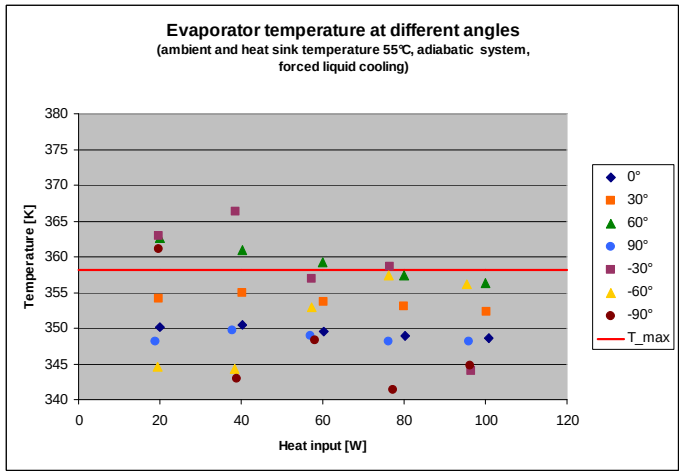

Figure 9: Evaporator temperatures of first LHP at different angles γ for an ambient and heat sink temperature of 55 °C

At an ambient and heat sink temperature of 55 °C the evaporator temperature exceeds the specified maximum evaporator temperature of is 85 °C (358.15 K).

Therefore a second LHP was build with an increased heat sink in order to provide more cooling power to the condenser section.

RESULTS OF THE SECOND LHP

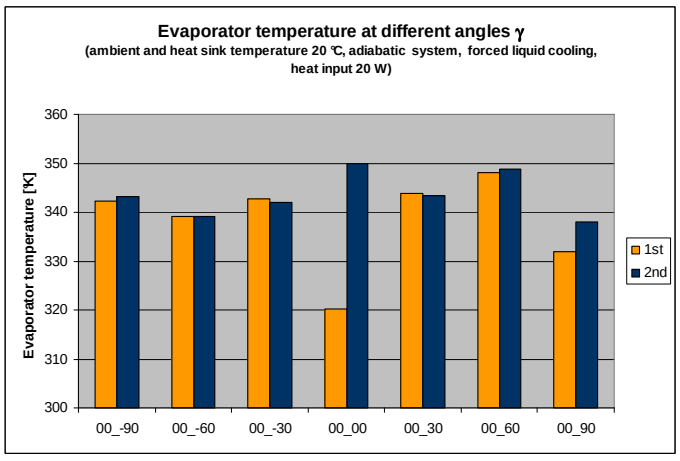

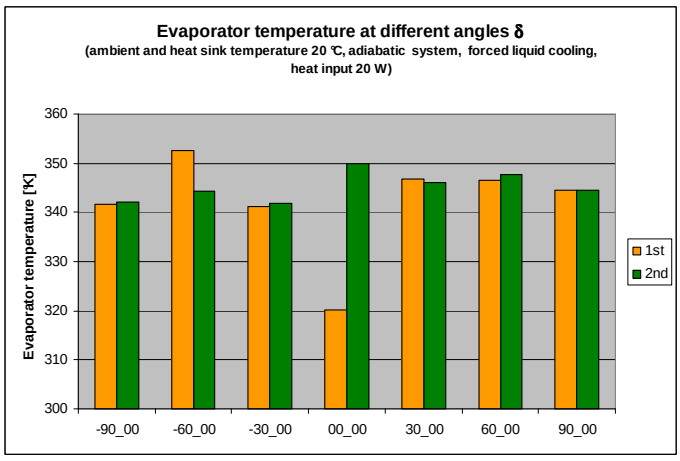

Figure 10: Evaporator temperatures of second LHP at different angles γ / δ for an ambient and heat sink temperature of 20 °C and a heat input of 20 W

In agreement with INSA, who do the simulation work only measurements with forced convection liquid cooling at the condenser section and isolated liquid and vapor lines have been realized. The maximum heat input for different angles γ and δ is 20 W. Higher heat inputs result in evaporator temperatures exceeding the specified maximum evaporator temperature of 85 °C.

Second measurements show similar results than the first one except at an angle of 0 ° where the difference between the first and second measurement of the evaporator temperature is about 29 K.

Consultations with ITP result in an agreement that the filling rate of the second LHP was not optimized for the forced convection but for the free convection case.

CONCLUSIONS

The first LHP works well at different angles γ for free convection air cooling at an ambient temperature of 20 °C, but exceeds its maximum evaporator temperature of 85 °C at an ambient temperature of 55 °C.

With forced liquid cooling, insulated lines and a sink temperature of 20 °C the evaporator temperatures are below the maximum evaporator temperature. But with a sink temperature of 55 °C at some angles the evaporator temperature exceeds the maximum evaporator temperature of 85 °C.

The variation of the angle δ has almost no influence on the evaporator temperature.

The second LHP does not work well for forced liquid cooling at a sink temperature of 20 °C. There have not been done any measurements at a sink temperature of 55 °C, because even at a sink temperature of 20 °C a heat input of only 20 W could be realized. At higher heat inputs the evaporator temperature exceeds the maximum evaporator temperature.

A second set of measurement under the same conditions show similar results than the first measured evaporator temperature, except for an angle of 0 ° where the temperature difference is 29 K.

1.2.3 WP 2300 : LHP DEVELOPMENT

1.2.3.1 Euro Heat Pipe developments

Euro Heat pipe has designed and developed in cooperation with INSA de Lyon and USTUTT a new LHP adapted to the specification defined in WP1000.

A trade-off of the potential cooling system designs has been done.

This analysis is based on comparative assessments of several LHP solutions regarding to performance (hydraulic, thermal, mechanical) and manufacturing aspects.

Safety aspects have also been considered for the selection of adequate working fluid (toxicity, flammability,…).

The selection of the body and wick material is based on compatibility analyses as well as performances regarding to parasitic flux aspects.

A comparative analysis has been done on the evaporator geometry with the selection of an evaporator with integrated reservoir to reach a compact design: No additional volume is so taken by an external reservoir.

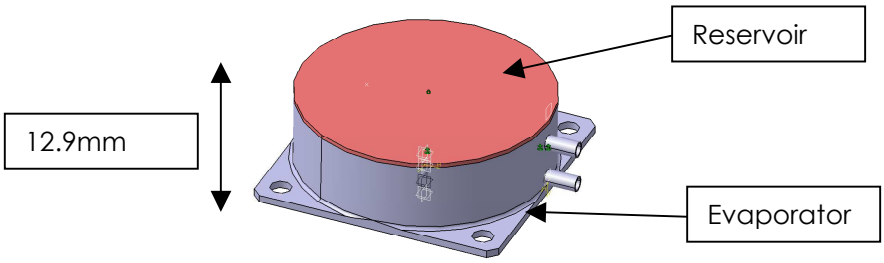

Figure 1-11: Geometry of evaporator and reservoir

The evaporator + reservoir cavity thickness has been limited to 12.9mm for integration reasons. This requirement allowsw mounting the evaporator + reservoir cavity either on lateral face of SEB (like in WE5000) or under the SEB so that it can be integrated in the shroud enveloppe volume.

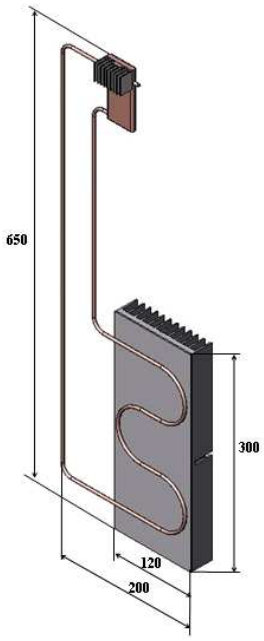

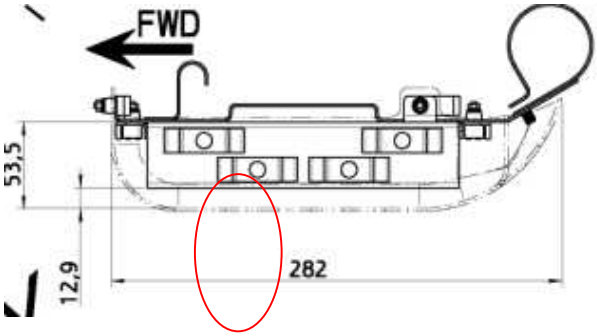

Figure 1-12 : SEB shroud available volume

The design analyses lead to select to possible options for the COSEE LHP:

Option 1:

Fluid: R245fa (HFC fluid) ***(*)***

Wick material: Nickel

Body material: Stainless steel

The fluid lines and condenser are in stainless steel for this configuration.

(*) Regarding the guidelines of the Montreal protocol, the production of HCFC shall be stopped in 2010 because they largely contribute to ozone layer depletion in addition to global warming.

As replacement refrigerant fluids, HFC, which don't contribute to ozone depletion, are recommended and today, no end of production and use perspectives for these fluids are foreseen.

Based on these considerations, R245fa is an adequate selection.

Option 2:

Fluid: Ultra pure water

Wick material: Titanium

Body material: Titanium

The fluid lines and condenser are in copper (and not in Titanium) for this configuration for cost reasons.

1.2.3.2 Institut (ITP) developments

ITP took part in the determination of the technical specifications for LHP. The work was performed in touch with USTUTT and INSA. In accordance with the agreed specification, first experimental mock-up

of copper-water LHP with flat evaporator was developed, made and preliminary tested and had permitted to validate the INSA model.

During preliminary tests under the ambient temperature and free air convection, the LHP demonstrated the following technical characteristics:

- ✓ Maximal 100W heat load under the horizontal orientation and under +45° and + 90° slope (the evaporator is above the condenser)
- ✓ Maximal temperature of the heat source was 81.2°C, its change under different orientations does not exceed 4 °C
- ✓ Minimum starting heat load of 20 W
- ✓ Maximal temperature gradient of 8.5 °C under the 100W heat load
- ✓ Maximal heat sink temperature of 72.7 °C

Figure 13: Scheme and overall LHP dimensions of the first prototype.

ITP has developed and tested a new variant of the copper-water LHP with a flat evaporator (LHP2) and an increased condenser.

It was demonstrated that the increase of the condenser length and the heat sink dimensions allows decreasing the temperature of the latter from X °C to Y °C. At the same time the heat source temperature does not exceed the maximal value of 85 °C at the heat sink cooling by the free air convection. Besides two copper-water LHPs were made (LHP-F1 and LHP-F2) to conduct freezing tests.

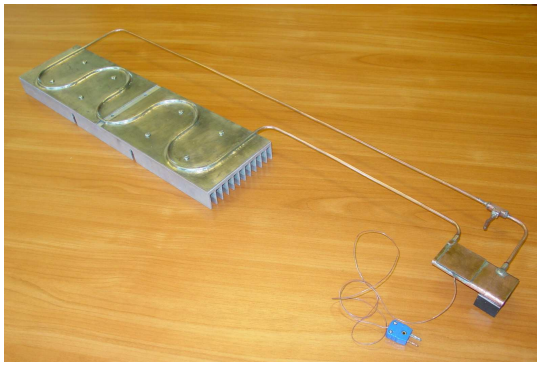

LHP2 general view

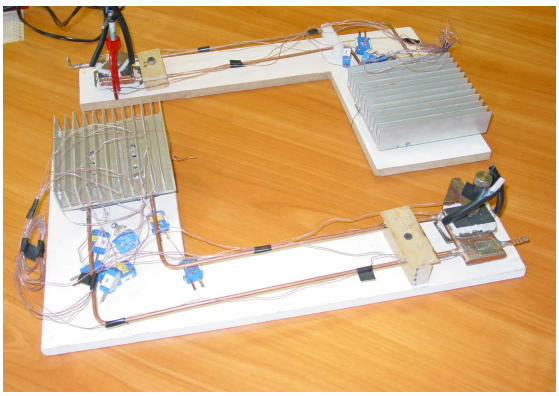

Copper-water LHP-F1 and LHPF-2

One of them (LHP-F2) was supplied with a special polymeric insert which was supposed to increase the LHPs resistance to the internal pressure that appear when water is freezing. It was showed that LHP-1F (without insert) stood 65 freezing cycles while LHP-2F stood 85 cycles.

As far as none of the copper-water LHPs stood the desired 200 freezing cycles, two LHPs with Freon R141b were made as an alternative. Both LHPs were made of the stainless steel and had cylindrical evaporators 10mm in diameter supplied with the nickel wicks.

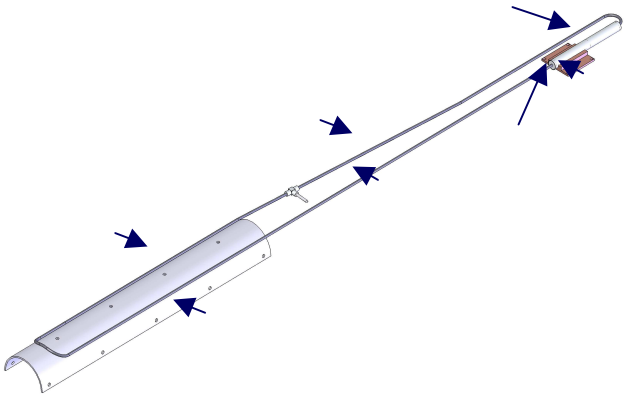

Freon R141b was chosen as a working fluid because its usage is allowed in Europe up to 2020 and also as it is fire-safe, explosion-proof and nontoxic. Besides it was intended that later it can be replaced by another working fluid e.g. R245fa which has approximately the same thermophysical properties but is more expensive.

Figure 14: General view of the SS-Ni-Freon 141b LHP

Tests of the LHPs with Freon R141b showed that the thermal characteristics of the devices correspond to the specification at the heat load under 50W, but the heat sink temperature remained higher than the specified one at the free air convection. It was demonstrated as well that even a light forced air convection (0.7 m/sec) near heat sink allows considerable decreasing of the heat source and heat sink temperatures.

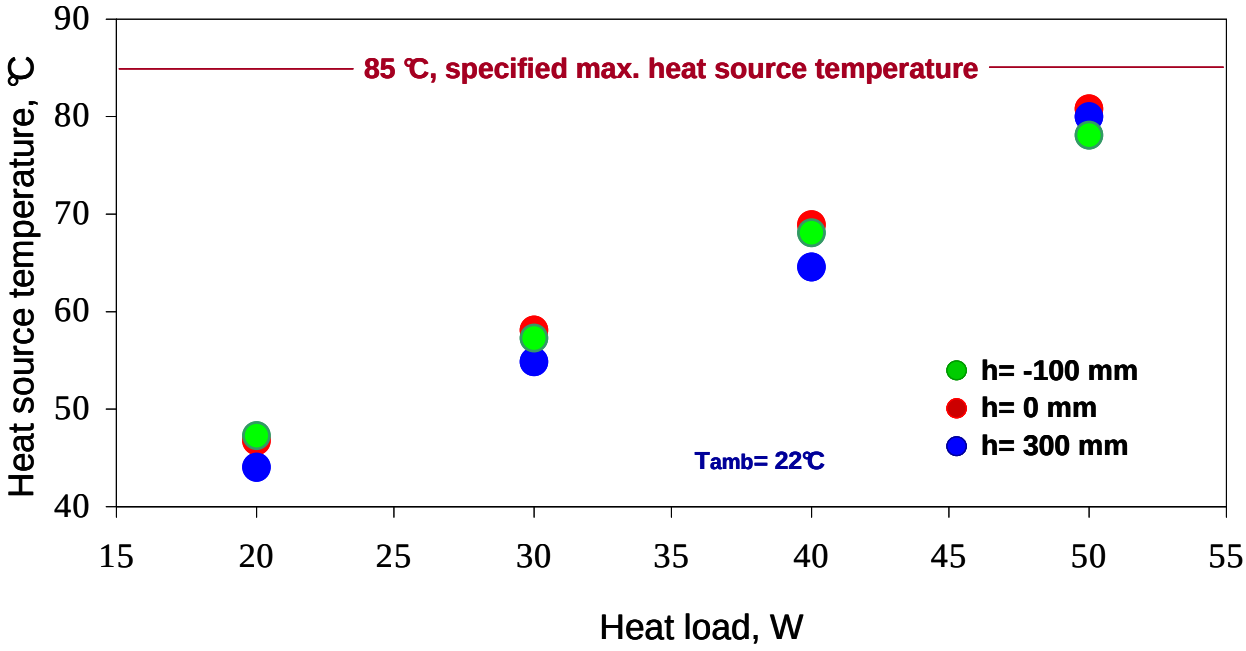

Figure 15: Heat source temperature vs haet load with different hights

Thermal test results of the LHP with Freon R141b as a working fluid.

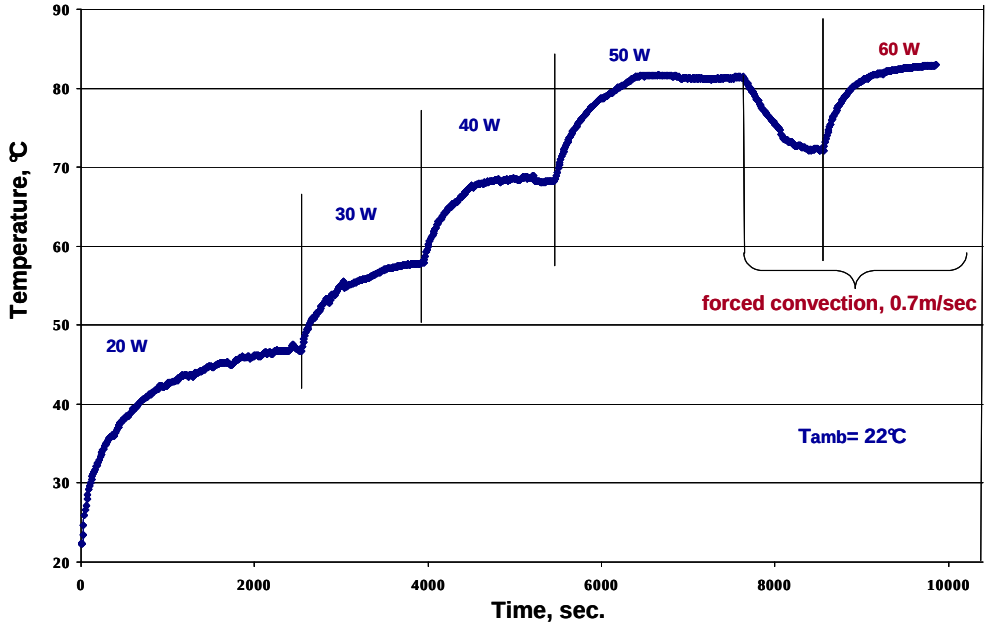

Figure 16 : Heat source temperature vs haet load

When the cooled object (SEB) is situated below the heat sink (seat beam) and in the operational process their mutual position will not change radically, the opportunity appears to use the Loop Thermosyphon (LTS), which is a simpler and cheaper heat transfer device in comparison with the LHP.

In order to demonstrate the possibility to use this device as an alternative for the LHP, a Loop Thermosyphon was developed and tested in ITP with Freon R141b as a working fluid. By its physical configuration and sizes the LTS is very close to the LHP, but its evaporator doesn't contain the capillary structure. Scheme and general view of the LTS are presented in Fig. 5 and Fig. 6.

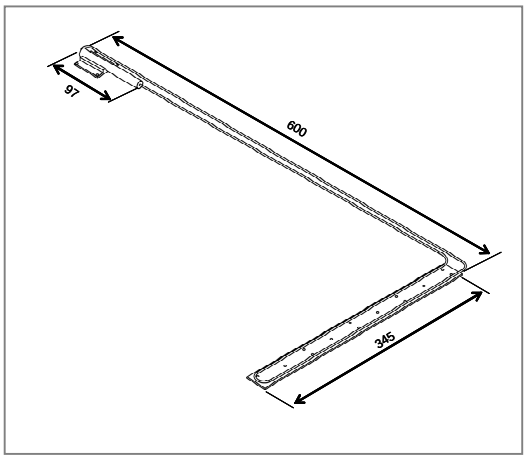

Figure 17: Scheme of the LTS

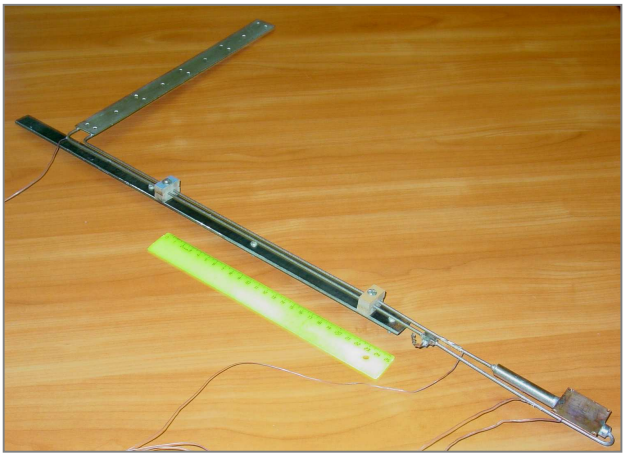

Figure 18: General view of the LTS

The LTS test results in form of heat source temperature dependences on the heat load are presented in Fig 7. The results were obtained at different angles of slope relative to the vertical axis.

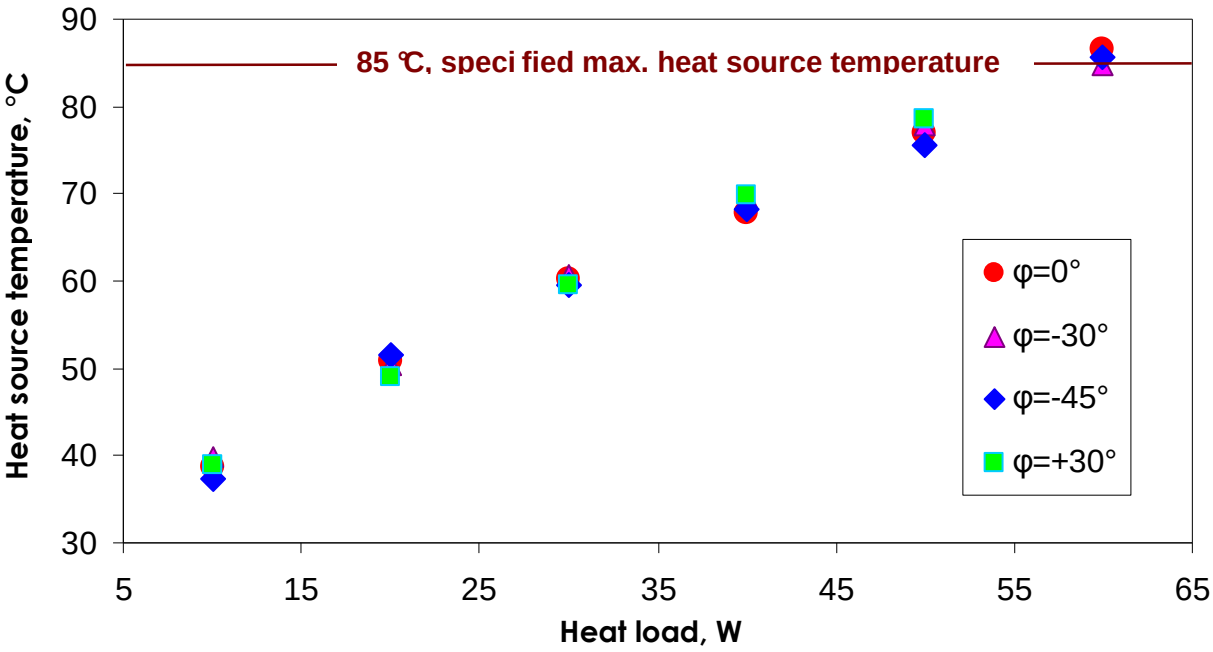

Figure 19: Heat source temperature vs heat load for different angles of slope

Conclusions:

- The max. specified heat source temperature of 85 °C was not reached in all test conditions in the heat load range of 20-50W.
- The heat sink max. average temperature of 55.5 °C was demonstrated at the heat load of 50W in the horizontal position (h=0 mm). At the same time the heat sink max. temperature reached the magnitude of 65 °C.
- The heat load of 40W can be considered as a nominal one, because the evaporator thermal resistance reached at this load its minimum at the level of 0.12-0.14 °C/W.
- The main limitation in the total thermal resistance of the system is the thermal resistance on the cold side between vapor and ambient which is in the range of 0.92-0.97 °C/W and at the same time the thermal resistance on the hot side between heat source and vapor is 0.13-0.23 °C/W
- It is shown that even a light forced air convection (0.7 m/sec) near heat sink allows considerable decreasing of the heat source temperature.
- The highest level of temperatures exists at the horizontal position of the heat sink. Its slope improves the natural convection and decreases temperatures.

The copper-water LHP was transferred for further tests to IKE and two LHPs with Freon R141b were transferred to Thales Avionics for integration on the seat.

- ✓ The principal possibility of the LHPs making in conformity with the specification was demonstrated
- ✓ It is necessary to proceed efforts aimed on the further device optimization and search of the methods that will allow solving the problem of the water freezing in the LHPs.

1.3 WP 3000 : SYSTEM INTEGRATION DESIGNS

WP 3000 objective is to design and optimize the interfaces of the equipment and connecting

structure (seat and aircraft) in order to minimize the thermal resistance and take full benefit of the new cooling system.

The system mock-up design shall be representative of existing and future technologies implemented by the end-users.

1.3.1 WP 3100 : EQUIPMENTS INTEGRATION

For interchangeability reasons most of the boxes follow the ARINC (Aeronautical Radio Inc) regulation that defines the external shapes sizes and connectors. The ARINC 600 defines a range of sizes, and taking the example of a 2 MCU (Modular Concept Unit) nearly equivalent to the existing SEB (L = 318 mm, l = 57,2 mm, h = 194 mm) will permit to illustrate and compare these different techniques.

A standard SEB is shown just under :

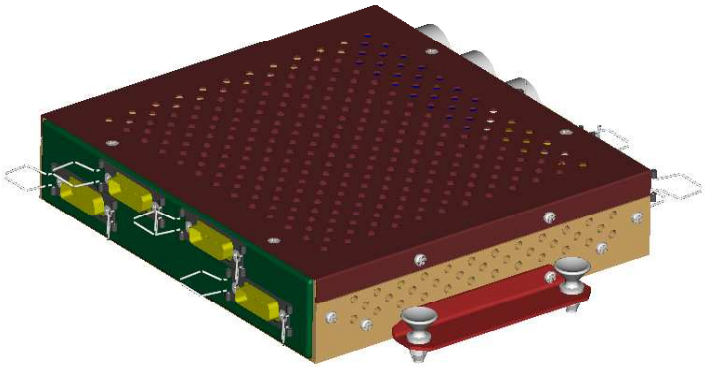

The SEB is made of two electronics cards with one hottest zone. The goal is to take off the heat from this zone by a loop heat pipe and to bring it to an evaporation zone located in the seat.

Two pcb have been designed. Each pcb could be powered up to 50W.

The pcb has two PQFP 208 each of them with two PMOS4 embedded. All the card is filled by 32 TO220 (330 Ω) grouped in 4 zones of 8 TO220.

The resistances are mounted in parallel in each zone and each zone can be connected between them to allow 32 resitances of 330 Ω in parallel.

With thess four possibilities we can obtain :

- One cell: equivallent resistance : ≈ 41,2 Ω
- Two cells: equivallent resistance : ≈ 20,6 Ω
- Three cells: equivallent resistance : ≈ 13,8 Ω
- Four cells : equivallent resistance : ≈ 10,3 Ω

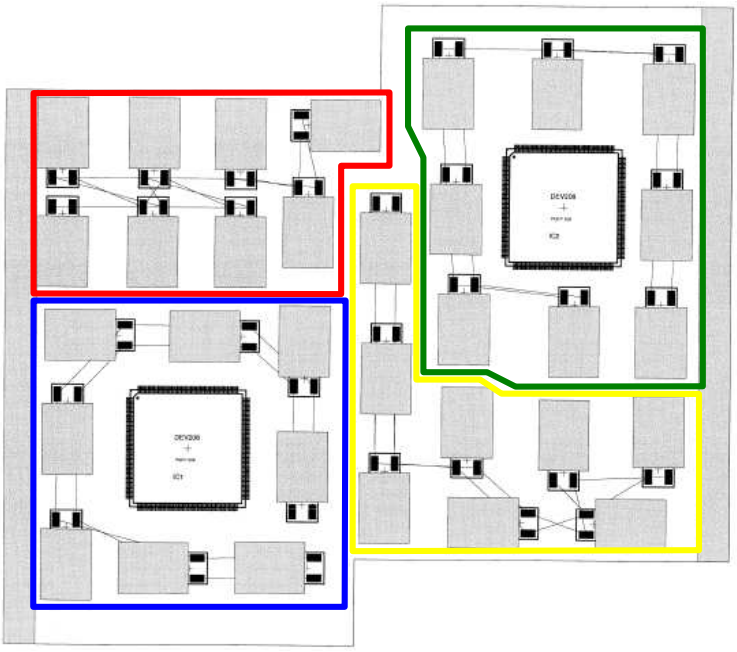

With a four power supply of 20W: 80W spreaded can easily apply on the two pcb on with another power supply of 20W 5W on each PQFP of the two cards could be applied.

Considering a new strategy for flowing out the calories mainly by conduction implies a complete reorganization of the internal equipment packaging. In conduction closed boxes, all the dissipate elements have to be linked to the thermal drain and this drain is then bridged to the heat sink

structure.

Based on typical existing SEB and ADB designs, thermal simulations will be performed to measure the maximum (ΔT) delta of temperature between ambient and box case obtained.

Thermal simulations

This simulation tools based on existing software: Flowtherm from Flomerics and PCB thermal from pacific numerix will be used to design improved conductive packaging options.

Different route have been followed to optimize the equipment internal structure. The problem to be solved is to channel the heat to one point or limited area where the heat pipe will be connected.

Among the options foreseen and simulated we have:

- A mechanical structure, a plate type, reproducing the exact counter part of the components so that this plate once in place will collect the heat of each dissipation component via some interface materials to cope with the height discrepancies and the manufacturing gaps. The LHP will be connected to one side of this plate.
- Thick interface "matelas" that will pick the heat on top of dissipative component and bring the heat to the cover. The LHP will be linked in this case on the cover itself.
- Another internal micro loop heat pipe or MHP having its evaporator connected on the dissipative components and its condenser linked to the cover. The external LHP will connect the evaporator to the condenser of the first LHP or HP via a thermal plug.

The optimisation and selection process based on simulations is on going to define the best option.

Maintainability and cost also be considered for the selection. Thermal simulations of the box have been realised with Flotherm V7.2. Two electronic cards are mounted in the SEB and the dissipative components of the cards are all figured.

The following simulations have been made considering the location of the loop heat pipe, the use of TIM (Thermal Interface Material), small internal heat pipe with different optioons: gluing, brazing, pinching.

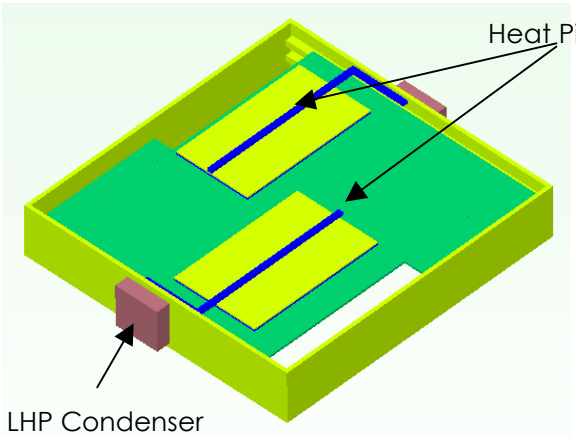

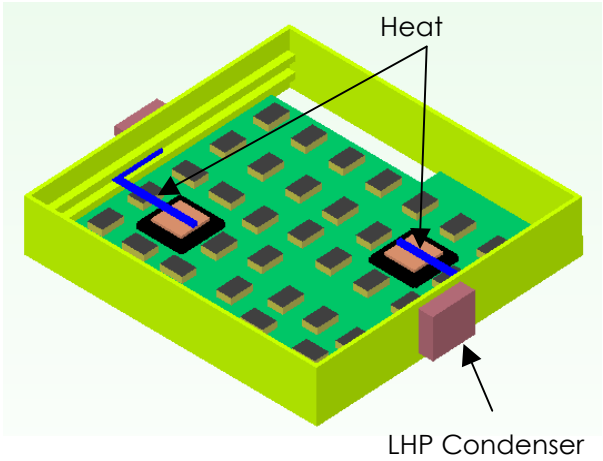

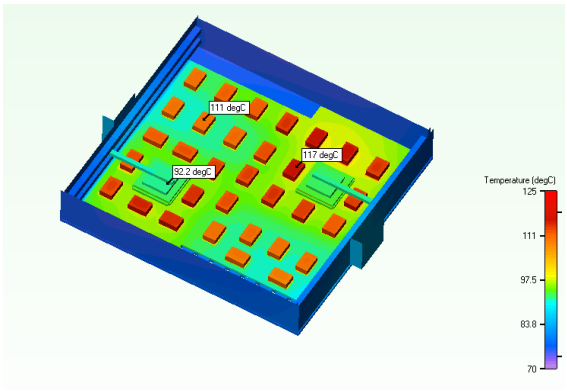

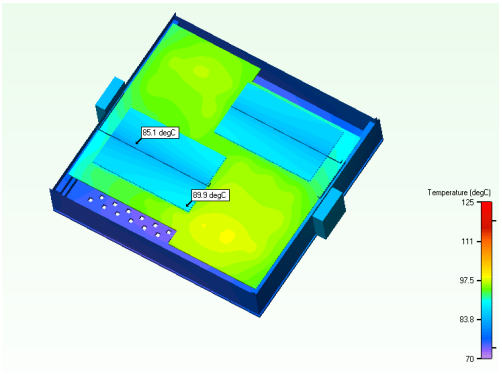

The conclusions of this preliminary simulations are:

- In order to be efficient, the Loop Heat Pipe must be associated with one or more internal standard heat pipe for the cooling of the SEB.
- The LHP evaporator can be reported on the SEB cover : this solution is very efficient for the cooling of discrete components but cannot be applied if there is more than 2 cards in the SEB or if there are too many components to cool.
- The best solution is to report the LHP evaporator on the side of the SEB near the slides. This solution allows to use the thermal conductivity of the PCB for the cooling of all the components located on the card. Local solutions with heat pipes link to the slide side permit to have an efficient cooling even for large dissipating components.

1.3.2 WP 3200-3300-3400 : SEATS INTEGRATION*

Existing seats are not necessarily optimized to receive electronic equipment that means that most of the time the boxes are installed where room is left.

Considering the interface requirement defined in WP 1000. The seat manufacturers will study novel interfaces by modification of existing base seat frames.

Simulation tools will be used to quantify the possible future modifications.

Different cases have to be considered:

- adaptation of the system on existing platforms
- development of new products

In both cases ΔT between seat and SEB will be evaluated and also ΔT between seat and ambient temperature.

Avio and Recaro have presented their seat integration with different possibilities. In case of over heating it will be possible to mount a plastic shroud on the evaporator.

INTEGRATION IN RECARO SEAT:

Integration of the evaporator on Recaro seat:

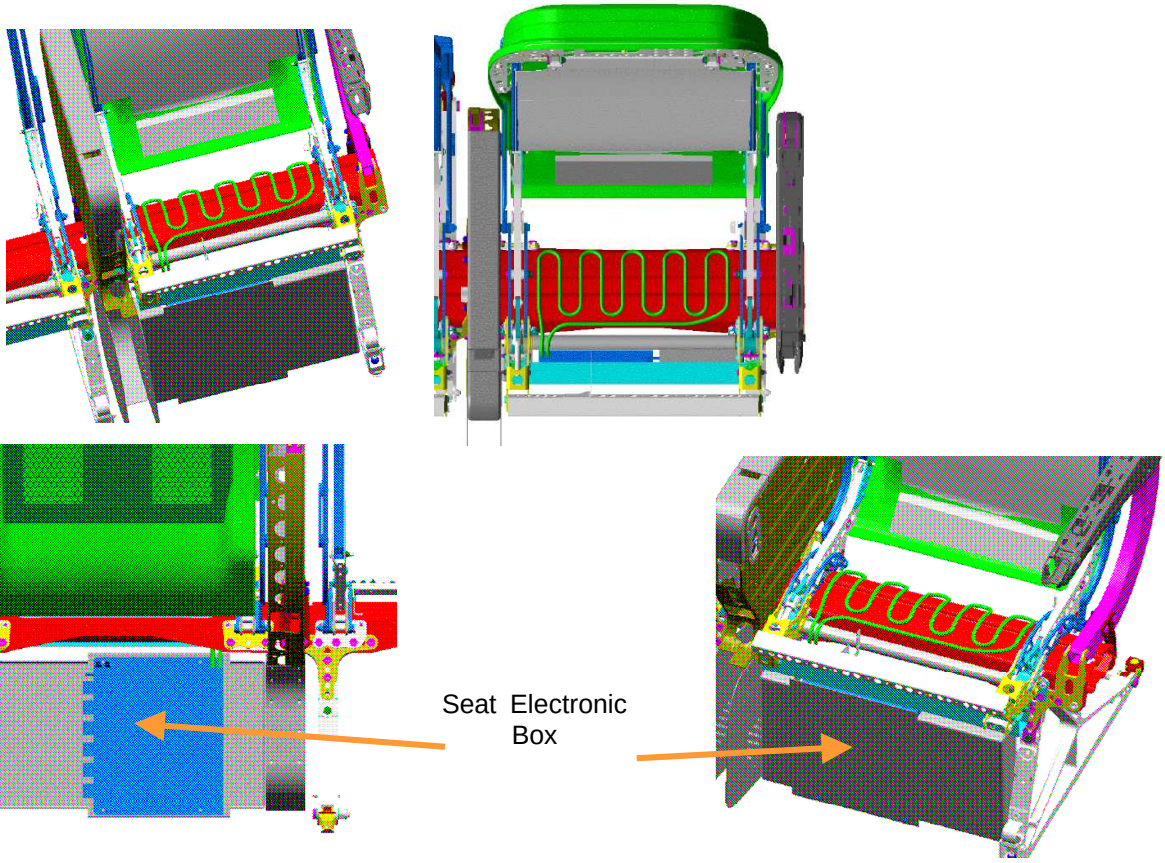

The seat electronic box is positioned in vertical position:

INTEGRATION ON AVIO SEAT

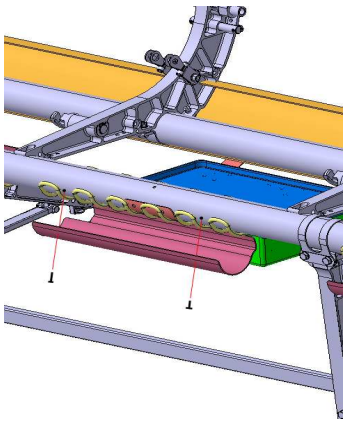

Front beam has been modified to allow the heat pipe installation: it will be fixed between the beam and the protective plate. This last component must be installed on the beam through screws.

Hence the front beam presents additional holes and screwed insert required to fix the fixation screws of the protective plate

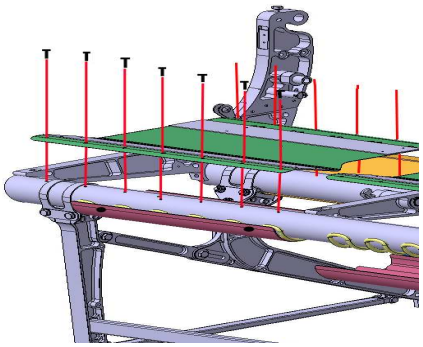

Seat pan has been modified to allow the easy removeability ot it. This to guarantee a quick and easy access to LHP system in case of necessity.

The standard seat pan is fixed on the rear and front beam by rivets.

The adaptation consists of the replacement of rivets by screws (with consequently different holes on the front and rear beams where those rivets were installed: the holes must be modified to host the screwed inserts for the seat pan fixation screw).

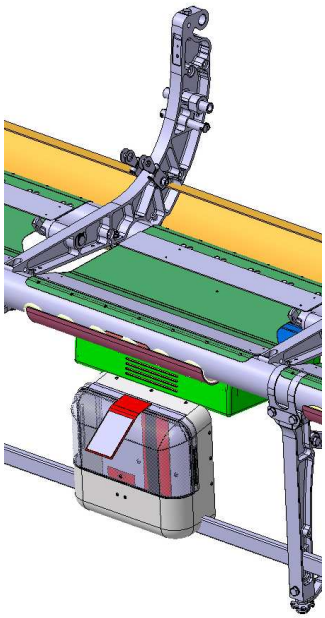

In standard E/C seats (like the Phoenix model) the life vest container is a pouch made of fabric and fixed under the seat pan by tie raps (plastic clamps).

Since the presence of the BOX under the seat pan, this standard pouch can not be used any more.

To stow the life vest a rigid box (made of metallic and plastic parts) has been designed. This box is fixed directly under the electronic box support plate in vertical position.

PAIG INTEGRATION

Without any information from PAIG no integration of the evaporator has been investigated on PAIG seat.

1.4 WP 4000 : SYSTEM MOCKUP DEVELOPMENT

1.4.1 WP 4100 : LHP MANUFACTURING

1.4.1.1 Euro Heat Pipe Manufactured LHP's and testing

1.4.1.1.1 First version LHP's : BB LHP's

Two types of prototypes have been realized and tested. The manufacturing of these 1st versions LHP's allows tuning some manufacturing processes mainly relative to the evaporator primary parts and sub-assy.

Prototype 1:

Fluid: R245fa

Wick material: Nickel

Body material: Stainless steel

The fluid lines and condenser are in stainless steel for this configuration.

Figure 1-20 : Evaporator and reservoir design for 1st version LHP in SS-R245fa

Prototype 2:

Fluid: Ultra pure water

Wick material: Titanium

Body material: Titanium

The fluid lines and condenser are in copper (and not in Titanium) for this configuration for cost reasons.

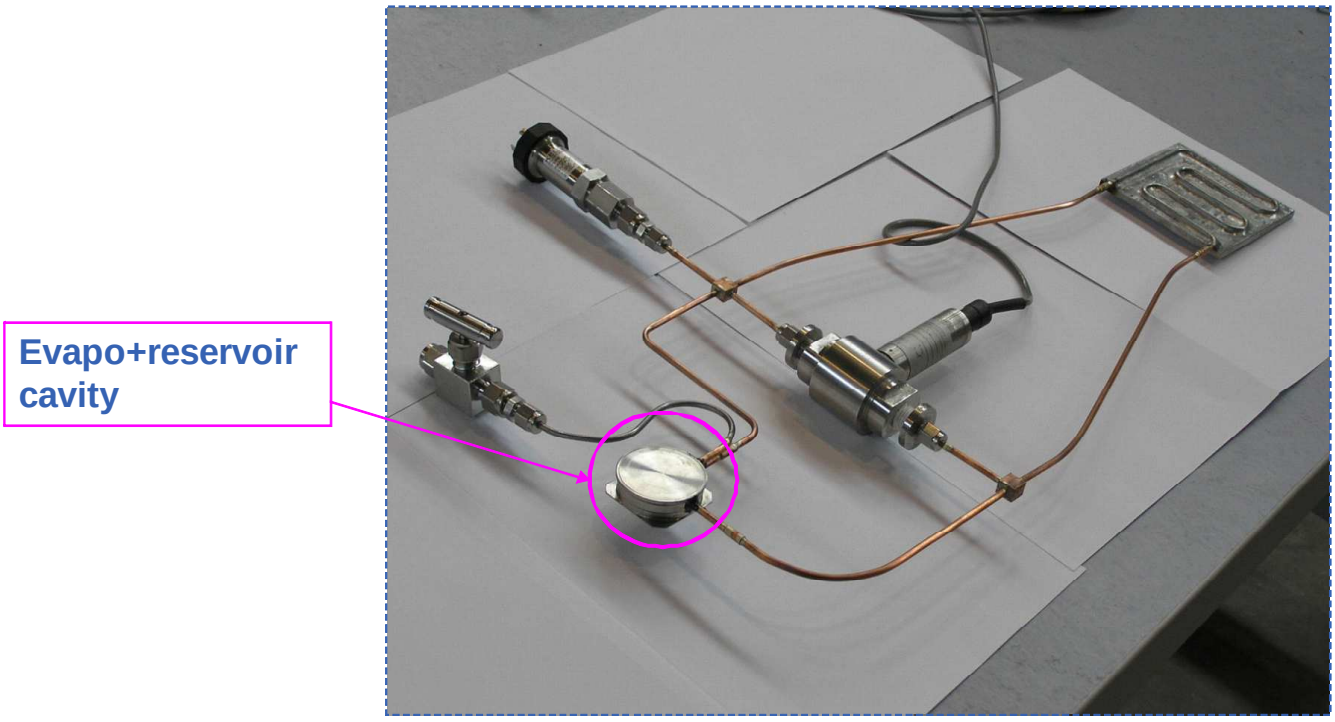

Figure 1-21 : LHP design for LHP in Ti/Cu/ultra pure water

These prototypes have been tested to characterize the BB LHP's functioning and so validate the design and manufacturing technology.

BB LHP's Test Set-up

- **Evaporator in horizontal position:**

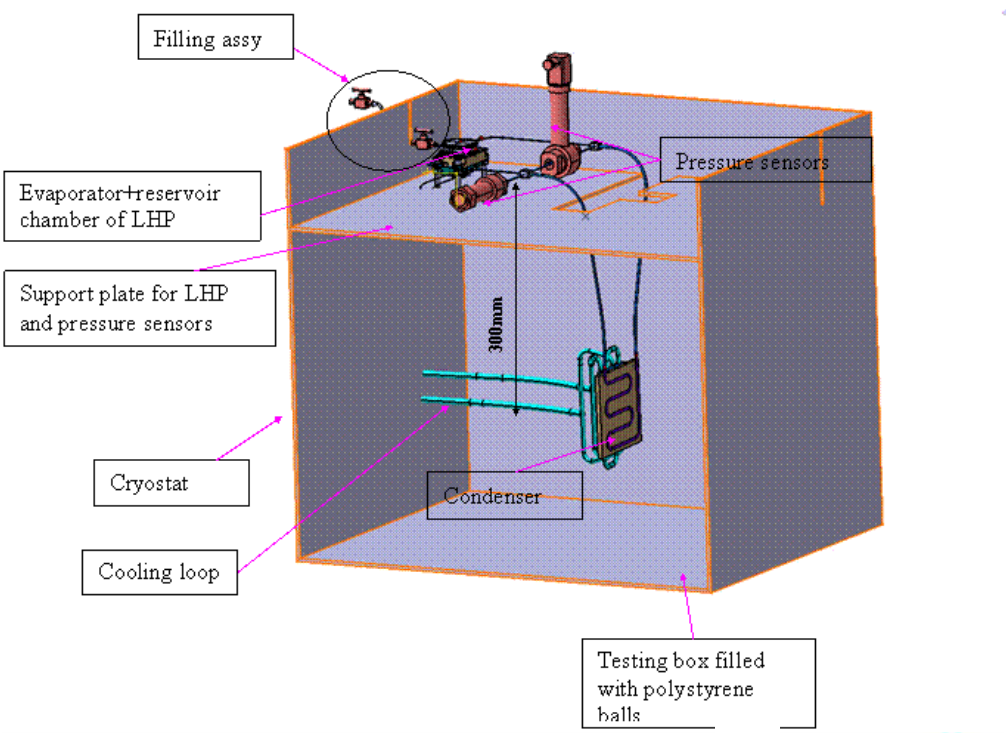

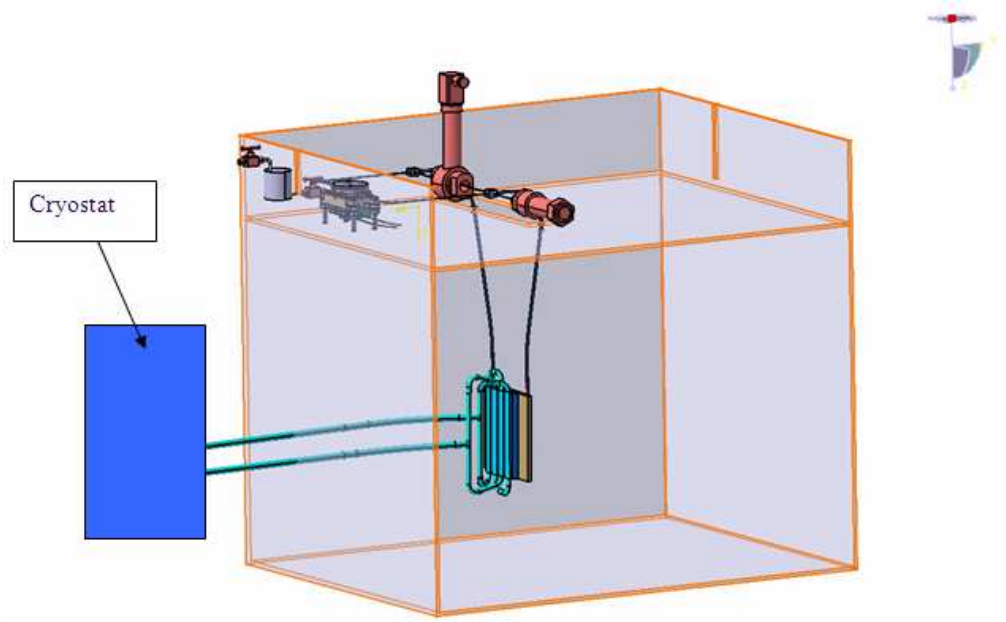

Figure 1-22: Testing of LHP with configuration of evaporator in horizontal position

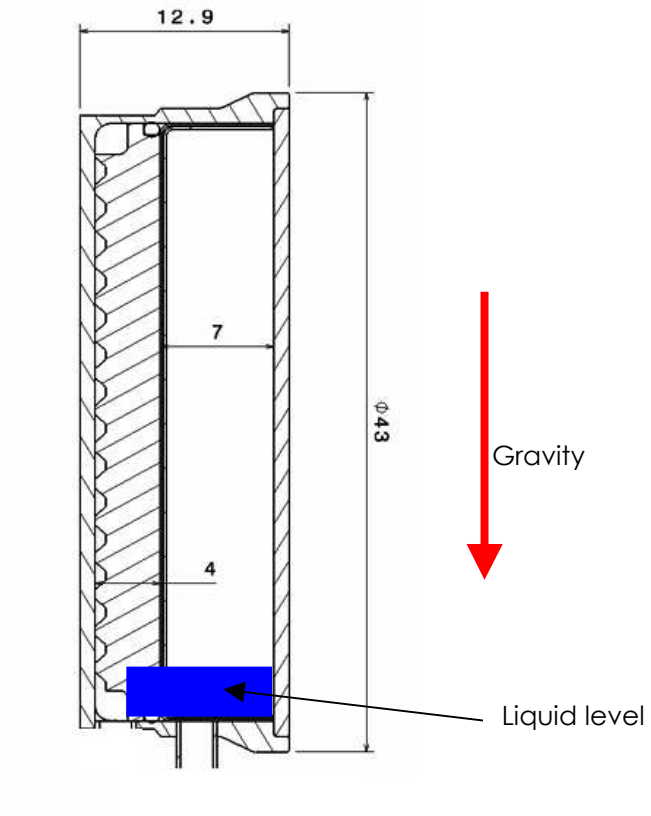

- Evaporator in vertical position:

Figure 1-23: Testing of LHP with configuration of evaporator in vertical position

Based on these tests results, the solution with R245fa was kept as nominal configuration for COSEE mini-LHP's.

The solution with water needs still some improvements and is considered as back-up.

1.4.1.2 Second version LHP's : LHP's mounted on aircraft seat

The objective of the 2nd version LHP is to modify the SS-R245fa LHP condenser design so that it can be mounted on the seat interfaces.

The condenser new design is based on the geometry of the seat I/F. The seat model that has been selected for mounting the EHP LHP's is the RECARO one.

Two SS-R245fa LHP's have been manufactured; one LHP presents the condenser plate on the right side and the other presents the condenser plate on the left side.

The adaptation of the LHP's on the seat can be done thanks to the possible manual routing of the fluid lines (ductile due to material in annealed state and low diameters).

Each LHP evaporator saddle is mounted on a SEB lateral wall so that the complete dissipation of the SEB components can reach 100W (2*50W/LHP).

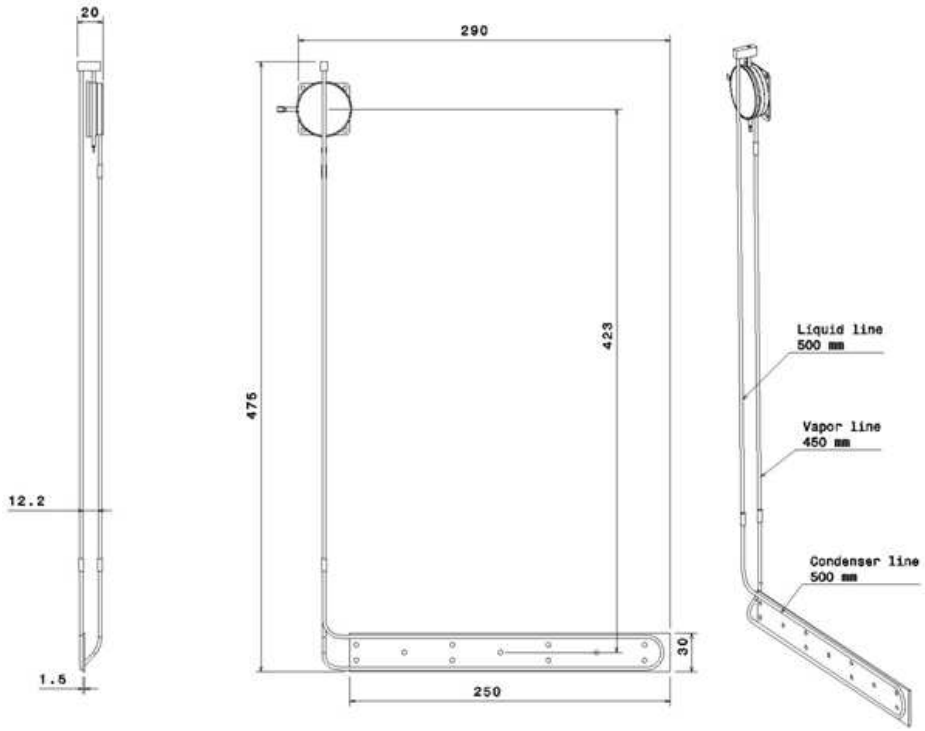

Figure 1-24: Description of SS-245fa mini-LHP with condenser on the right side

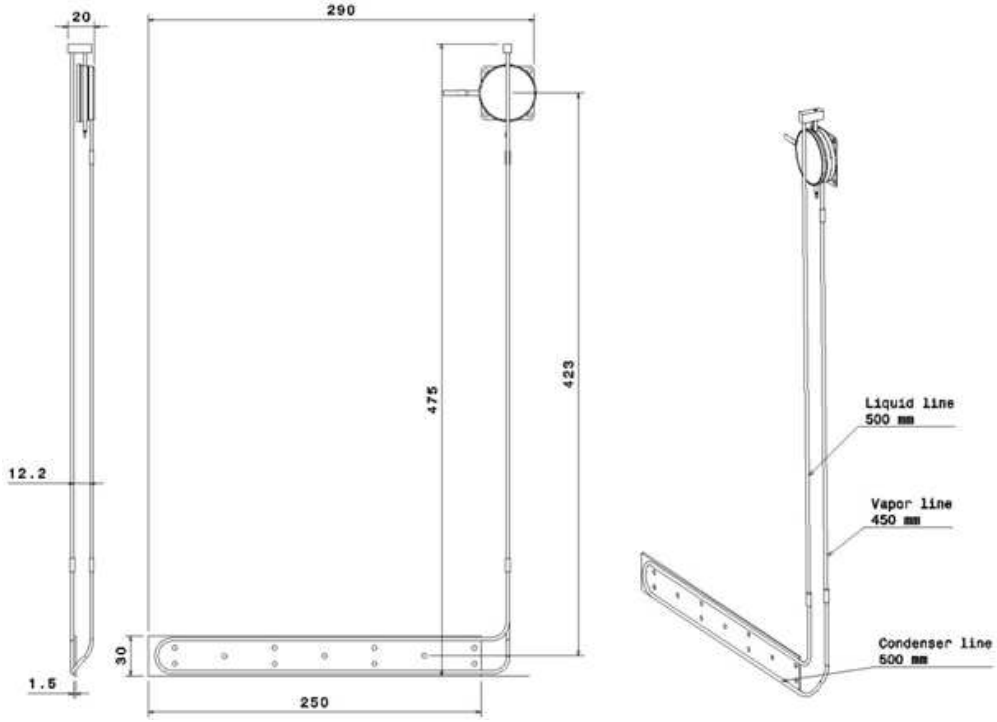

Figure 1-25: Description of SS-245fa mini-LHP with condenser on the left side

Pictures of SS-R245fa mini-LHP's before delivery

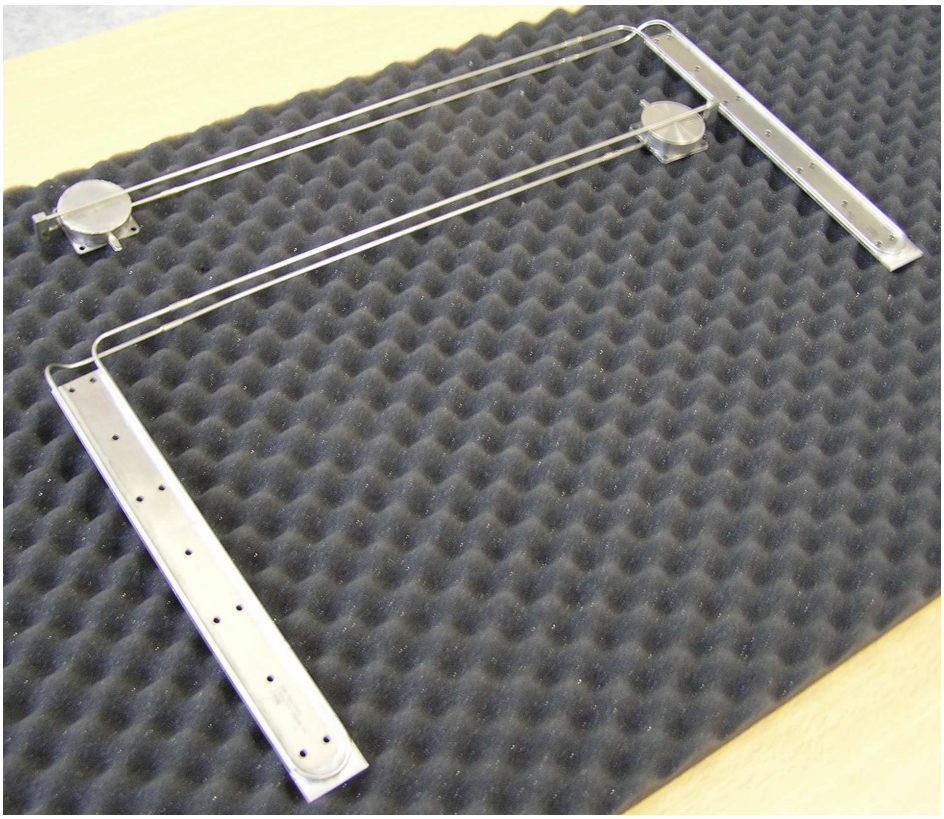

Figure 1-26: View of both mini-LHP's in stainless steel and filled with R245fa

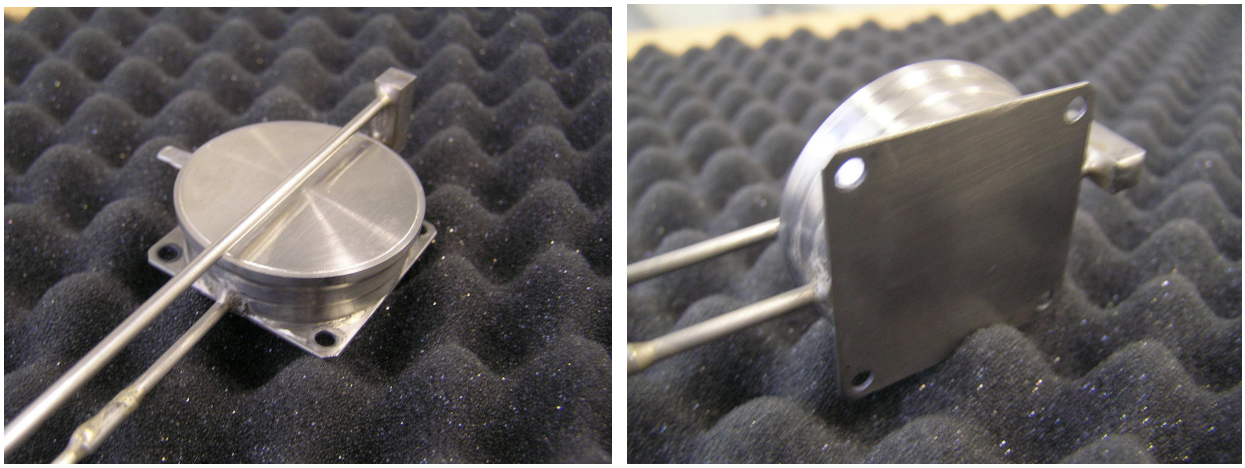

Figure 1-27: Evaporator views of mini-LHP in stainless steel and filled with R245fa

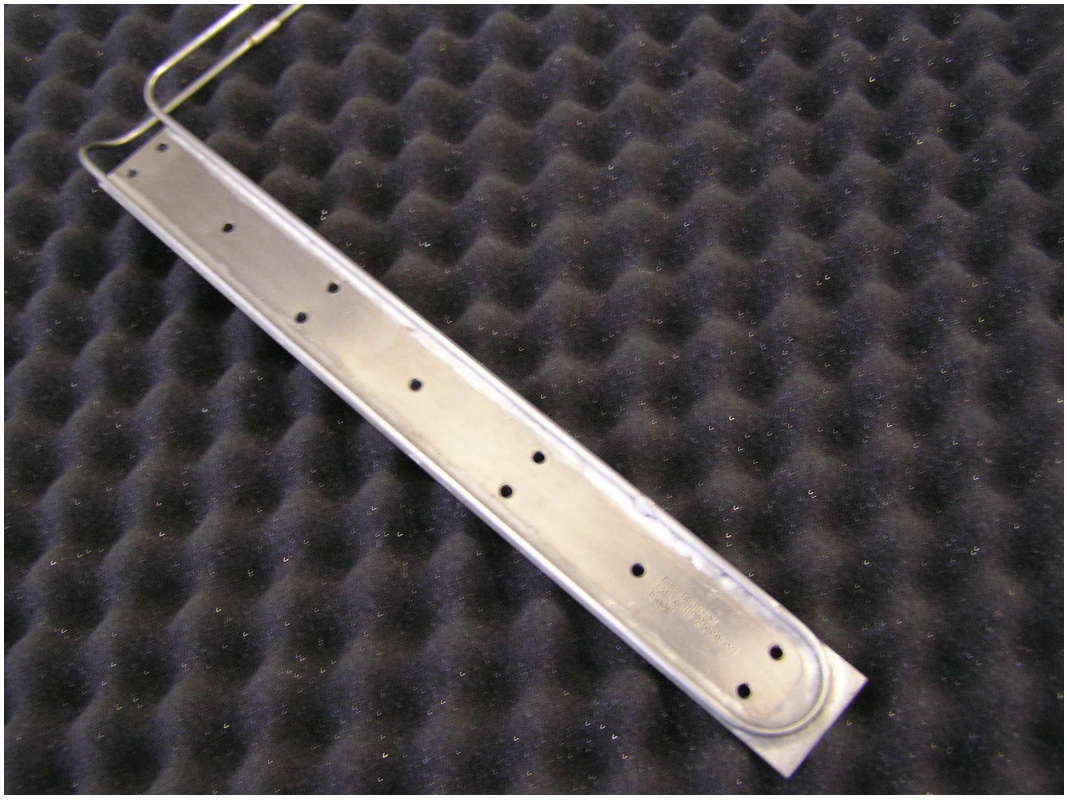

Figure 1-28: Condenser view of mini-LHP in stainless steel and filled with R245fa

Mass Status of SS-R245fa mini-LHP's

Part number	LHP mass (g)	R245fa quantity (g)	Quantity of LHP's
12E16-11-10000-01	131.82	6.81	1
12E16-21-10000-01	127.36	6.81	1

Table 1-3: Mass status of SS-R245fa mini-LHP's

Acceptance tests on 2nd version LHP before delivery

Only evaporator in vertical position has been tested to simulate the mounting configuration in the SEB (mounted on the lateral walls). **The LHP's have been tested with a tilt of 500mm between evaporator and condenser.**

No insulation is made around the LHP, only natural convection is present. The cooling is applied directly on the condenser plate.

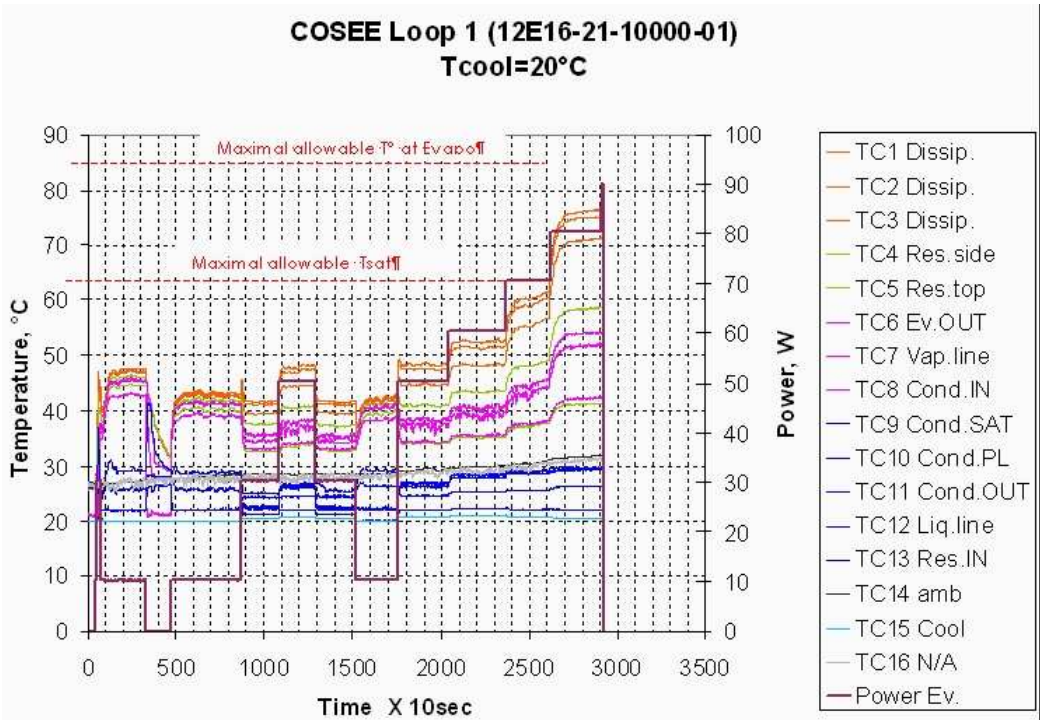

Figure 1-29 : Thermal acceptance tests results for loop 1 at Tcondenser = +20°C

For the acceptance tests of loop 1 at a condenser T° of +20°C, start-up has been achieved at 10W then power could be increased up to 80W.

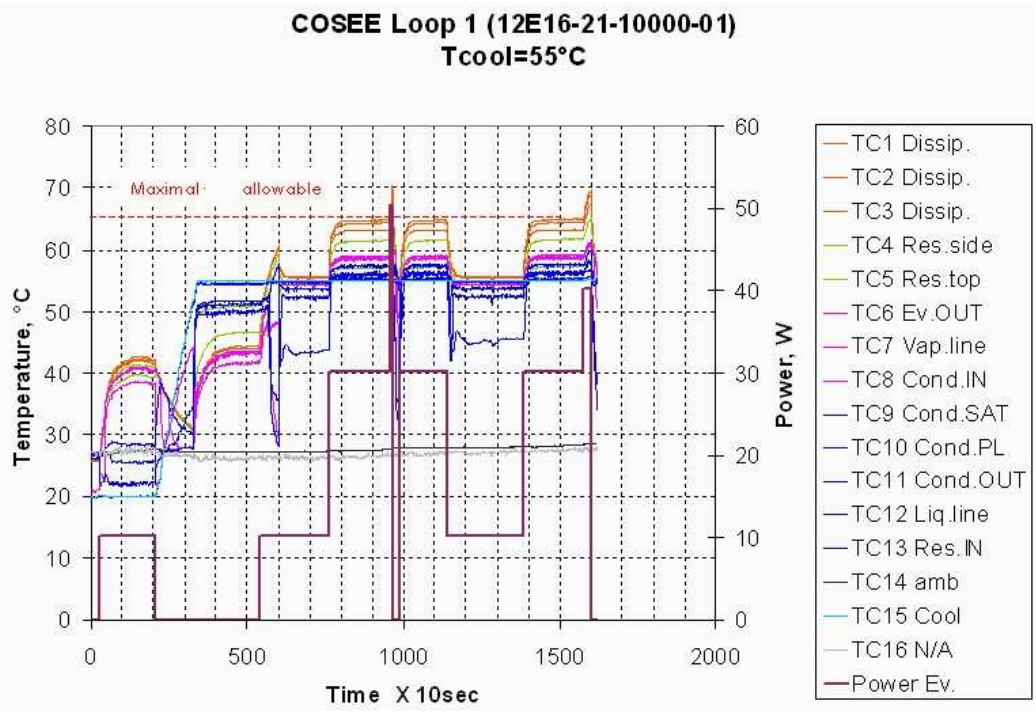

Figure 1-30 : Thermal acceptance tests results for loop 1 at Tcondenser = +55°C

For the acceptance tests of loop 1 at a condenser T° of +55°C, start-up has been achieved at 10W then power could be increased up to 30W. The maximal heat load has been limited by the saturation temperature that can not exceed +65°C.

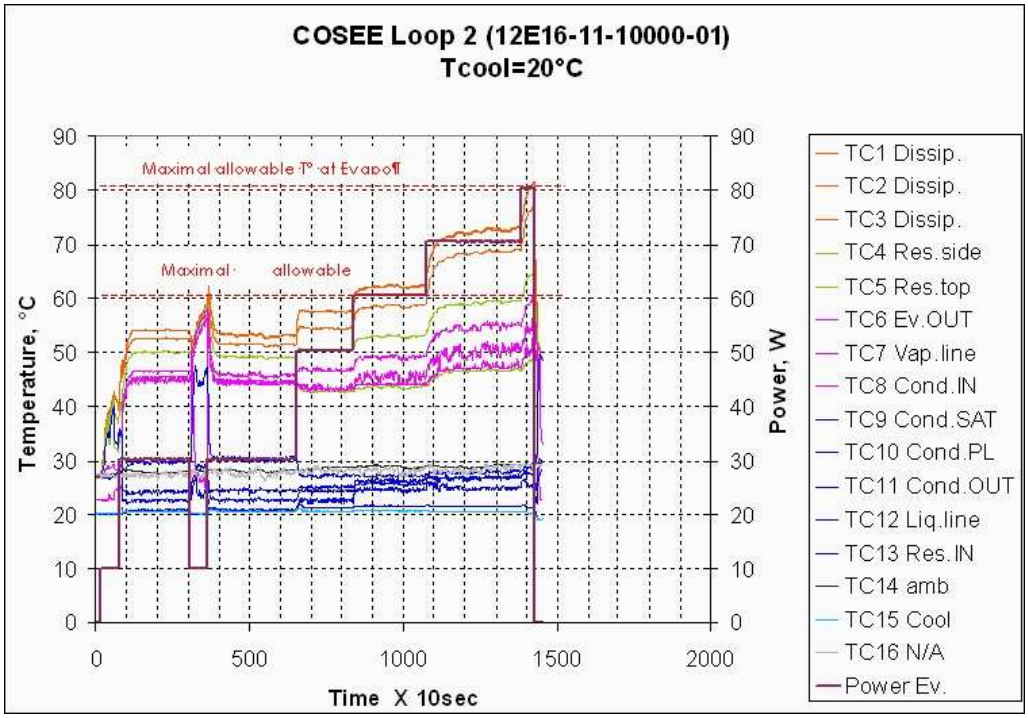

Figure 1-31 : Thermal acceptance tests results for loop 2 at Tcondenser = +20°C

For the acceptance tests of loop 2 at a condenser T° of +20°C, start-up has been achieved at 10W then power could be increased up to 70W.

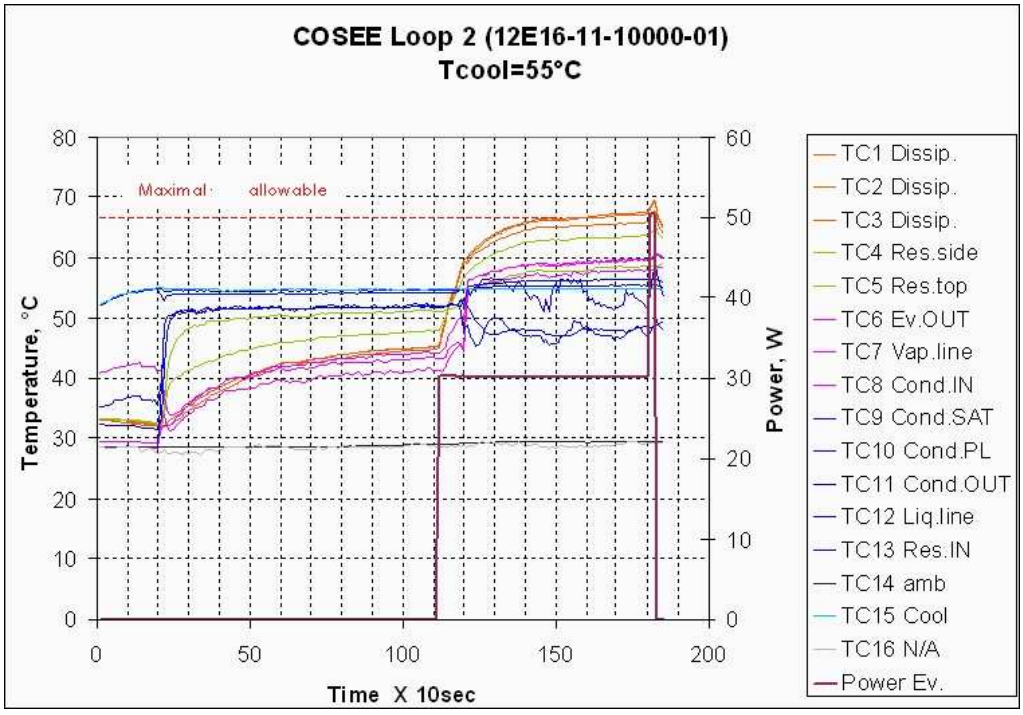

Figure 1-32 : Thermal acceptance tests results for loop 2 at Tcondenser = +55°C

For the acceptance tests of loop 2 at a condenser T° of +55°C, start-up has been achieved at 30W. Power could not be increased over 30W because of the saturation temperature limitation at +65°C.

1.4.1.3 INSTITUT of THERMAL PHYSICS LHP MANUFACTURING

Config in Stainless Steel and R245fa : New condenser design

Fluid lines tubes : diam ext = 2.5mm / SS 316L in annealed state

Allows bending for integration of LHP on the seat interfaces.

LHP's shall be delivered to Thalès for mounting on seat.

ITP has delivered two LHP based on freon R141b fluid.

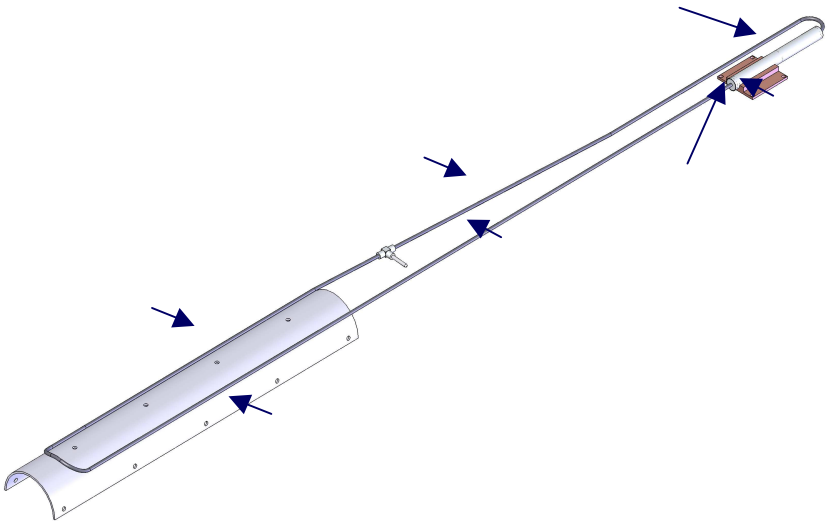

1.4.2 WP 4200: EQUIPMENTS ADAPTATIONS

Two complete new electronic boxes have been realised. The two boxes have the same sizes than the commercial one actually used on IFE sytems and are representative of power distributions.

The new box has received a modified flange with a specific area dedicated to the external heat pipe evaporator. Additional internal heat pipes have been added to channel the heat to these flanges. Internal modifications have been made to screw the clamping system of the internal heat pipes.

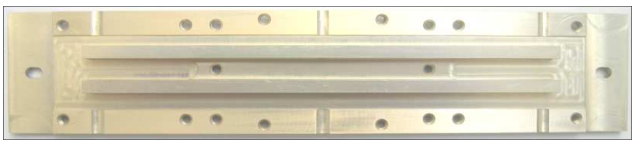

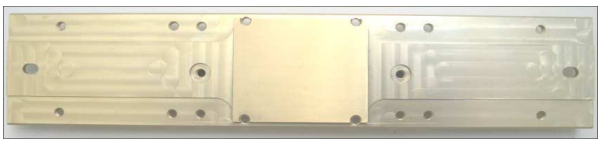

The internal heat pipes are two phases heat transfer systems. They are made of an unique tube of copper: liquid (water) and vapor flows in counter-flow in the tube. In our application for the cooling of the local component the heat pipe length would be around 120mm and the power per heat pipe around 10W.

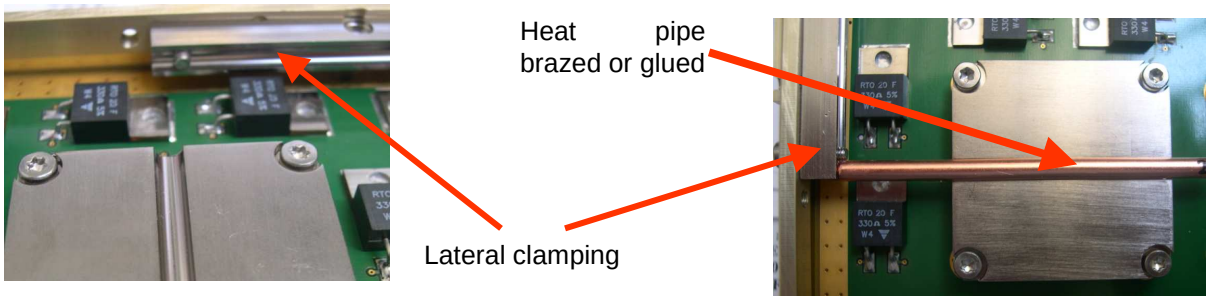

The heat pipe can be shapped (bended, flattened) and brazed or glued on metal clamping part in order to have a good contact between the heat pipe and the heat sources.

The electronic pcb have been designed to improve the heat transfer to the side of the card using a large copper mass plan and using thermal vias under each components.

Each card can be powered up to 50W, with two cards in the box the maximum of 100W could be reached.

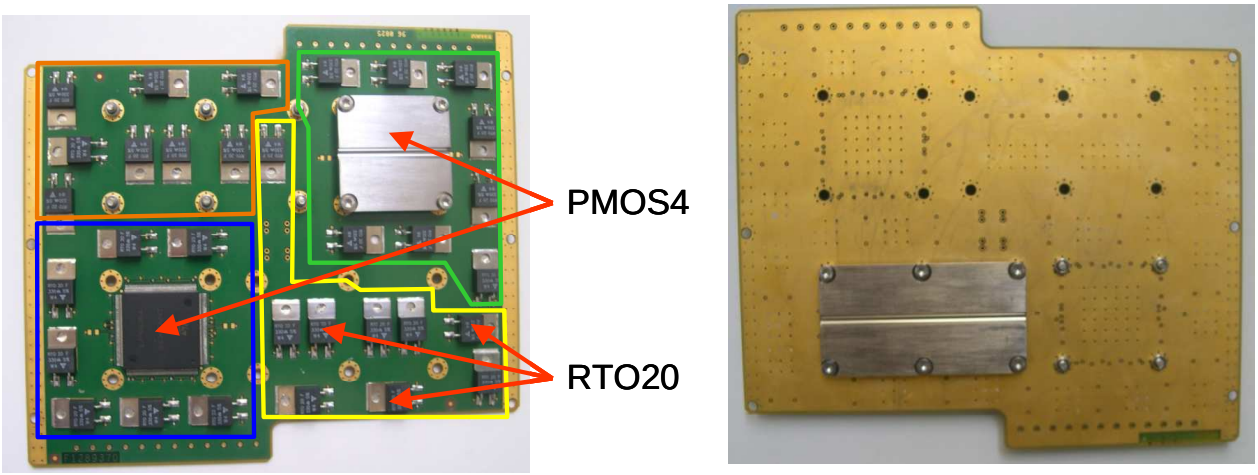

1.4.3 WP 4300-4400-4500 : SEATS INTEGRATION*

Two type of seat have been send to Thales avionics for the preliminary ambient thermal validations.

One type of the seat is an Avio economic seat with an aluminium structure and the other one is a carbon economic seat from RECARO. Unfortunaly no seat fron PAIG has been send.

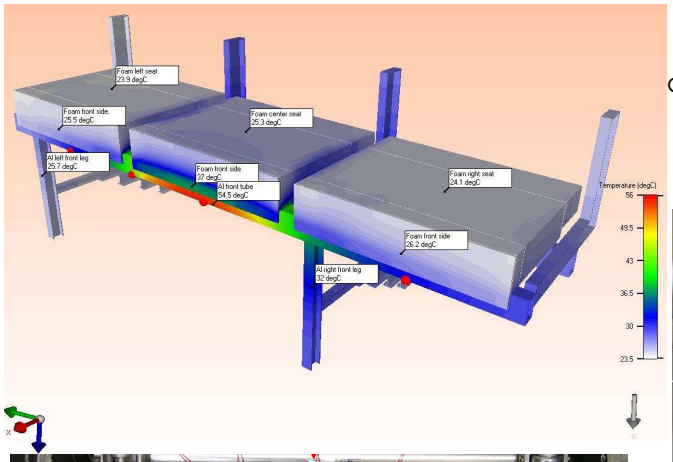

a

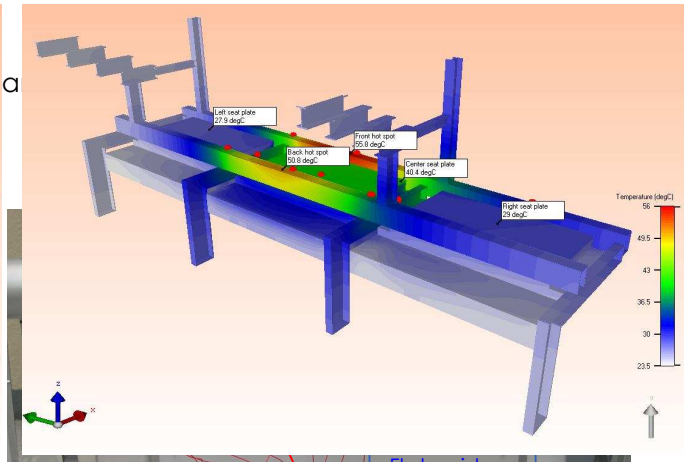

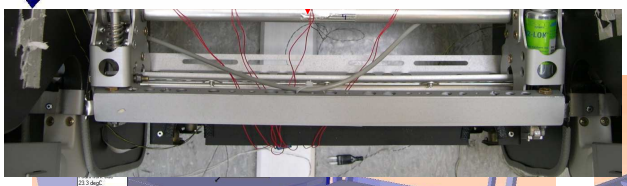

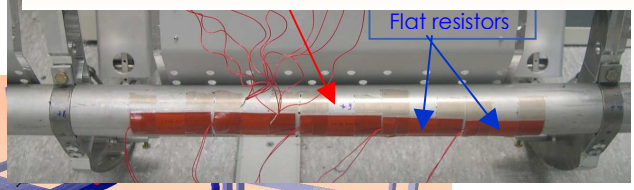

A power of 100W can be applied with the resistors that simulate the heat source (Loop heat pipe condenser) and the thercouples measure the temperatures along the beam of the seat to get a thermal field of seat structure.

With these measurments a modelisation of the two seats heve been realised to look after the influence of the location of the loop heat pipe evaporator. The seats have been simulated with the foam and to see the real temperature in th ebeam the foam is extracted from the model.

Results on Avio seats:

the temperatures reached a ΔT of 59°C (between ambient and maximum temperature on the beam) for a heat load of 100W

- the heat spread is located to a small area
- the natural convection is too weak for a sufficient cooling
- measurement are a little pessimistic regarding to a real LHP condenser.

One improvement will be the increasing of the emissivity of the aluminium beam by black painting, this improvement is limited the benefit is only 4°C.

To allow a better result the beam could be increased from its cross section.

Results on Recaro seats:

- the temperatures reached ΔT 125°C for for 100W heat loads
- there is not heatspread along the carbon beam (plane conductivity less than 50 W/mK)

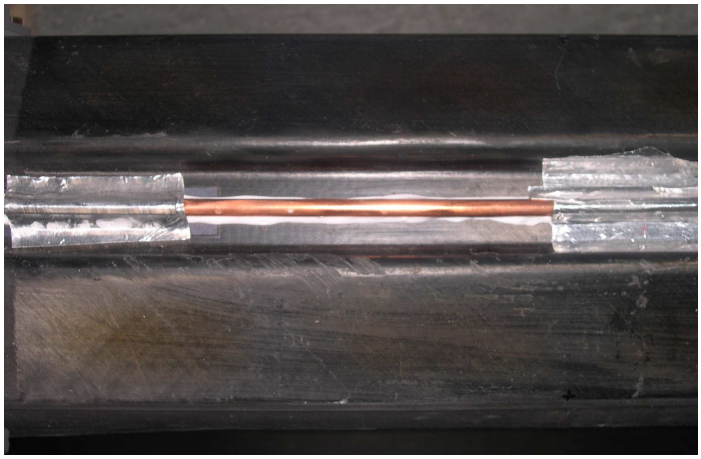

- the natural convection is too weak for a sufficient cooling
- measuramentare pessimist regarding to a real LHP condenser
- To increase the conductivityof carbon composite a small heat pipe could be use.

Moreover, to split the condenser region in two parts could also decrease the temperature.

With these two improvements the heat dissipation has been largely increased. At least there is a 50°K temperature drop near the condenser zone 20°K is coming from the heat pipe and 30°K from the condenser location.

GENERAL CONCLUSION

The thermal conductivity of the two seat are too weak for the application targetted:

for Avio seats it comes from the small cross section of the beam. It canot be incresed as a matter of weight

for Recaro seat the difficulty lies in the thermal conductivity of the carbon beam (1W/mK in the vertical direction) and too small in the rorizontal plane (50 W/mK)

A simple solution for Recaro and Avio seats would be the use of a copper heat pipe fixed on the main structure alumlinium beam or carbon beam.

Additional heat pipes would reduced the LHP condenser temperaute the main problem is to integrate the copper heat pipe in the beams. Painting on the hottest areas of the Avio seats allows some additional cooling.

With the present design and with standard power (30W to 50W) the LHP condenser temperature are acceptable but must be confirmed with real experiments) :

Avio seat : ΔT 25°C

Recaro seat ΔT 40°C

These temperature levels are compatible with SEB cooling.

1.5 WP 5000 : PERFORMANCE EVALUATION

1.5.1 WP 5100 : THERMOMECHANICAL PERFORMANCES EVALUATIONS

During this phase, the seats equipped with representative electronic equipments have been submitted to the test programme defined in WE 1400.

1.5.2 EHP mini-LHP's thermomechanical performance evaluation

1.5.2.1 Thermal performance tests on LHP's mounted on the RECARO seat

Test configuration:

The RECARO seat has a composite structure: Carbon/Epoxy.

Each LHP condenser is fixed to a seat beam face.

The SEB is placed on the back of the seat and each LHP evaporator is mounted on the SEB lateral face.

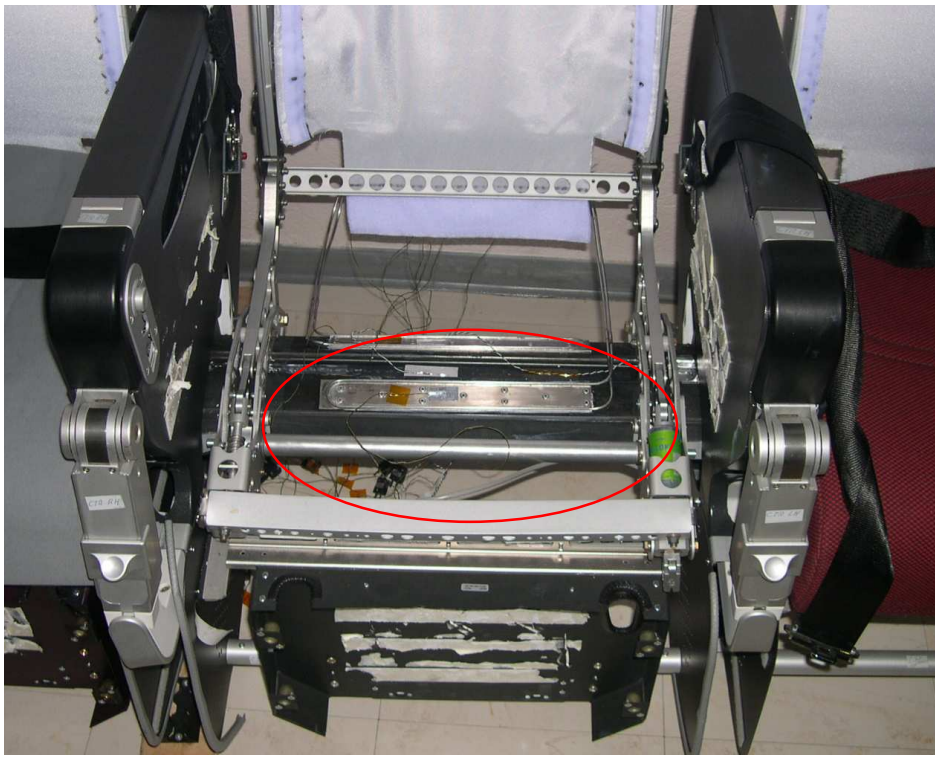

Figure 1-33 : Mounting of LHP's condensers on the RECARO seat beam

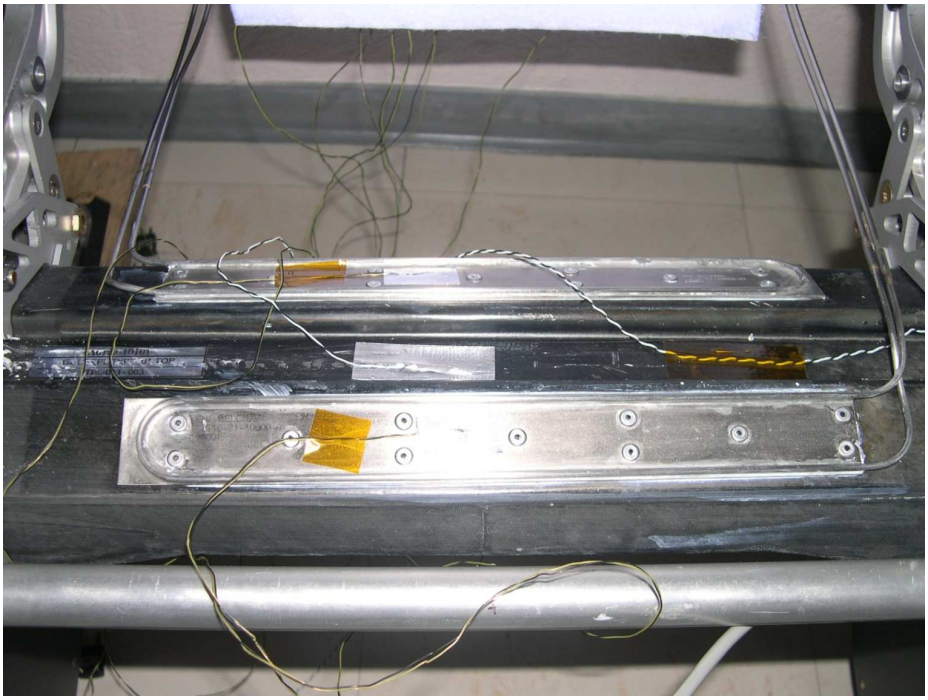

Figure 1-34 : Detailed view of the condenser mounting on RECARO seat

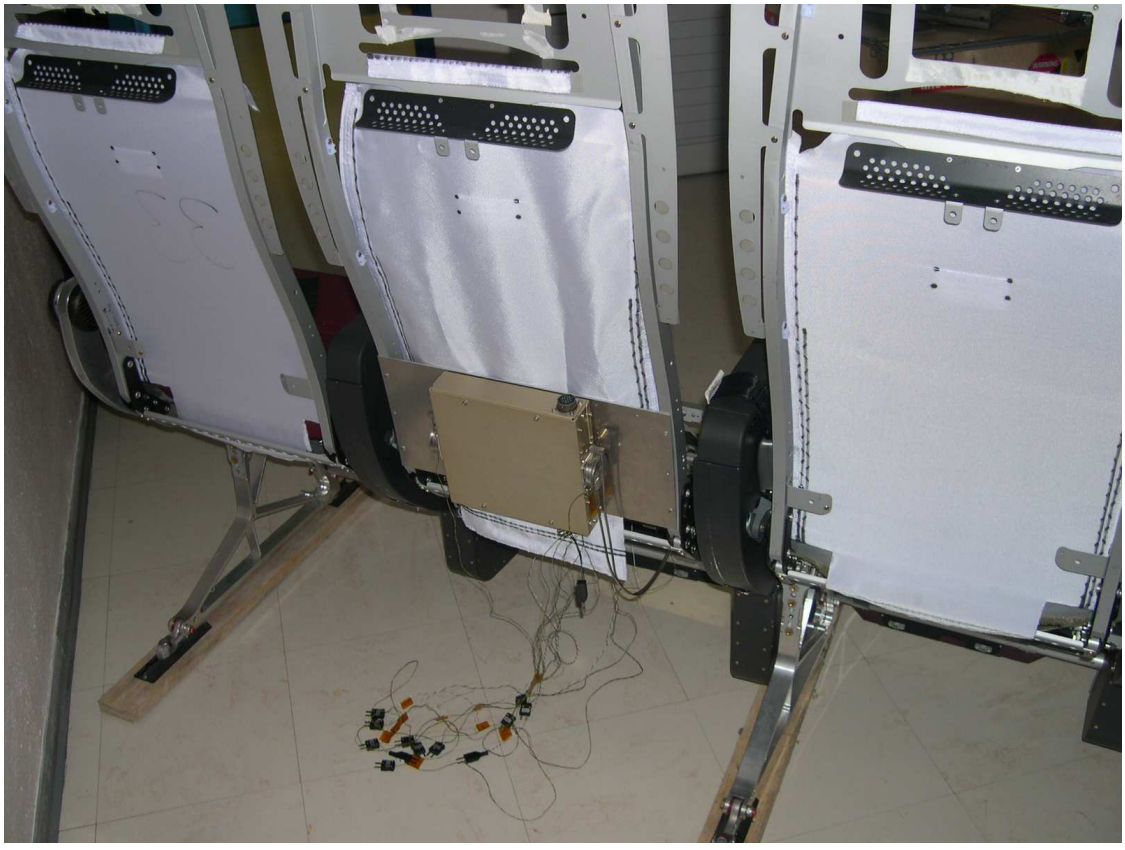

Figure 1-35 : View of SEB mounting on the seat back.

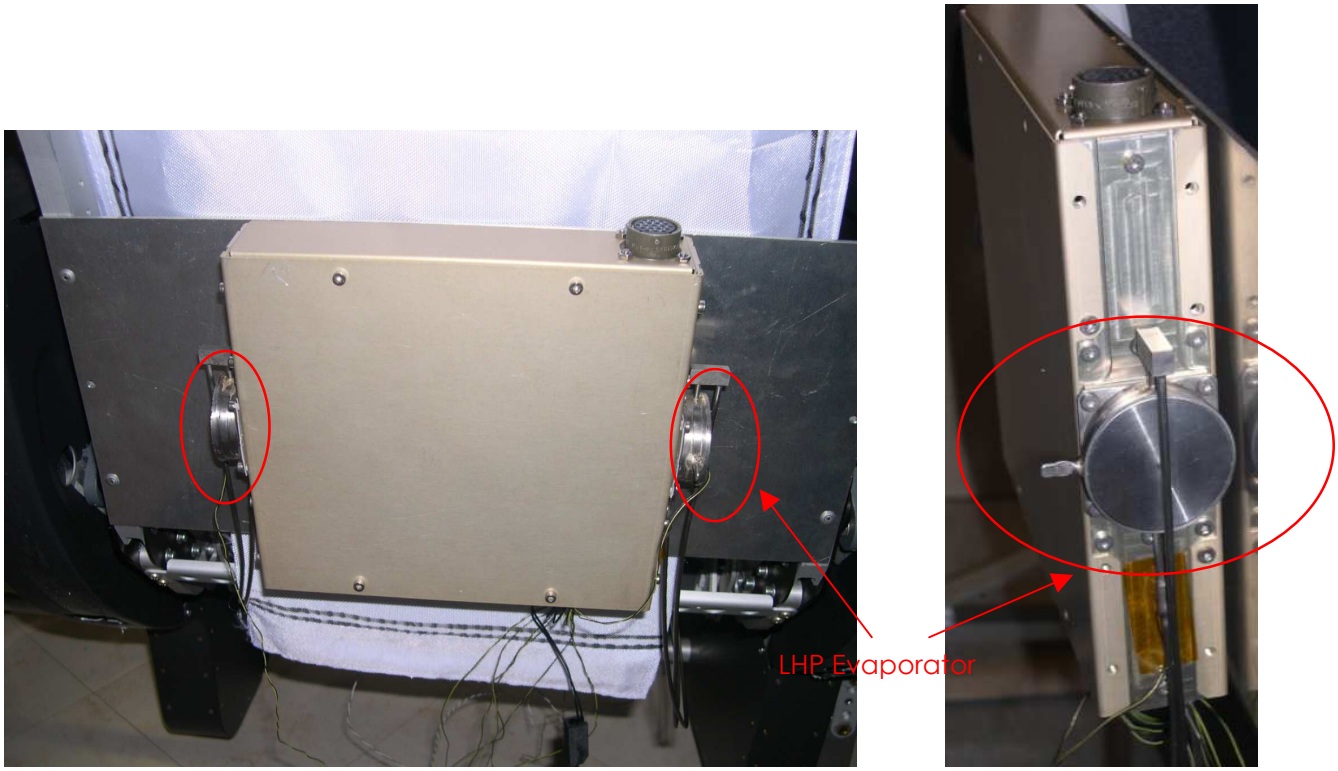

Figure 1-36 : Detailed view of LHP evaporator on the SEB.

Tests results:

The tests have been done considering the evaporator above the condenser with a tilt of 500mm.

The ambient T° is of +20°C.

Only radiation and convection have been considered.

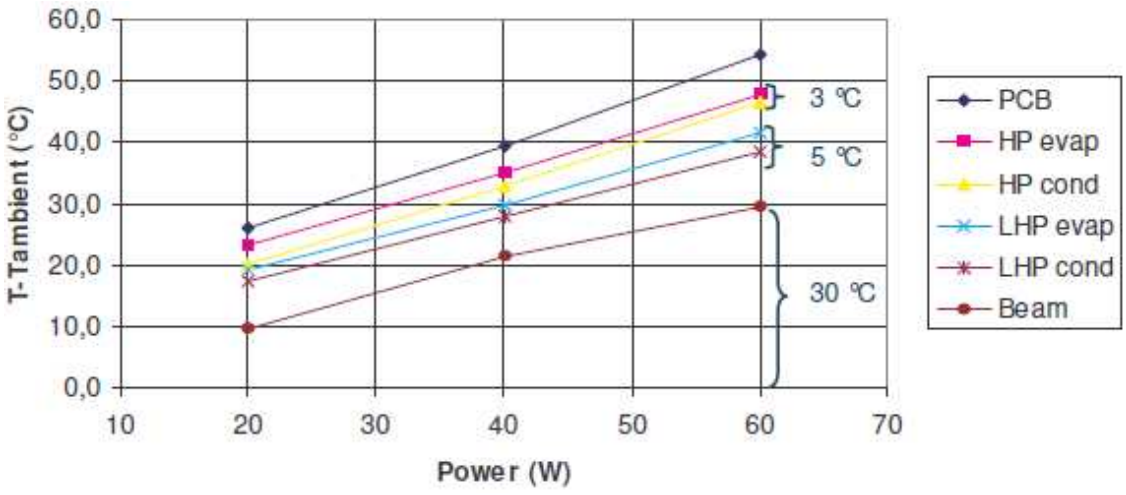

Figure 1-37 : Temperatures distribution

We can observe from the upper figure:

- **An average of heat dissipation in the seat structure (λxy = 50W/mK and λz = 1W/mK) as it is in composite.**

  ⇒ Strong gradient in the beam near the LHP condenser.

- The HP thermal gradient is about 3°C.

- The LHP thermal gradient is about 5°C.

So the improvement of the SEB cooling efficiency is limited by the beam thermal conductivity. **However the LHP efficiency is good : 5°C of thermal gradient whereas the tilt between evaporator and condenser is of 500mm.**

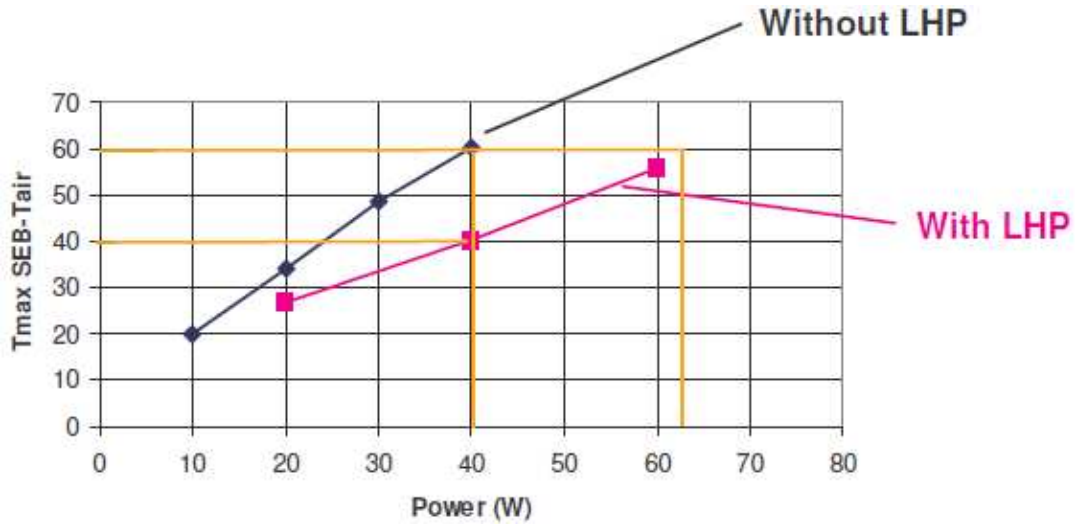

Figure 1-38 : Impact of LHP using in the SEB temperature limitation

For a constant power of 40W ⇒ 20°C of T° reduction (30% benefit on temperature)

For a constant thermal gradient = 60°C⇒ the dissipated power capability goes from 40 to 65W (60% increase).

2 CONCLUSION

All the objectives of the COSEE project have been realised.

The main objective was to develop and integrate an advanced cooling technique based on heat pipes located between the seat or the aircraft structure and the dissipative equipment through :

- evaluation and thermal simulation of the heat dissipation capability of the different cooling options
- design and development of a specific and reliable loop heat pipes adapted to aerospace specifications
- adaptation of the equipment and seat structure to optimize the use aof the new cooling technique
- performance evaluation on representative mock-up against the aeronautic specifications.

All the objectives: technological, strategic and collaborative have been met and even surpassed.

The final testing has shown that the two developed technologies are able to divide by a **factor of two the temperature elevation** on the critical components or **to multiply by two the power dissipated**.

The heat transportation distance between the box and the structure initially 500mm has been increased to 700 mm with a good flexibility of the tubes.

Software and simulation tools associated with experimental measurement techniques have provided good design optimizations.

This project was very challenging in deifferent areas of innovations :

- Two cooling techniques have been developed with the combination of heat pipes in the electronic box and loop heat pipe for the long distance heat transportation.
- The performance achieved with a conductivity of 80000 W/m°K is equivalent to 200 times the bare copper capability. The 3 mm tubes would be equivalent to a copper rod of 80mm diameter.
- Simulation tools and measurement techniques have been established.
- Examination on the possibility to exploit the results on avionics equipment is on-going as well as other opportunities for the LHP manufacturers

The quality and excellent cooperation within the consortium has permitted to successfully terminate the project.

NOMENCLATURE

A	cross-sectional area, m²
c_p	specific heat, J kg^{-1} K^{-1}
D	diameter, m
e	thickness, m
g	gravity, m.s^{-2}
h	convective heat transfer coefficient, W m^{-2} K^{-1}
h_C	condensation heat transfer coefficient, W m^{-2} K^{-1}
ΔH	condenser elevation, m
k	thermal conductivity, W m^{-1} K^{-1}
l_v	latent heat of vaporization, J kg^{-1}
L	length, m
$\dot{m}$	mass flow rate, kg s^{-1}
P	pressure, Pa
Q	heat transfer rate, W
R	thermal resistance, K W^{-1}
S	heat exchange area, m²
T	temperature, K

Subscripts:

A	ambient
C	condenser or condensation
E	evaporator
eff	effective
i	input or inlet or inner
l	liquid
L	liquid line
NCG	Non Condensable Gas
o	out or outlet or outer
R	reservoir
sink	heat sink
v	vapour
w	wick
wall	container wall
η	two-phase

REFERENCES

Amidieu M., Tjiptahardja T., Van Oost S., Mullender B., STENTOR CPL: Ground test and modelling results, in: International Conference On Environmental Systems, Toulouse, July 2000, (SAE paper 2000-01-2454), 9 p.

Baker C.L., Bienert W.B., Ducao A.S., Loop heat pipe flight experiment, in: International Conference On Environmental Systems, Danvers, July 1998, (SAE paper 981580) 7 p.

Baumann J., Rawal S., Viability of loop heat pipes for space solar power applications, in: AIAA Thermophysics Conference, 35th, Anaheim, CA, 11-14 June 2001, (AIAA 2001-3078), 10 p.

Boo J. H., Chung W. B., Thermal performance of a small-scale loop heat pipe with PP wick, in: 13th IHPC, Shanghai, China, 21-25Sept. 2004, pp. 259-264.

Bugby D., Heat pipe architecture offers flexible thermal control, COTS Journal, July 2005. Available on: http://www.cotsjournalonline.com/home/article.php?id=100367 (consulted on July 11th, 2006).

Cao Y., Faghri A., Conjugate analysis of a flat-plate type evaporator for capillary pumped loops with three-dimensional vapor flow in the groove, Int. J. Heat Mass Transfer 37 (3) (1994) 401-409.

Chen Y., Groll M., Mertz R., Maydanik Y.F., Vershinin S.V., Steady-state and transient performance of a miniature loop heat pipe, International Journal of Thermal Sciences, In Press, Corrected Proof, Available online 9 March 2006, 7 p.

Chuang P-Y.A., An improved steady-state model of loop heat pipes based on experimental and theoretical analyses, PhD Thesis, The Pennsylvania State University, 2003, 271 p.

Cheung K.-H., Hoang T., Ku, J., Kaya T., Thermal performance and operational characteristics of loop heat pipe (NRL LHP), in: International Conference On Environmental Systems, Danvers, July 1998, (SAE paper 981813) 9 p.

Delil A.A.M., Baturkin V., Friedrikhson Yu., Khmelev Yu., Zhuk S., Experimental results on heat transfer phenomena in miniature loop heat pipe with a flat evaporator, in: 12th IHPC, Moscow, 19-24 May 2002, 8 p.

Delil A.A.M., Maydanik Y.F., Gerhart C., Development of different novel loop heat pipes within the ISTC-1360 project, in: International Conference On Environmental Systems, Vancouver, July 2003, (SAE paper 2003-01-2383) 12 p.

Dickey J.T., Peterson G.P., Experimental and analytical investigation of a capillary pumped loop, J. Thermophysics and heat Transfer 8 (3) (1994) 602-607.

Douglas D., Ku J., Kaya T., Testing of the Geoscience Laser Altimeter System (GLAS) prototype loop heat pipe, in: 37th Aerospace Sciences Meeting and Exhibit, Reno, NV, 1999 (AIAA-1999-0473).

Figus C., Le Bray Y., Bories S., Prat M., Heat and mass transfer with phase change in a porous structure partially heated: continuum model and pore network simulations, Int. J. Heat Mass Transfer 42 (1999) 2557-2569.

Grob E., Baker C., McCarthy T., In-flight thermal performance of the geoscience laser altimeter system (GLAS) instrument, in: International Conference On Environmental Systems, Vancouver, July 2003, (SAE paper 2003-01-2421) 11 p.

Hamdan M., Cytrynowicz D., Medis P., Shuja A., Gerner F., Loop heat pipe (LHP) development by utilizing coherent porous silicon (CPS) wicks, in: 8th Inter Society Conference on Thermal Phenomena, San Diego, California, 29 May-2 June 2002, pp. 457-465.

Hamdan M.O., Loop heat pipe (LHP) modelling and development by utilizing coherent porous silicon (CPS) wicks, PhD Thesis, University of Cincinnati, 2003, 161 p.

Hamdan M., Gerner F.M., Henderson H.T., Steady-state model of a loop heat pipe (LHP) with coherent porous silicon (CPS) wick in the evaporator, in: 19th Annual IEEE SEMI-THERM, San Jose, California, 11-13 March 2003, 9 p.

Hoang T.T., Ku J., Advanced loop heat pipes for spacecraft thermal control, in: 8th AIAA/ASME Joint Thermophysics and Heat Transfer Conference, St. Louis, Missouri, 24-26 June 2002, (AIAA-2002-3094) 8 p.

Hoang T.T., Ku J., Miniature loop heat pipes for electronic cooling, in: InterPack2003-35245, Maui, Hawaii, USA, 6-11July 2003, 9 p.

Kaya T., Ku J., A parametric study of performance characteristics of loop heat pipes, in: International Conference On Environmental Systems, Denver, July 1999, (SAE paper 1999-01-2006) 7 p.

Kaya T., Ku J., Ground testing of loop heat pipes for spacecraft thermal control, in: 33rd Thermophysics Conference, Norfolk, VA, 28 June - 1 July 1999, 8 p.

Kaya T., Ku J., Thermal operational characteristics of a small loop heat pipe, Journal of Thermophysics and Heat Transfer 17 (4) (2003) 464-470.

Ku J., Operating characteristics of loop heat pipes, in: International Conference On Environmental Systems, Denver, July 1999, (SAE paper 1999-01-2007) 16 p.

Ku J., Ottenstein Rogers P., Cheung K., Investigation of low power operation in a loop heat pipe, in: 31st International Conference On Environmental Systems, Orlando, July 2001, (SAE paper 2001-01-2192) 10 p.

Ku J., High frequency low amplitude temperature oscillations in loop heat pipe operation, in: International Conference On Environmental Systems, Vancouver, July 2003, (SAE paper 2003-01-2387) 9 p.

Ku J., Rodriguez J.I., Low frequency high amplitude temperature oscillations in loop heat pipe operation, in: International Conference On Environmental Systems, Vancouver, July 2003, (SAE paper 2003-01-2386) 12 p.

Launay S., Sartre V., Bonjour, J., Parametric analysis of Loop Heat Pipe operation: a literature review, Int. J. Therm. Sci. 46 (7) (2007) 621-636.

Lee W.-H., Lee K.-W., Park K.-H., Lee K.-J., Study on working characteristics of loop heat pipe using a sintered metal wick, in: 13th IHPC, Shanghai, China, 21-25 Sept. 2004, pp. 265-269.

Liao Q., Zhao T.S., Evaporative heat transfer in a capillary structure heated by a grooved block, Journal of Thermophysics and Heat Transfer 13 (1) (1999) 126-133.

Maydanik Y.F., Fershtater Y.G., Theoretical basis and classification of loop heat pipes and capillary pumped loops, in: 10th IHPC, Stuttgart, Germany, 21-25 Sept. 1997, 15 p.

Maydanik Y.F., Miniature loop heat pipes, in: 13th IHPC, Shanghai, China, 21-25Sept. 2004, pp. 23-35.

Maydanik Y.F., Loop heat pipes, Applied Thermal Engineering 25 (5-6) (2005) 635-657.

Mena F., Supper W., Puillet C., Design and development of loop heat pipes, in: International Conference On Environmental Systems, Toulouse, July 2000, (SAE paper 2000-01-2315) 13 p.

Mishkinis D., Ochterbeck J. M., Sodtke C., Ku J., Butler D., Non-dimensional analysis and scaling issues in loop heat pipes in: AIAA Aerospace Sciences Meeting and Exhibit, 41st, Reno, Nevada, 6-9 Jan. 2003, (AIAA 2003-0341).

Nikitkin M.N., Bienert W.B., Goncharov, K.A., Non-condensable gases and loop heat pipe operation, in: International Conference On Environmental Systems, Danvers, July 1998, (SAE paper 981584).

Nikitkin M., Cullimore B., CPL and LHP technologies: What are the differences, what are the similarities? in: International Conference On Environmental Systems, Danvers, July 1998, (SAE paper 981587) 10 p.

Orlov A.A., Goncharov K.A., Kotliarov E.Y., Tyklina T.A., et al., The loop heat pipe experiment on board the GRANAT spacecraft, in: 27th ICES, Noordwijk, The Netherlands, 20-22 May 1997, 13 p.

Pastukhov V.G., Maidanik Y.F., Vershinin C.V., Korukov M.A., Miniature loop heat pipes for electronics cooling, Applied Thermal Engineering 23 (2003) 1125-1135.

Platel V., Fudym O., Butto C., Briend P., Coefficient de transfert, à l'interface de vaporisation, d'une boucle de fluide diphasique à pompage capillaire, Rev. Gén. Therm. 35 (1996) 592-598.

Riehl R.R., Comparing the behaviour of a loop heat pipe with different elevations of the capillary evaporator, in: International Conference On Environmental Systems, Colorado Springs, July 2004, (SAE paper 2004-01-2510).

Riehl R.R., Evaluating the behaviour of loop heat pipe with different compensation chamber configurations, in: 13th IHPC, Shanghai, China, 21-25Sept. 2004, pp. 107-112.

Riehl R.R., Siqueira T., Heat transport capability and compensation chamber influence in loop heat pipes performance, Appl. Therm. Eng. 26 (11-12) (2006) 1158-1168.

Rodriguez J.I., Pauken M., Performance characterization and model verification of a loop heat pipe, in: International Conference On Environmental Systems, Toulouse, July 2000, (SAE paper 2000-01-2317) 7 p.

Van Oost S., Mullender B., Bekaert G., Legros J.-C., Secondary wick operation principle and performance mapping in LHP and FLHP evaporators, in: Space Technology and Applications International Forum,

Albuquerque, New Mexico, 3-7 February 2002, pp. 94-103.

Wolf D.A., Bienert W.B., Investigation of temperature control characteristics of loop heat pipes, in: 24th ICES, Friedrichshafen, Germany, 20-23June 1994, (SAE paper 941576) 8 p.

Yao W., Miao J., Shao X., Parametric analysis on LHP/CPL evaporator performance and critical heat flux by two-dimensional calculation, 13th IHPC, Shanghai, China, 21-25Sept. 2004, pp. 125-132.

Zhao T.S., Liao Q., On capillary-driven flow and phase-change heat transfer in a porous structure heated by a finned surface: measurements and modelling, Int. J. Heat Mass Transfer 43 (7) (2000) 1141-1155.

Boo, J.H., Chung, W.B., Thermal performance of a small scale loop heat pipe with PP wick, Proc. of the 13th IHPC, Shanghai, 2004, p. 259-264.

Chuang, P.-Y. A. An improved steady-state model of loop heat pipes based on experimental and theoretical analyses, PhD Thesis, The Pennsylvania State University (2003).

Maydanik Y.F., Loop Heat Pipes, Applied Thermal Engineering 25 (2005) 635–657

Launay S., Sartre V., Bonjour, J., Parametric analysis of Loop Heat Pipe operation: a literature review, Int. J. Therm. Sci. 46 (7) (2007a) 621-636.

Launay, S., Sartre, V., Bonjour, J., Effect of fluid thermophysical properties on loop heat pipe operation, 14th IHPC, Florianópolis, Brazil, (April 22-27, 2007b).

Launay, S., Sartre, V., Bonjour, J., Simulation du fonctionnement d'une boucle de fluide à pompage capillaire dans un système embarqué, Congrès Français de Thermique, Ile des Embiez (29 mai -1er juin 2007c) 47-53.

Launay S., Sartre V., Bonjour J., An analytical model for characterization of Loop Heat Pipes, Journal of Thermophysics and Heat Transfer 22 (4) (2008) 623-631.

Loop Heat Pipe specificities – Typical loop heat pipe experimental results					
	Riehl 2005	**Maidanik 1995**	**Pauken 2000**	**Pauken 2000**	**Kaya 2003**
Fluid	Acetone	Ammonia	Ammonia	Propylene	Ammonia
LHP specificities					
LHP size	Miniature	Miniature	Macro	Macro	Miniature
Liquid line length and diameter	0.85 m – ∅ 2.85 mm	3 m – ∅ 2 mm	1.04 m – ∅ 4.5 mm	1.04 m – ∅ 4.5 mm	0.13 m – ∅ 2.5 mm
Vapour line length and diameter	0.55 m – ∅ 2.85 mm	3 m – ∅ 3 mm	1.04 m – ∅ 4.5 mm	1.04 m – ∅ 4.5 mm	0.16 m – ∅ 2.5 mm
Evaporator: - design - materials - length	cylinder ∅ 16.5 mm stainless steel 67 mm	cylinder ∅ 12 mm stainless steel 120 mm	cylinder aluminium	cylinder aluminium	cylinder ∅ 13 mm aluminium 120 mm
Vapour grooves	Porous wick	Porous wick			
1st wick characteristics – materials ∅ pore (µm) porosity permeability (m^2)	polyethylene 6 0.5 $1. 10^{-13}$	Sintered Ni powder 2-3 0.70	Sintered Ni 2.4 0.6 $4. 10^{-14}$	Sintered Ni 2.4 0.6 $4. 10^{-14}$	Sintered Ni 2.4 0.6 $4. 10^{-14}$
2^{nd} wick characteristics – materials					
Reservoir: - materials - volume	Stainless steel ≈ 20 cm3	Stainless steel ≈ 25-30 cm3	Stainless steel ≈ 115 cm3	Stainless steel ≈ 115 cm3	Aluminium ≈ 2.3 cm3
Evap/reservoir specificities	Bayonet	Bayonet			
Condenser design: -shape - materials - length	tube – ∅ 2.85 mm aluminium saddle 1 m	annular ∅ 12 mm aluminium saddle 120 mm	tube – ∅ 4.1 mm aluminium 3.8 m	tube – ∅ 4.1 mm aluminium 3.8 m	tube heat exchanger Cu block 100 mm
Experimental study					
LHP operation conditions	Steady state/transient		Steady state	Steady state/transient	Steady state/transient
Power range	2-80 W	10-130 W	20-800 W	20-200 W	5-250 W
Maximum heat flux					
Sink temperature range	0 to 5 °C	30 °C	-10 to 20 °C	-10 to 20 °C	-40 to 0 °C
Total conductance	1 W/K	26 W/K (H) 5.4 W/K (V – 60 cm)	170 W/K ?	44 W/K ?	2.8 W/K
Specific studies	- evap/reservoir designs - power cycle test	- orientation (0-60 cm)	- fluid effect	- fluid effect - gravity - start-up	- orientation - start-up - power cycle test - acceleration

Loop Heat Pipe specificities – Typical loop heat pipe experimental results					
	Pastukhov 2003	**Pastukhov 2003**	**Lee 2004**	**Lee 2004**	
Fluid	Ammonia	Ammonia	Water	Water	
LHP specificities			Flat evaporator	Flat evaporator	
LHP size	Miniature	Miniature	Miniature	Miniature	
Liquid line length and diameter	0.34 m – ∅ 1.3 mm	0.24 m – ∅ 1.2 mm	0.5 m – $\varnothing_{OD}$ 3.2 mm	0.5 m – $\varnothing_{OD}$ 3.2 mm	
Vapour line length and diameter	0.21 m – ∅ 1.3 mm	0.52 m – ∅ 1.2 mm	0.5 m – $\varnothing_{OD}$ 6.35 mm	0.5 m – $\varnothing_{OD}$ 6.35 mm	
Evaporator: - design - materials - length	cylinder ∅ 6 mm stainless steel 40 mm	cylinder ∅ 5 mm stainless steel 10 mm	Flat 52x52 mm² Copper 10 mm thick	Flat 52x52 mm² Copper 10 mm thick	
Vapour grooves			Evaporator wall	Evaporator wall	
1st wick characteristics – materials ∅ pore (µm) porosity permeability (m²)	Ti	Stainless steel	Sintered brass wick 4.8 0.4	Sintered SS wick 9.5 0.53	
2nd wick characteristics – materials			No 2nd wick	No 2nd wick	
Reservoir: - materials - volume	Stainless steel ≈ 1-2 cm3	Stainless steel	Stainless steel ≈ 20 cm3	Stainless steel ≈ 20 cm3	
Evap/reservoir specificities			Reservoir above evapora	Reservoir above evaporator	
Condenser design: -shape - materials - length	tube – ∅ 1.3 mm Al plate/air cooling ≈ 0.6 m	tube – ∅ 1.3 mm Al fins/air cooling ≈ 0.12 m	water heat exchanger	water heat exchanger	
Experimental study					
LHP operation conditions	Steady state	Steady state	Steady state	Steady state	
Power range	2-40 W	2-30 W	40-160 W ?	40-160 W ?	
Maximum heat flux			5.92 W/cm²	5.92 W/cm²	
Sink temperature range	24 °C	22 °C	20 °C	20 °C	
Total conductance	0.6 W/K	0.5 W/K	2 W/K (at 160 W) ? (H)	2 W/K (at 160 W) ? (H)	
Specific studies	- gravity - condenser design	- gravity - condenser design - air or water cooling - evap saddle materials	- fill charge effect - wick charcateristics	- fill charge effect - wick charcateristics	

APPENDIX 2: DESCRIPTION OF THE LHP MODEL EQUATIONS

1.1. Energy balance on each LHP component

The energy balance at the evaporator expresses that a part of the heat input Q_i is transferred to the reservoir by conduction through the evaporator wall and another part to the liquid-vapour interface:

$$Q_i = \frac{T_E - T_R}{R_{wall}} + \frac{T_E - T_v}{R_E} \qquad (1)$$

where R_E is the thermal resistance between the heat source to the vaporization interface at the porous wick surface. The heat transferred to the liquid-vapour interface includes latent and sensible heat, plus conduction to the evaporator core through the wick (Hamdan et al., 2003):

$$\frac{T_E - T_v}{R_E} = \dot{m} l_v + \dot{m} c_{p,l} (T_v - T_R) + \frac{T_v - T_R}{R_w} \qquad (2)$$

A convective-conductive heat transfer is considered inside the wick:

$$R_w = \frac{exp\left(\frac{\dot{m} c_{p,l} e_w}{k_{eff} A_w}\right) - 1}{\dot{m} c_{p,l}}$$ for a flat evaporator,

$$R_w = \frac{exp\left(\frac{\dot{m} c_{p,l}}{2\pi k_{eff} L_w} ln \frac{D_{wo}}{D_{wi}}\right) - 1}{\dot{m} c_{p,l}}$$ for a cylindrical one.

The value of the wick thermal conductivity k_w is usually experimentally measured. As suggested by Prof. Maydanik (ITP), it can also be estimated using the Odelevski formula:

$$k_w = k \frac{1 - \varepsilon}{(1 + \varepsilon)^b} \qquad (3)$$

where k is the solid material thermal conductivity, ε the porosity and b a coefficient, whose value is 2.1 for the sintered structures. Thus, the effective thermal conductivity k_{eff} of the porous material saturated with gas or liquid is determined by the correlation:

$$k_{eff} = \varepsilon k_l + k \frac{1 - \varepsilon}{(1 + \varepsilon)^b} \qquad (4)$$

In the reservoir, the heat leaking by conduction through the wall and through the wick is balanced by the heat exchange to ambient and the returning liquid subcooling:

$$\dot{m} c_{p,l} (T_R - T_{Ri}) = \frac{T_E - T_R}{R_{wall}} + \frac{T_v - T_R}{R_w} + \frac{T_A - T_R}{R_A} \qquad (5)$$

The energy balance of the condenser is:

$$Q_o = \dot{m}c_{p,v}(T_v - T_C) + \dot{m}l_v + \dot{m}c_{p,l}(T_C - T_{Co}) \tag{6}$$

$$\dot{m}l_v = \frac{\pi L_\eta}{1/h_C D_{C,i} + 1/h_{Sink} D_{C,o}}(T_C - T_{Sink}) \tag{7}$$

The condensation coefficient h_C is calculated by Chato (1962) correlation for stratified flow inside smooth horizontal tube:

$$h_C = 0.555\left[\frac{g}{(T_C - T_{wall})D_c}\right]^{1/4}\left[\frac{\rho_l(\rho_l - \rho_v)l_v k_l^3}{\mu_l}\right] \tag{8}$$

(8)

For high vapour velocities, the flow regime may be of annular type and the Shah correlation is used. In the condenser subcooled region, the condenser outlet temperature T_{co} is calculated considering a convective heat transfer with the heat sink:

$$T_{Co} = T_{Sink} + (T_C - T_{Sink})exp\left(-\frac{\pi D_C (L_C - L_\eta)}{\dot{m}c_{p,l}(1/h_l + D_C/h_{Sink}D_{C,o})}\right) \tag{9}$$

The convective heat transfer coefficient h_l between the liquid and the tube wall is calculated by considering a constant Nusselt number for laminar flow, and using the Colburn correlation for turbulent flow. The heat exchange between the liquid line and the ambient is expressed in a similar form, to yield the reservoir inlet temperature T_{Ri}:

$$T_{Ri} = T_A + (T_{Co} - T_A)exp\left(-\frac{\pi D_L L_L}{\dot{m}c_{p,l}(1/h_l + D_L/h_A D_{L,o})}\right) \tag{10}$$

1.2. Heat transfer coefficient reservoir wall – ambient

This part of the model has been specifically developed for the LHP fabricated by ITP, as it includes a finned radiator pressed on to the reservoir.

For the finned radiator at vertical position, the Chaddock correlation is used to determine the convective heat transfer coefficient:

$$h_{R-A} = h_{ref}\left(\frac{S_b}{S_t} + \varepsilon\left(1 - \frac{S_b}{S_t}\right)\right) \tag{11}$$

where S_b is the base area and S_t the total area of the finned surface. The fin efficiency ε is given by:

$$\varepsilon = \frac{1}{1 + \frac{2}{3}\frac{h_{ref}\, a^2}{k_A\, t}} \tag{12}$$

where *a* is the fin height, *t* the fin thickness and *L* the fin length. The Nusselt number is related to the space between to adjacent fins, *s*:

$$\mathrm{Nu} = \frac{h_{ref}\, s}{k_A} = 0.112\left(\mathrm{Gr}_s \mathrm{Pr}\frac{s}{L}\right)^{0.534}\left(1 - \exp\left(-\frac{129}{\mathrm{Gr}_s \mathrm{Pr}\frac{s}{L}}\right)\right)^{0.284} \tag{13}$$

$$\mathrm{Gr}_s = \frac{g\beta(T_{wall} - T_A)s^3}{\nu^2} \tag{14}$$

where the air properties are taken at $T_{ref} = T_A + 0.62(T_{wall} - T_A)$

For the finned radiator at horizontal position, the correlation is:

$$\mathrm{Nu} = \frac{h_{R-A}\, s}{k_A} = 6.7\times10^{-4}\mathrm{Gr}_s \mathrm{Pr}\left(1 - \exp\left(-\frac{0.746\times10^4}{\mathrm{Gr}_s \mathrm{Pr}}\right)^{0.44}\right)^{1.7} \tag{15}$$

When the LHP is oriented at an intermediate position between horizontal and vertical, the heat transfer coefficient $h_{R\text{-}A}$ is deduced from the values calculated at 0° and 90° using linear interpolations.

1.3. Heat transfer coefficient liquid line – ambient

For the liquid line at vertical position, the correlation valid for a thin cylinder and large Grashof numbers is used:

$$\mathrm{Nu}_L = \frac{h_{L-A}L}{k_A} = \frac{4}{3}\left(\frac{7\mathrm{Gr}_L \mathrm{Pr}^2}{5(20 + 21\mathrm{Pr})}\right)^{1/4} + \frac{4}{35}\frac{272 + 315\mathrm{Pr}}{64 + 63\mathrm{Pr}}\frac{L}{D} \tag{16}$$

For the liquid line at horizontal position, the correlation of Churchill and Chu is used:

$$\mathrm{Nu}_D = \frac{h_{L-A}D_L}{k_A} = \left(0.60 + \frac{0.387(\mathrm{Gr}_D \mathrm{Pr})^{1/6}}{\left(1 + (0.559/\mathrm{Pr})^{9/16}\right)^{8/27}}\right)^2 \tag{17}$$

When the LHP is oriented at an intermediate position between horizontal and vertical, the heat transfer coefficient $h_{L\text{-}A}$ is deduced from the values calculated at 0° and 90° using linear interpolations.

1.4. Thermodynamic equations

As the LHP configuration for which the reservoir may be completely filled is not considered (case of excessive fill charge), there are three saturation states that are thermodynamically related. They are located in the evaporator grooves, in the reservoir and in the condenser. Thus, the following conditions must be satisfied:

$$T_v - T_C = \left(\frac{\partial T}{\partial P}\right)\Delta P_v \tag{18}$$

$$T_C - T_R = \left(\frac{\partial T}{\partial P}\right)\left(\Delta P_l - \rho_l g \Delta H\right) \tag{19}$$

In Eq. 19, a positive elevation ΔH means that the condenser is placed above the evaporator and a negative elevation, that the condenser is placed under the evaporator. The slope of the pressure-temperature saturation curve $\partial T/\partial P$ can be related to the thermophysical properties of the working fluid using the Clausius-Clapeyron equation:

$$\frac{\partial T}{\partial P} = \frac{T\left(1/\rho_v - 1/\rho_l\right)}{l_v} \tag{20}$$

The pressure drops ΔP_v and ΔP_l, due to the friction forces in the vapor and the liquid lines, depend on the fluid flow regime. They are calculated as follows:

$$\Delta P = \frac{f}{2\rho D}\left(\frac{\dot{m}}{A}\right)^2 L \tag{21}$$

Considering a hydraulically smooth tube wall of diameter *D* and length *L*, f is expressed by (Bejan and Krauss, 2003):

$$\begin{cases} f = 64/\mathrm{Re} & \text{for laminar flow } (\mathrm{Re} \le 2000) \\ f = 0.316\,\mathrm{Re}^{-0,25} & \text{for turbulent flow } (\mathrm{Re} \ge 9510) \end{cases}$$

The friction factor for the transition flow between laminar and turbulent regimes is assumed to be constant in order to ensure the continuity in calculation of the pressure drops with the flow regimes, i.e. $f = 0.032$ for $2000 < \mathrm{Re} < 9510$.

Eqs. (1) to (21) constitute the LHP global model under the form of a non-linear system of equations. The numerical solution of this system leads to the prediction of the temperature and pressure distribution along the LHP, and of the LHP performance as well.

APPENDIX 3: PRELIMINARY VALIDATION OF THE MODEL WITH THE LITERATURE RESULTS

A preliminary validation of the model was performed from experimental or numerical results available in the open literature.

2.1 Validation with experimental results

The LHP steady-state model was first run to check its ability to predict LHP performance when changing the working fluid. Detailed experimental results are presented by Boo and Chung (2004), using methanol, ethanol and acetone as working fluids. The LHP container and tubing are made of stainless steel (liquid: 2 mm ID, vapour: 4 mm ID, length 500 mm), and a polypropylene porous wick is used as the capillary structure (porosity: 0.4 to 0.5; $k_w \approx$ 0.2 $Wm^{-1}K^{-1}$; pore size from 0.5 to 25 µm). The experimental results were obtained for heat inputs ranging from 10 to 80 W. Each performance test was conducted until the heater surface temperature T_E reached 90°C, in order to protect the PP wick from permanent deformation. The maximum thermal load is then determined at this temperature.

Figure 1 shows the comparison between the experimental results (symbols) and the predictions (dashed lines) for the vapour and evaporator temperatures, versus Q_i, of three different working fluids (methanol, ethanol and acetone). The temperature difference between the evaporator and the vapour is strongly linked to the thermal resistance R_E between the heat source and the interface. R_E is difficult to estimate as it depends on the mechanical contact between the container and the wick, and also on the wettability of the liquid with the porous wick. Indeed, a highly wetting fluid has a better ability to fill the porous medium and thus, to

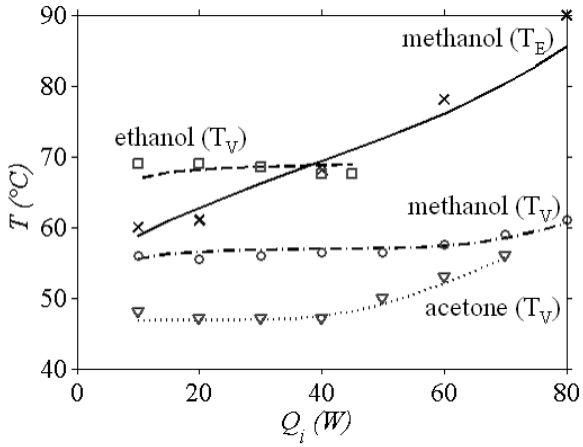

Figure 1: Comparison of T_v and T_E (symbols) measured by Boo and Chung (2004) to predicted temperatures (lines) for various working fluids.

reduce the thermal resistance between the container wall and the evaporation interface. As such characteristics are not detailed in Boo & Chung's study, R_E had to be adjusted in the model in order to obtain a good agreement between experimental and model results. It must nevertheless be stated that R_E was fixed to a constant value for each working fluid, and that it was strictly kept constant for a given fluid, whatever the heat flux. R_E was adjusted at the maximum thermal load, for which the evaporator temperature T_E is near 90°C. R_E is the lowest for methanol and is the highest for ethanol. The value of this constant might reflect the difference between the wettabilities of these fluids on a propylene surface, but no contact angle measurement for these fluids on such surface under saturation conditions could be found in the literature to confirm this explanation.

Finally, after this single adjustment, the data predicted by the model are in good agreement with the experimental results.

2.2 Validation with Chuang's theoretical model

The present LHP simulation results were also compared to Chuang's results (Chuang, 2003), which concern a cylindrical evaporator LHP filled with ammonia. The reservoir temperature T_R is depicted in figures 2 and 3 as a function of the evaporator heat input and the condenser elevation above the evaporator (H), for the present model and Chuang's model, respectively. $H < 0$ situation is called "adverse elevation" (less favorable situation for the best performance of the LHP, condenser below evaporator) and "positive elevation" refers to $H > 0$. The ambient temperature is T_A = 19 °C and the heat sink temperature T_{sink} = 5 °C. This curve has a typical shape corresponding to $T_A > T_{sink}$. In the decreasing part of the curve, the LHP operates in variable conductance mode. In the increasing part of the curve, the LHP operates in fixed conductance mode. The condenser elevation has a weak effect in case of high heat flux, because the pressure losses due to friction predominate over the pressure drop due to gravity. For low heat flux, an adverse elevation induces a T_R increase and a positive elevation induces the opposite effect.

A good accordance is obtained between our model results (figure 2) and Chuang's results (figure 3). Discrepancies are due to the fact that in Chuang's study, the model of the condensation heat transfer coefficient is different, the pressure losses are included in the condenser model and the conductive resistance through the wall R_{wall} is calculated differently.

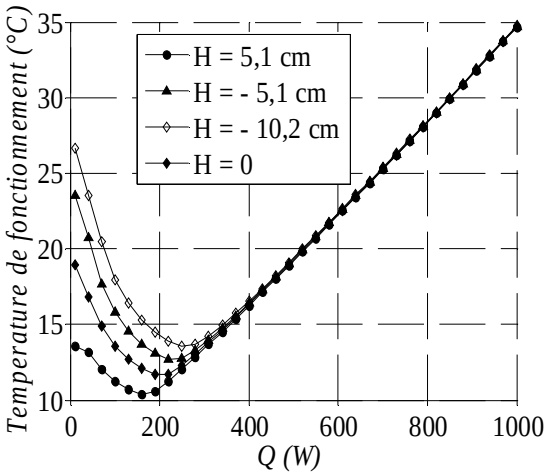

Figure 2 : Gravity effect on the operating temperature (present model)

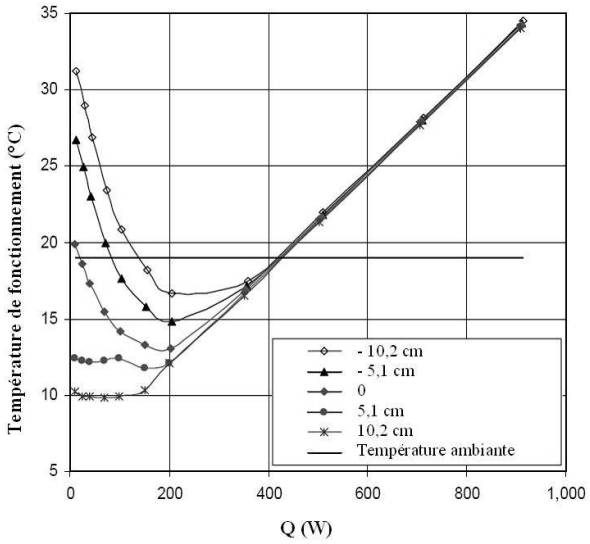

Figure 3 : Gravity effect on the operating temperature (Chuang's model, 2003)

APPENDIX 4: Geometrical and thermophysical data of the LHP fabricated by ITP and of the LHP fabricated by EHP

	LHP of ITP	LHP of EHP
Evaporator		
Dimensions (mm)	85 × 40 × 7	40 (OD) × 4.8
Wall thickness (mm)	0.5	0.8 (bottom); 1 (side wall)
Heated zone (mm²)	40 × 40	40 (OD)
Material	copper	titanium
Reservoir		
Dimensions (mm)	20 × 40 × 7	40 (OD) × 8.3
Wall thickness (mm)	0.5	0.8 (bottom); 1-4 (side wall)
Material	copper	titanium
Capillary structure		
Dimensions (mm)	55 × 39 × 7	39 (OD) × 4
Material	copper	titanium
Porosity	0.69	0.63
Pore diameter (µm)	16	13
Permeability (m²)	$2.15\ 10^{-12}$	$11\ 10^{-13}$
Thermal conductivity (W/m/K)	40	1.05
Number of vapour grooves	12	23
Vapour groove cross sectional area (mm²)	2.5447	0.4875
Liquid line		
Length (mm)	765	500
Inner diameter (mm)	3	2.5
Wall thickness (mm)	0.5	0.25
Material	copper	copper
Vapour line		
Length (mm)	358	500
Inner diameter (mm)	3	2.5
Wall thickness (mm)	0.5	0.25
Material	copper	copper
Condenser		
Length (mm)	562	500
Inner diameter (mm)	3	2.5
Wall thickness (mm)	0.5	0.25
Material	copper	copper
Working fluid		
	water	water

APPENDIX 5: IDENTIFICATION OF THE UNKNOWN MODEL PARAMETERS WITH THE EXPERIMENTAL RESULTS OF IKE

A new LHP model was developed, to account for the specificities of the LHP fabricated by ITP and of the experimental test bench of IKE. Since the thermal resistance network remains unchanged (figure 1), the model is based on the same set of equations as described in part 2. It has been adapted to enable the identification of the thermal resistances R_E and R_{wall}, which are difficult to predict accurately:

- R_E is the thermal resistance between the evaporator wall and the liquid-vapor interface in the wick. It includes heat conduction in the evaporator wall, heat transfer across the contact evaporator wall/wick, heat conduction in the porous medium filled with a two-phase fluid. So, its value will depend on many parameters e.g. the wick thermal conductivity, the mechanical contact between wick and container, the fluid/wick material wettability, the operating conditions (pressure, temperature, heat flux, LHP elevation …). The model convergence is very sensitive to this parameter.
- R_{wall} is a combination of axial heat conduction in the evaporator wall and convective heat transfer with the liquid flowing in the capillary structure. Thus, the evaporator wall acts as a fin to transfer the axial heat leak to the reservoir. This resistance is difficult to predict because: 1/ the liquid temperature varies along the capillary structure, 2/ the boundary condition at the "fin" tip is not clearly known.
-

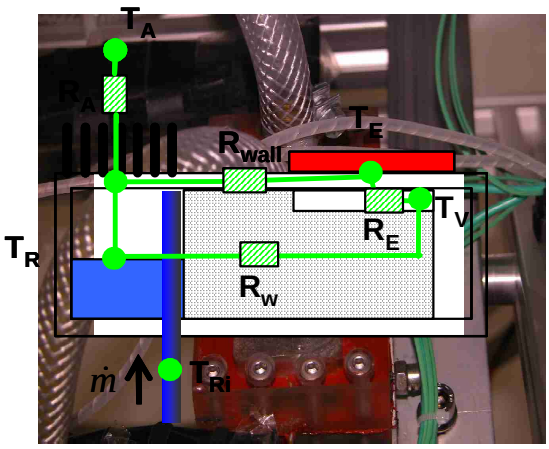

Figure 1: *Thermal resistance network for the evaporator model of the LHP fabricated by ITP*

Figure 2 : *Photography of the LHP heat sink (forced water circulation)*

The mass flow rate is an input data of this model, deduced from the experimental heat dissipation at the condenser:

$$\dot{m} = \frac{Q_C}{\Delta h_v} \qquad (1)$$

In this equation, it is assumed that the heat evacuated by latent heat is much greater than the heat dissipated by sensible heat, for the fluid desuperheating and subcooling. The experimental reservoir temperature (T_CC measurement) is used as an input data of the model, to determine the vapour temperature T_V. As the fluid in the reservoir and the vapour are assumed to be at equilibrium, there is a relationship between the temperature $(T_V\text{-}T_R)$ difference and the pressure difference $(P_V\text{-}P_R)$.

Using the Clausius-Clapeyron approximation, this relationship is expressed by:

$$T_v = T_R \frac{\left(1 + \frac{(v_v - v_l)}{2\Delta h_v} \Delta P_t\right)}{\left(1 - \frac{(v_v - v_l)}{2\Delta h_v} \Delta P_t\right)} \tag{2}$$

The energy balance of the reservoir is used to determine the evaporator wall temperature:

$$T_E = R_{wall}\left(\dot{m}c_{pl}\left(T_R - T_{Ri}\right) - \frac{\dot{m}c_{pl}}{exp\left(\frac{\dot{m}c_{p,l}e_w}{k_{eff}A_w}\right) - 1}\right) + \frac{T_R}{R_{wall}} + \frac{\left(T_R - T_A\right)}{R_A} \tag{3}$$

In Eq. (3), the reservoir temperature and the reservoir inlet temperature are provided by the experimental data. As the liquid line is thermally insulated, we have $T_{Co} = T_{Ri}$. The energy balance of the evaporator wall is used to determine the thermal resistance R_E:

$$R_E = \frac{T_v - T_E}{\frac{T_E}{R_{wall}} - Q_E - \frac{T_R}{R_{wall}}} \tag{4}$$

With equations (1) to (4), minimizing differences between the predicted and experimental values of the evaporator wall temperatures allows identifying the thermal resistances R_E and R_{wall}. The value of R_E is identified for each value of the heat load, tilt angle and heat sink temperature, which are the most important governing parameters.